ELSEVIER

Coordination Chemistry Reviews
156 (1996) 1–89

COORDINATION CHEMISTRY REVIEWS

Lanthanides and actinides. Annual survey of their organometallic chemistry covering the year 1994

Yurii K. Gun'ko, Frank T. Edelmann

Chemisches Institut der Otto-von-Guericke-Universität Magdeburg, Magdeburg, Germany

Accepted 8 March 1996

Contents

PII S0010-8545(96)01253-2

Keywords: Lanthanide; Actinide; Organometallic chemistry

---

1. Introduction

The review presents complexes of the lanthanides, actinides and also scandium and yttrium, which contain metal–carbon bonds as defined by the section 29 of Chemical Abstracts. Abstracts of papers presented at conferences, dissertations, and patents have mostly been excluded.

2. Lanthanides

2.1. Lanthanide complexes without supporting cyclopentadienyl ligands

2.1.1. Alkyl and arene complexes

Eaborn et al. [1] reported the synthesis and crystal structure of bis{tris(trimethylsilyl)methyl}ytterbium, $Yb[C(SiMe_3)_3]_2$, which was obtained from the reaction between YbI_2 and $K[C(SiMe_3)_3]$ in benzene. The most interesting and surprising feature of the structure of $Yb[C(SiMe_3)_3]_2$ (Fig. 1) is that the C–Yb–C angle is 137°. All other known bis{tris(trimethylsilyl)methyl}metal species, whether neutral or anionic, are linear. The authors also described the preparation and structure of an Yb analogue of a Grignard reagent. The reaction of $Yb[C(SiMe_3)_3]_2$ with iodomethane led to the unusual cleavage of one Yb–C bond formation of a new Yb(II) compound, $[Yb\{C(SiMe_3)_3\}I \cdot (OEt_2)]_2$. The same compound was isolated from the reaction between Yb metal and $(Me_3Si)_3CI$ in diethyl ether. According to the X-ray structure the molecule $[Yb\{C(SiMe_3)_3\}I \cdot (OEt_2)]_2$ (Fig. 2) has a centre of symmetry so that the central Yb_2I_2 ring is planar, as is usual in such a system. The angle at Yb is slightly larger and that at I, being slightly smaller than 90°.

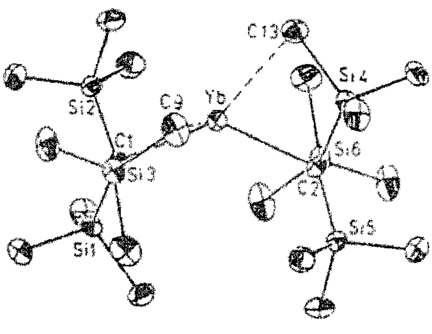

Fig. 1. Molecular structure of $Yb[C(SiMe_3)_3]_2$.

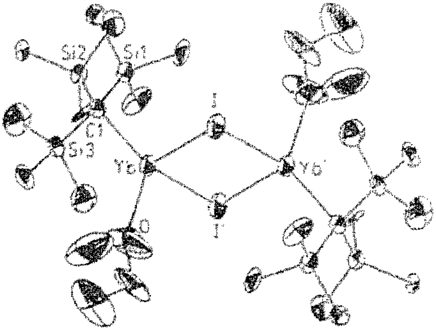

Fig. 2. Molecular structure of $[Yb\{C(SiMe_3)_3\}I(OEt_2)]_2$.

Mashima et al. [2] reported the synthesis and structure of the diene-bridged dilanthanum complex, $[LaI_2(THF)_3(\mu\text{-}\eta^4{:}\eta^4\text{-}PhCH{=}CHCH{=}CHPh)LaI_2(THF)_3]$. The complex was obtained from metallic lanthanum, 1,4-diphenylbuta-1,3-diene and iodine in THF.

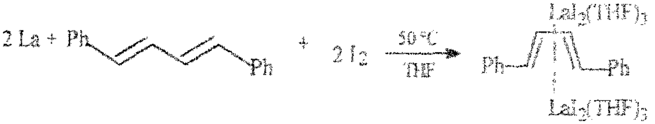

The complex crystallizes as a centrosymmetric molecule (Fig. 3). Each La atom exhibits a pseudooctahedral six-coordination through one η^4-interaction with the bridging diene unit. Three THF molecules are in mer-arrangement and two iodo ligands are trans to each other. The La–I distances are 3.176(1) and 3.179(1) Å, the average La–C is 2.805 Å.

Perry and Goddard [3] determined the Sc^+–alkyl bond strengths. The authors calculated dissociation energies for Sc^+–alkyl bonds and predicted thermochemistry for the σ-bond metathesis reaction: $Sc(R)^+ + R'H \rightarrow Sc(R')^+ + RH$. The results for $R = CH_3$, C_2H_5, i-C_3H_7 and t-C_4H_9 suggest that the Sc^+–R bond strengths decrease in the order methyl > primary > secondary > tertiary, correlating with the electron affinities of the radicals. The results for $R = C_2H_5$ and n-C_3H_7 suggest that the Sc^+–R bond strengths increase with the size of the ligand. The chemistry in gas-phase σ-bond metathesis reactions of $Sc(CH_3)_2^+$ with alkanes (C_2H_6, C_3H_8 and n-C_4H_{10}) can be readily explained by the trends in the pertinent Sc^+–alkyl bond strengths.

$$Sc(CD_3)_2^+ + CH_3CD_2CH_3 \xrightarrow{>90\%} Sc(CD_3)(CH_3CD_2CH_2)^+ + HCD_3$$

$$\xrightarrow{<10\%} Sc(CD_3)(CD(CH_3)_2)^+ + CD_4$$

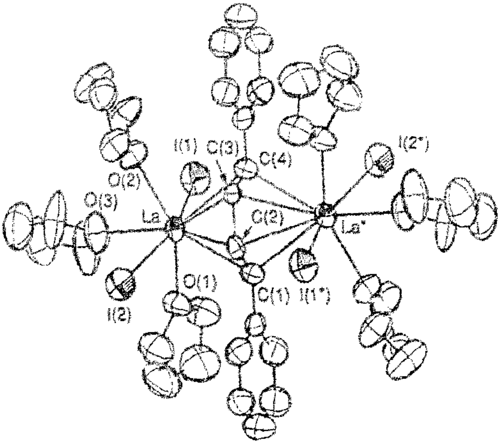

Fig. 3. Molecular structure of [$LaI_2(THF)_3(\mu-\eta^4:\eta^4-PhCH=CHCH=CHPh)LaI_2(THF)_3$].

Crellin et al. [4] used Fourier transform ion cyclotron resonance mass spectrometry to show that $Sc(CD_3)_2^+$ reacts with saturated alkanes larger than ethane in the gas phase by a four centre σ-bond metathesis reaction with methane elimination (Scheme 1). These processes involved little or no activation energy and occur preferentially with primary carbon–hydrogen bonds.

Lipshutz et al. [5] investigated the reactions of α-epoxytriisopropylsilane with selected nucleophiles including n-$BuCeCl_2$ and n-Bu_2CeCl. The reaction led to α-silyl alcohols which are readily oxidized to the corresponding triisopropylsilyl acyl silanes. The yields for the cerium complexes were less than 35%.

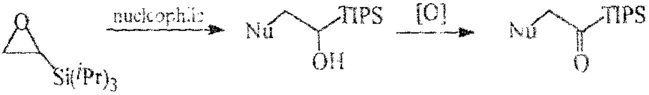

TIPS - triisopropylsilyl

Murakami and Ito [6] reported new carbon–carbon bond forming reactions via new organosamarium(III) intermediates. (α-Iminoalkyl)samarium(III) intermediates

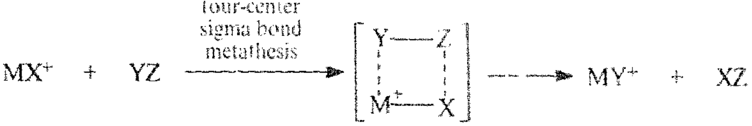

Scheme 1.

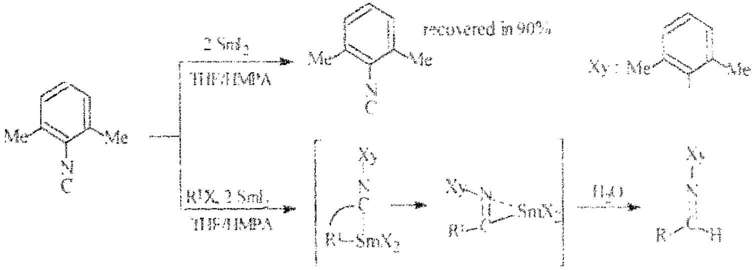

Scheme 2.

were generated by treatment of organic halides and 2,6-xylyl isocyanide with SmI_2 (Scheme 2).

When a carbonyl compound was added to the reaction mixture, α-hydroxy imine was formed (Scheme 3).

Unsymmetrical α-diketones were obtained by autoxidation of the resulting α-hydroxy imines. 4-(*tert*-Butyldimethylsiloxy)-2,6-xylyl isocyanide was used in the SmI_2-mediated three-component coupling reaction for the stereoselective syntheses of 2-amino alcohols via reduction and subsequent oxidative *N*-de-arylation. Double insertion of 2,6-xylyl isocyanide into an organic halide mediated by SmI_2 provided a synthetic method for hydroxy diketones and vicinal triketones.

Liang et al. [7] described the arene complexes $Ln(\eta^6\text{-}C_6Me_6)(AlCl_4)_3$, which were synthesized by the reaction of $LnCl_3$ with $AlCl_3$ and C_6Me_6 in the molar ratio of 1:3:1.2.

$$LnCl_3 + 3AlCl_3 + C_6Me_6 \xrightarrow{\text{toluene}} Ln(\eta^6\text{-}C_6Me_6)(AlCl_4)_3 \cdot MeC_6H_5$$

Ln = Nd, Sm, Gd, Yb

In the molecular structure of $Yb(\eta^6\text{-}C_6Me_6)(AlCl_4)_3 \cdot MeC_6H_5$ (Fig. 4) the coordination polyhedron of the Yb atom is a distorted pentagonal bipyramid. Five chlorine atoms are located in an equatorial plane; the sixth chlorine atom Cl(2) occupies one apical position and C_6Me_6 occupies the other one. The mean distances of $Yb–Cl^b$

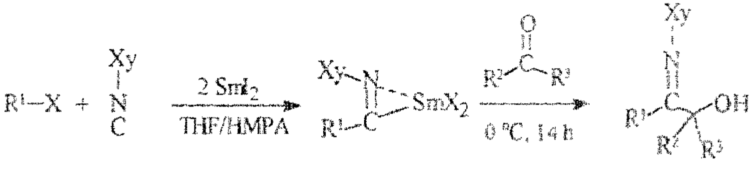

Scheme 3.

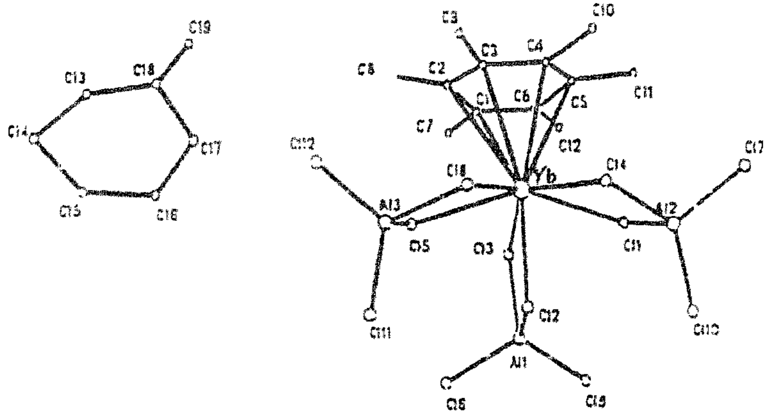

Fig. 4. Molecular structure of $Yb(\eta^6\text{-}C_6Me_6)(AlCl_4)_3 \cdot MeC_6H_5$.

(Cl in the plane) and Yb–Cl^a (Cl in the apical position) are 2.795(7) Å and 2.734(10) Å respectively.

Boje and Magull [8] reported the reaction between $SmBr_3$ and $[(biph)Li_2]$ in THF, which led to the complex $[(C_{24}H_{16})SmBr(thf)_2]_2 \cdot [C_{24}H_{14}]$.

$$6SmBr_3 + 6[(biph)Li_2] \xrightarrow{THF} [(C_{24}H_{16})SmBr(thf)_2]_2 \cdot [C_{24}H_{14}] + 2Sm + 2SmBr_2 + H_2 + 12LiBr$$

As result of this reaction, two biphenyl units are coupled to afford $[(C_{24}H_{16})SmBr(thf)_2]_2 \cdot [C_{24}H_{14}]$ with the hydrocarbon $C_{24}H_{14}$ intercalated. In the dimeric structure of $[(C_{24}H_{16})SmBr(thf)_2]_2 \cdot [C_{24}H_{14}]$ (Fig. 5) the Sm ions are bridged by two Br^-. The Sm–Br distances are 2.986(2) and 2.992(2) Å. Each Sm ion is octahedrally coordinated.

2.1.2. Complexes with phosphine ligands

Karsch et al. [9] described the dimeric complex $[Sm\{CH(PMe_2)_2\}_3]_2$, obtained from $[Sm(O_3SCF_3)_3]$ and $[LiCH(PMe_2)_2]$.

$$[Sm(O_3SCF_3)_3] + 3[LiCH(PMe_2)_2] \rightarrow [Sm\{CH(PMe_2)_2\}_3]_2$$

An X-ray structure determination revealed a centrosymmetric dimer in a chair conformation, formed by two bridging diphosphinomethanide ligands via the P(2) and C(1) atoms (Fig. 6). Together with P(1), C(1) is also a member of a three-membered ring (SmCP) as a substructural unit. Both samarium atoms are additionally ligated by two diphosphinomethanide ligand in a π-type coordination. Thus the complex contains four π-type and two bridging σ-type coordinated ligands.

Gambarotta and coworkers [10] prepared and characterized the complexes

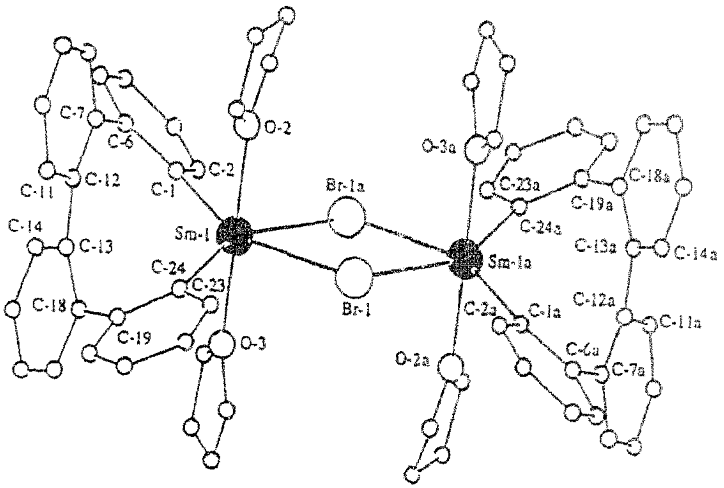

Fig. 5. Molecular structure of $[(C_{24}H_{16})SmBr(thf)_2]_2 \cdot [C_{24}H_{14}]$.

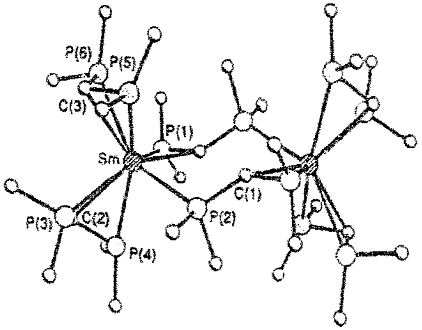

Fig. 6. Molecular structure of $[Sm\{CH(PMe_2)_2\}_3]_2$.

$[Cr\{Ph_2PC(H)PPh_2\}_2](\mu\text{-}Cl)[\mu\text{-}C(H)(PPh_2)_2][Cr\{Ph_2PC(H)PPh_2\}]$ and $Sm[\eta^3\text{-}Ph_2PC(H)PPh_2]_2$. The samarium complex was obtained by the reaction of $[LiCH(PPh_2)_2]$ with $SmCl_3(THF)_3$ in THF. $Sm[\eta^3\text{-}Ph_2PC(H)PPh_2]_2$ is monomeric with the Sm atom nine-coordinated by three identical diphosphinomethanide ligands (Fig. 7). The Sm–C and Sm–P distances range from 2.720(9) to 2.787(9) Å and from 2.818(3) to 2.903 Å respectively.

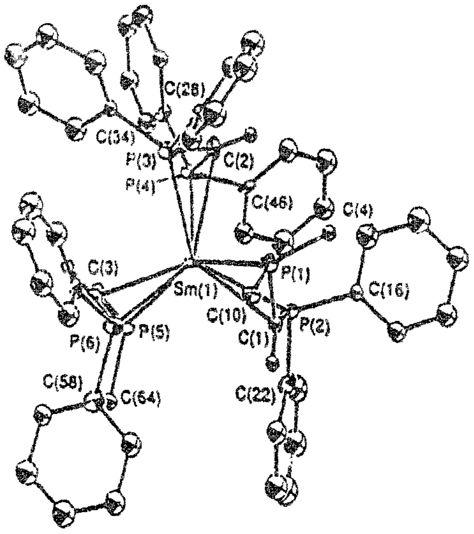

Fig. 7. Molecular structure of $Sm[\eta^3\text{-}Ph_2PC(H)PPh_2]_2$.

2.1.3. *Alkoxides and aryloxides*

Barnhart et al. [11] reported the synthesis, properties, and X-ray structures of several lanthanide arene-bridged aryloxide dimers. The reaction of 2,6-diisopropylphenol with the monomeric amides $Ln[N(SiMe_3)_2]_3$ ($Ln = Nd$, Sm, Er) in toluene under reflux gave the tris(aryloxide) complexes $Ln_2(O\text{-}2,6\text{-}i\text{-}Pr_2C_6H_3)_6$.

$$2Ln[N(SiMe_3)_2]_3 + 6HOAr \xrightarrow[\text{reflux}]{\text{toluene}} Ln_2(OAr)_6 + 6HN(SiMe_3)_2$$

The addition of a Lewis base such as THF to a benzene solution of $Ln_2(OAr)_6$ led to the cleavage of the dimeric unit and formation of monomeric THF bis-adducts $Ln(O\text{-}2,6\text{-}i\text{-}Pr_2C_6H_3)_3(THF)_2$.

$$Ln_2(OAr)_6 + 4THF \xrightarrow{\text{toluene}} 2Ln(OAr)_3(THF)_2$$

$$Ln = Nd, Sm, Er; Ar = 2,6\text{-}i\text{-}Pr_2C_6H_3$$

The bis(THF)adduct of lutetium $Lu(O\text{-}2,6\text{-}i\text{-}Pr_2C_6H_3)_3(THF)_2$ was prepared by the interaction of $Lu[N(SiMe_3)_2]_3$ with three equivalents of 2,6-diisopropylphenol in refluxing toluene in the presence of THF.

$$Lu[N(SiMe_3)_2]_3 + 3HOAr \xrightarrow[\text{reflux}]{\text{toluene/THF}} Lu(OAr)_3(THF)_2 + 3HN(SiMe_3)_2$$

$$Ar = 2,6\text{-i-}Pr_2C_6H_3$$

The reaction of anhydrous $LnCl_3$ (Ln = Sm, Pr, Gd and Yb) with KO-2,6-i-$Pr_2C_6H_3$ in THF also gave the bis(THF) adducts Ln(O-2,6-i-$Pr_2C_6H_3)_3(THF)_2$:

$$LnCl_3 + 3KOAr \xrightarrow{\text{THF}} Ln(OAr)_3(THF)_2 + 3KCl$$

$$Ln = Sm, Pr, Gd \text{ and } Yb;\ Ar = 2,6\text{-i-}Pr_2C_6H_3$$

Six lanthanide complexes containing 2,6-diisopropylphenoxide ligation have been examined by single-crystal X-ray diffraction techniques: $Ln_2(OAr)_6$ (Ln = Nd, Sm) and $Ln(OAr)_3(THF)_2$ (Ln = Er, Lu, Pr, Gd) (Ar = 2,6-i-$Pr_2C_6H_3$). The molecules of $Ln_2(OAr)_6$ contain centrosymmetric, dimeric $Ln_2(O\text{-}2,6\text{-i-}Pr_2C_6H_3)_6$ units bridged by intermolecular η^6-π-arene interactions of a unique aryloxide ligand (Fig. 8). The coordination geometry of each lanthanide atom approximates a three-legged piano stool. Each metal is bound to three terminal aryloxide oxygen atoms, and six carbon atoms of one of the aromatic rings of an aryloxide ligand are bound to the symmetry-related metal atom in the dimeric unit.

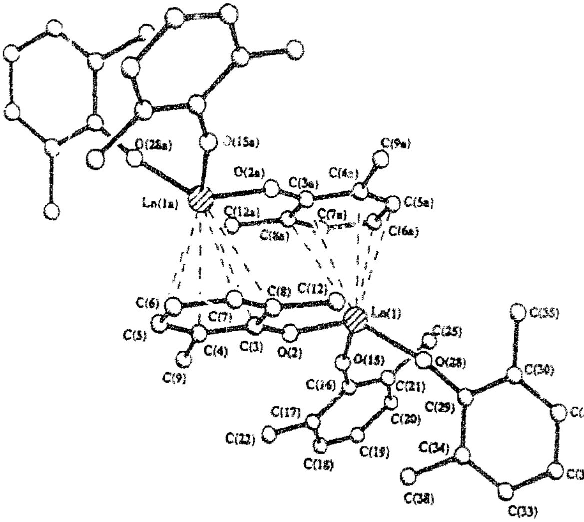

Fig. 8. Molecular structure of $Ln_2(OAr)_6$ (Ln = Nd, Sm).

Previously known 4f-element–π-arene complexes display the three basic structural types exemplified by $[(\eta\text{-arene})Ln(AlCl_4)_3]_x$ (**I**), $Yb(O\text{-}2,6\text{-}Ph_2C_6H_3)_3$ (**II**) and $(\eta\text{-arene})_2Gd$ (**III**) (Fig. 9). The π-arene-dimers $Ln_2(OAr)_6$ (Ln = Nd, Sm) represent a new structural type for 4f-element–π-arene complexes (**IV**).

The four bisadducts $Ln(O\text{-}2,6\text{-}i\text{-}Pr_2C_6H_3)_3(THF)_2$ (Ln = Er, Lu, Pr, Gd) are isostructural. The molecular structure consists of a lanthanide metal centre coordinated in a distorted trigonal bipyramidal fashion by three equatorial aryloxide and two axial THF ligands (Fig. 10).

Biagini et al. [12] described a series of new mixed-bridged alkyl–alkoxy lanthanide complexes. The complexes $[Ln(\mu\text{-}O^tBu)_3(\mu\text{-}Me)_3(AlMe_2)_3]$ (Ln = Pr, Nd, Y) were obtained from the reaction of $AlMe_3$ with $Ln(O^tBu)_3$ in toluene.

$$Ln(O^tBu)_3 + 3AlMe_3 \rightarrow [Ln(\mu\text{-}O^tBu)_3(\mu\text{-}Me)_3(AlMe_2)_3]$$

$$(Ln = Pr, Nd, Y)$$

The complex $[Nd(\mu\text{-}O^tBu)_3(\mu\text{-}Me)_3(AlMe_2)_3]$ was characterized by single-crystal X-ray diffraction. In the structure (Fig. 11) the Nd atom is bonded to three crystallographically equivalent moieties ((μ-O^tBu), (μ-Me), ($AlMe_2$)) giving rise to a highly

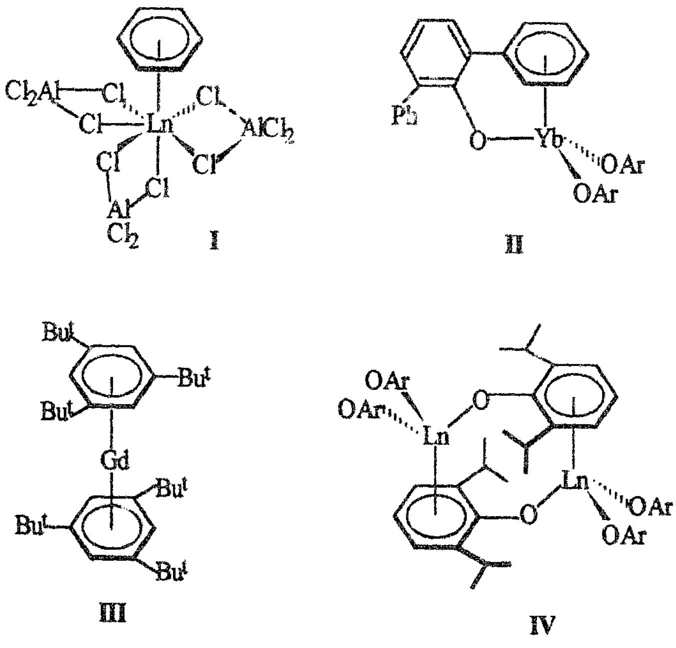

Fig. 9. Basic structural types of 4f-element–π-arene complexes.

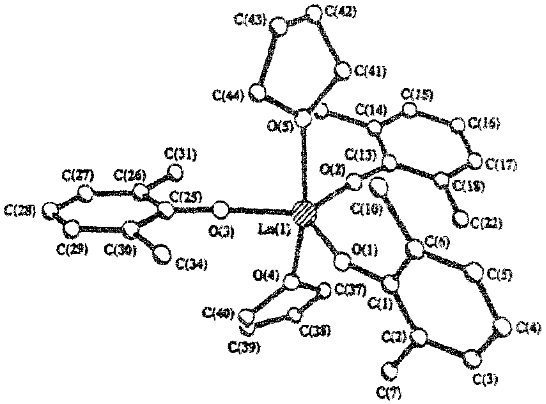

Fig. 10. Molecular structure of $Ln(O\text{-}2,6\text{-}i\text{-}Pr_2C_6H_3)_3(THF)_2$ (Ln = Er, Lu, Pr, Gd).

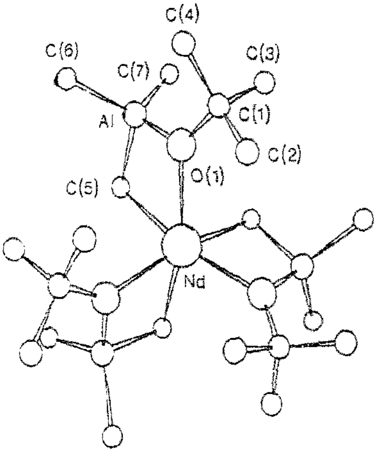

Fig. 11. Molecular structure of $[Nd(\mu\text{-}O^tBu)_3(\mu\text{-}Me)_3(AlMe_2)_3]$.

distorted octahedral coordination. The distances Nd–O(1) and Nd–C(5) are 2.303(7) Å and 2.784(11) Å respectively.

Greeves et al. [13] investigated the diastereoselective addition of organocerium reagents to aldehydes and cyclic ketones. The organocerium reagents were prepared according to Scheme 4.

The reagents were used in the reaction with the Cram's original aldehyde (Scheme 5) and with various cyclohexanones (Scheme 6).

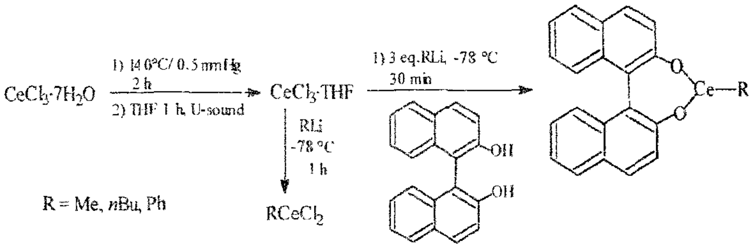

Scheme 4.

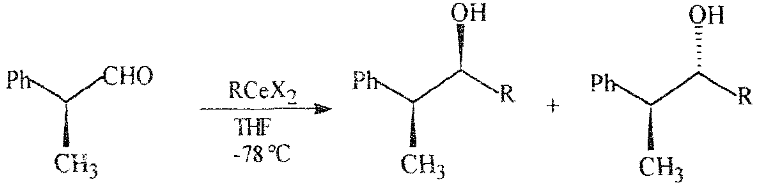

Scheme 5.

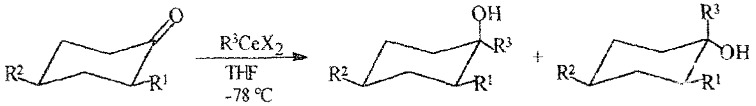

Scheme 6.

The diastereoselectivity of these chiral dialkoxy- and diaryloxyorganocerium reagents in the reactions was compared with that of conventional organocerium reagents.

2.1.4. Fullerenes

Capp et al. [14] reported an improved high-pressure toluene extraction of the lanthanum-containing fullerenes La@C_n for even n from 74 to 90. La@C_n was coaxed from the prewashed soot with a high-pressure, high-temperature extraction technique which could be called a 'bomb' extraction. Analysis of the toluene extract of the lanthanum bomb soot was accomplished by laser desorption Fourier transform ion cyclotron resonance mass spectrometry (LD/FT/ICR/MS). The positive ion mass spectrum was dominated by La@C_{82}^+ but also showed other La@C_n^+, including $n=74$, 76, 78, 80, 84, 86, 88 and 90. Analysis of peak intensities suggested that, by mass, the material was 20% La@C_n and 11% La@C_{82}. The average size of an empty fullerene in the sample was 100.9 carbon atoms.

2.2. Cyclopentadienyl complexes

2.2.1. Mono(cyclopentadienyl) complexes

Zhou et al. [15] reported the synthesis and structure of $CpYCl_2(THF)_3$ ($Cp = C_5H_5$). The complex was obtained by reaction of YCl_3 with one equivalent of sodium cyclopentadienyl in THF. The complex $CpYCl_2(THF)_3$ is monomeric with the central metal Y coordinated by one Cp, three oxygen atoms from three THF molecules, and two chlorine atoms to form a distorted octahedral geometry. The average Y–C(Cp) bond is 2.65(3) Å. The Y–Cl bond lengths are 2.630(8) Å and 2.625(7) Å respectively. The complex is isostructural with known organolanthanide derivatives of Nd, Gd, Ho, Er and Yb.

Depaoli et al. [16] reported the crystal structure of $CpEuCl_2(THF)_3$ (Fig. 12). The structure has a nonaxial symmetry about the Eu(III) ion in agreement with the observed asymmetry parameter of 0.46.

Evans et al. [17] published the synthesis and characterization of the pentamethylcyclopentadienyl complex of trivalent europium $[(C_5Me_5)Eu(OCMe_3)(\mu\text{-}OCMe_3)]_2$.

$$EuCl_3 + 2NaOCMe_3 \xrightarrow[\text{24 h, } -NaCl]{\text{THF}} \text{“}Eu_3(OCMe_3)_7Cl_2(THF)_2\text{”}$$

$$\text{“}Eu_3(OCMe_3)_7Cl_2(THF)_2\text{”} + 3KC_5Me_5 \xrightarrow[\text{18 h}]{\text{toluene}}$$

$$[(C_5Me_5)Eu(OCMe_3)(\mu\text{-}OCMe_3)]_2$$

The complex is dimeric (Fig. 13). The plane formed by two europium atoms and the two oxygen atoms of the bridging ligands is perpendicular to the plane formed by the two C_5Me_5 ring centroids and the oxygen atoms from the terminal $OCMe_3$ groups.

Edelmann and coworkers [18] reported the synthesis and structure of the $[(C_5Me_5)Sm\{S_2P(OMe)_2\}_2]_2$. The complex was obtained by the reaction of $(C_5Me_5)_2Sm(THF)_2$ with the $[(MeO)_2P(S)S]_2$.

$$2(C_5Me_5)_2Sm(THF)_2 + [(MeO)_2P(S)S]_2[(C_5Me_5)Sm\{S_2P(OMe)_2\}_2]_2$$

The structure of the complex is dimeric with triply bridging *O,O′*-dimethyldithiophosphate ligands in which one of the methoxy groups is involved in the coordination to samarium (Fig. 14). The samarium atom has a formal coordination number of nine. The Sm–S bond distances range from 290.9(2) to 304.7(2) Å.

Bercaw and coworkers [19] investigated the model Ziegler–Natta σ-olefin polymerization catalysts derived from $[\{(\eta^5\text{-}C_5Me_4)SiMe_2(\eta^1\text{-}NCMe_3)\}(PMe_3)Sc(\mu_2\text{-}H)]_2$ and $[\{(\eta^5\text{-}C_5Me_4)SiMe_2(\eta^1\text{-}NCMe_3)\}Sc(\mu_2\text{-}CH_2CH_2CH_3)]_2$. The scandium hydride complex $[(Cp^*SiNR)(PMe_3)Sc(\mu_2\text{-}H)]_2$ ($(Cp^*SiNR) = (\eta^5\text{-}C_5Me_4)SiMe_2(\eta^1\text{-}NCMe_3)$) was obtained by hydrogenation of $(Cp^*SiNR)ScCH(SiMe_3)_2$ in the presence of PMe_3. The reaction (Scheme 7) of the complex with two equivalents of ethylene leads to the ethylene-bridged scandium

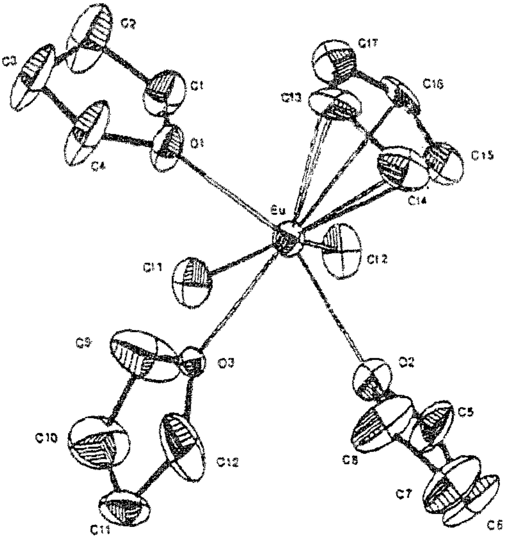

Fig. 12. Molecular structure of $CpEuCl_2(THF)_3$.

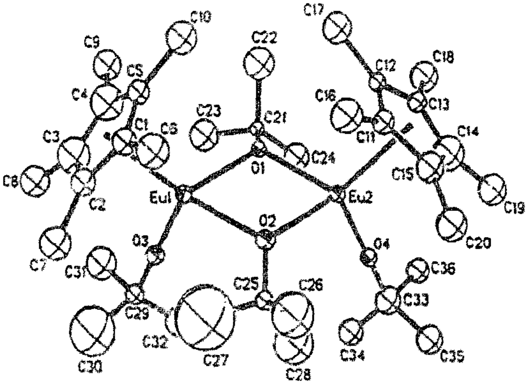

Fig. 13. Molecular structure of $[(C_5Me_5)Eu(OCMe_3)(\mu\text{-}OCMe_3)]_2$.

dimer $(\mu,\eta^2,\eta^2\text{-}C_2H_4)[(Cp^*SiNR)(PMe_3)Sc]_2$. In the structure of $(\mu,\eta^2,\eta^2\text{-}C_2H_4)[(Cp^*SiNR)(PMe_3)Sc]_2$ (Fig. 15) the $Sc_2(\mu,\eta^2,\eta^2\text{-}C_2H_4)$ core is the most unusual feature. The C–C bond length of the ethylene bridge (1.433(12) Å) is

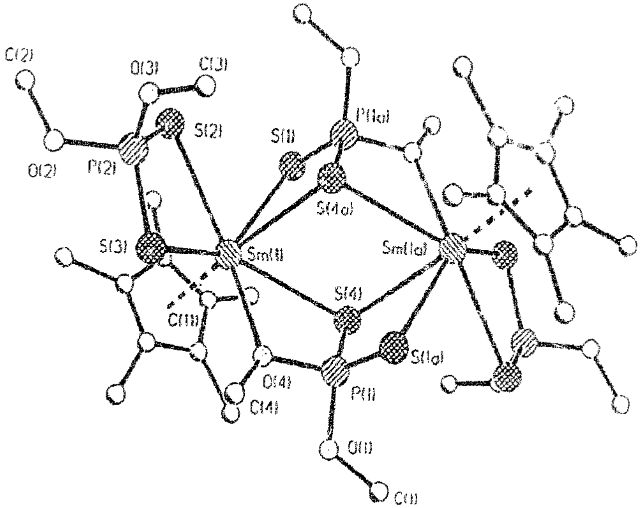

Fig. 14. Molecular structure of $[(C_5Me_5)Sm\{S_2P(OMe)_2\}_2]_2$.

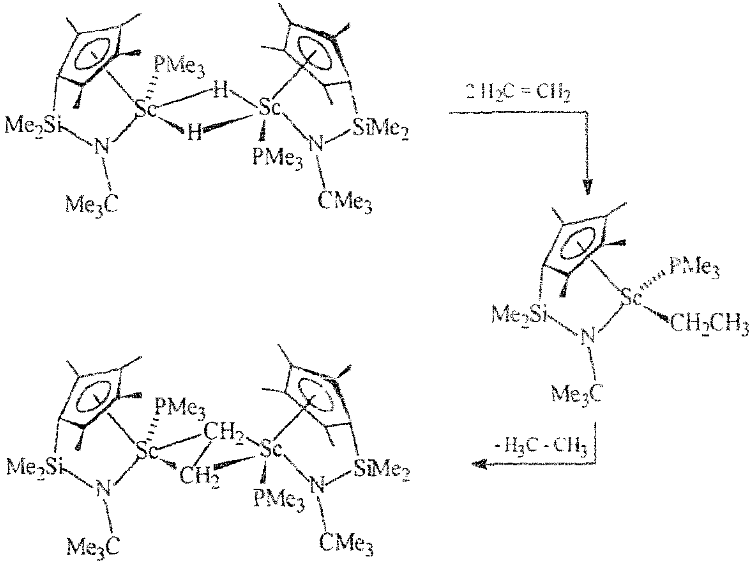

Scheme 7.

intermediate between that of a single and double C–C bond, comparable with the bond lengths observed in transition metal olefin complexes.

Reaction of $[(Cp^*SiNR)(PMe_3)Sc(\mu_2\text{-}H)]_2$ with one equivalent of propylene per scandium gave the PMe_3-free scandium propyl derivative $(\mu\text{-}CH_2CH_2CH_3)_2[(Cp^*SiNR)Sc]_2$ (Scheme 8).

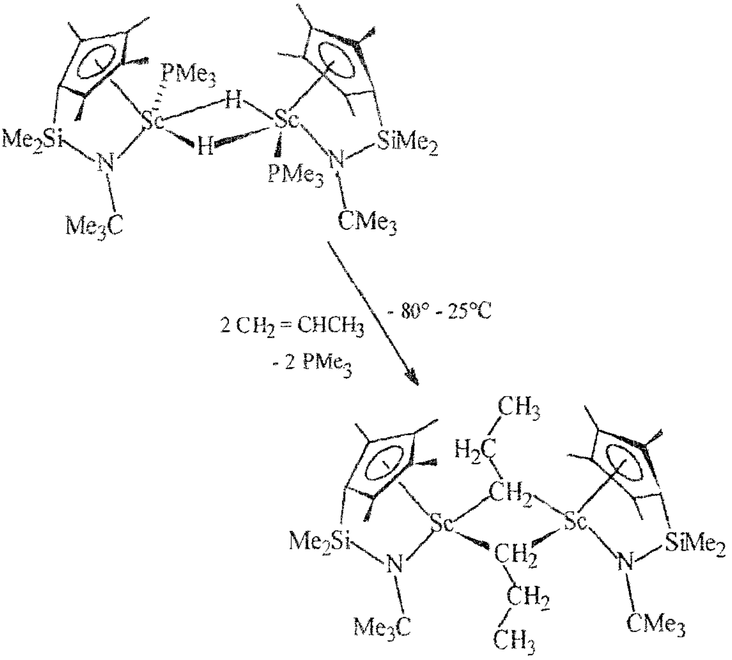

Scheme 8.

According to the X ray structure analysis, the complex $(\mu\text{-}CH_2CH_2CH_3)_2[(Cp^*SiNR)Sc]_2$ is a dimer with a three-centre, two-electron propyl-bridged core, $[Sc_2(\mu\text{-}CH_2CH_2CH_3)_2]$. The Sc–C–Sc bridge angle of 89.4(2)° is considerably more acute than the corresponding Sc–H–Sc angle (114.1°) in the $[(Cp^*SiNR)(PMe_3)Sc(\mu_2\text{-}H)]_2$. Bulkier alkyl ligands such as 2-methylpentyl and isobutyl do not form stable μ-alkyl bridges, as they readily and more competitively retain PMe_3 in their coordination sphere. Reaction of $[(Cp^*SiNR)(PMe_3)Sc(\mu_2\text{-}H)]_2$ with styrene led to a double-insertion product (Scheme 9) arising from sequential 1,2- and 2,1-styrene insertion.

The dimeric PMe_3-free alkyl complexes such as $(\mu\text{-}CH_2CH_2CH_3)_2$-$[(Cp^*SiNR)Sc]_2$ are considerably more active catalyst precursors for α-olefin polymerization than the $[(Cp^*SiNR)(PMe_3)Sc(\mu_2\text{-}H)]_2$.

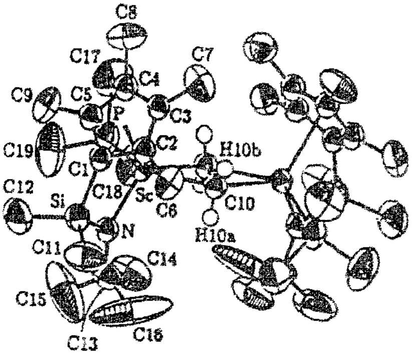

Fig. 15. Molecular structure of (μ-η^2,η^2-C_2H_4)[(Cp*SiNR)(PMe_3)Sc]$_2$.

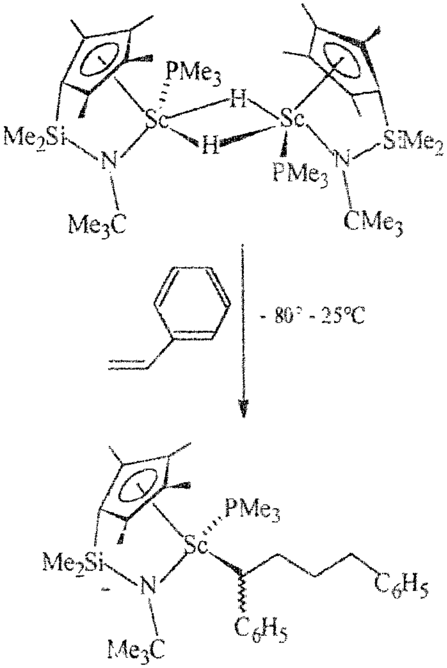

Scheme 9.

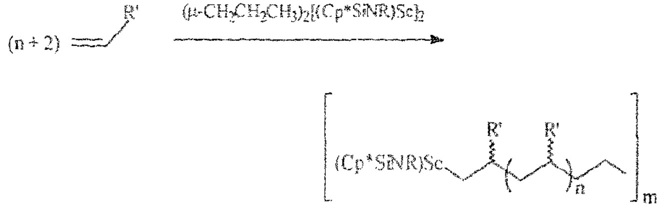

(R' = CH_3, CH_2CH_3, $CH_2CH_2CH_3$)

The kinetic analysis of 1-pentene polymerization catalysed by the above mentioned complexes has been discussed.

Shen et al. [20] reported the synthesis of new organolanthanide complexes $[CpLnLL']_2$ ($Cp = C_5H_5$; Ln = Gd, Tb, Dy, Ho, Er, Tm, Yb; HL = benzophenoneoxime; HL' = 8 – quinolinol) from Cp_3Ln in THF.

$$2Cp_3Ln + 2HL + 2HL' \xrightarrow[\text{reflux}]{\text{THF}} [CpLnLL']_2 + 2C_5H_6$$

$$L = (C_6H_5)_2CNO,\ L' = 8 - C_6H_7{:}CHCH{:}CH$$

The complexes have been characterized by elemental analyses, IR and MS spectroscopy. According to the data the complexes were considered to be oxo-bridged dimers.

Schaverien [21,22] published the synthesis of, reactivity of, and olefin polymerization by the μ-hydride–μ-alkyl compounds $[Y(C_5Me_5)(OC_6H_3^tBu_2)]_2(\mu\text{-H})(\mu\text{-alkyl})$. The hydrogenation of $Y(C_5Me_5)(OAr)CH(SiMe_3)_2$ in hexane under 10 bar of H_2 yielded $[Y(C_5Me_5)(OAr)(\mu\text{-H})]_2$ (Scheme 10). The latter reacted with terminal olefins $H_2C{=}CHR$ (R = H, Me, Et, *n*-Bu) to form the μ-*n*-alkyl complexes *trans*-$[Y(C_5Me_5)(OAr)]_2(\mu\text{-H})(\mu\text{-}CH_2CH_2R)$ (Scheme 11). The compounds polymerize α-olefins and dienes. The reaction of $[Y(C_5Me_5)(OAr)(\mu\text{-H})]_2$ with the terminal acetylene $HC{\equiv}CSiMe_3$ led to the acetylide derivative $[Y(C_5Me_5)(OAr)]_2(\mu\text{-H})(\mu\text{-}C{\equiv}CSiMe_3)$. Further treatment with excess of $HC{\equiv}CSiMe_3$ in the presence of THF gave the monomeric acetylide $Y(C_5Me_5)(OAr)C{\equiv}CSiMe_3(THF)_2$ (Scheme 12).

The methyl derivatives $[Y(C_5Me_5)(OAr)(\mu\text{-Me})]_2$ and $[Y(C_5Me_5)(\mu\text{-Me})_2]_3$ were prepared by the reactions of $Y(C_5Me_5)(OAr)_2$ with MeLi (one equivalent and 1.6 equivalents respectively). Cleavage of the derivatives $[Y(C_5Me_5)(OAr)(\mu\text{-Me})]_2$ by THF led to $Y(C_5Me_5)(OAr)(Me)(THF)_2$.

The synthesis and crystal structure of $[Li(THF)_4][(^tBuCp)Yb(NPh_2)_3]$ were described by Mao et al. [23]. The complex was synthesized from the t-butylcyclopentadienyl ytterbium dichloride and three equivalents of $LiNPh_2$.

$$(^tBuCp)YbCl_2 + 3LiNPh_2 \xrightarrow[-78\ ^\circ C]{\text{THF–hexane–toluene}} [Li(THF)_4][(^tBuCp)Yb(NPh_2)_3] + 2LiCl$$

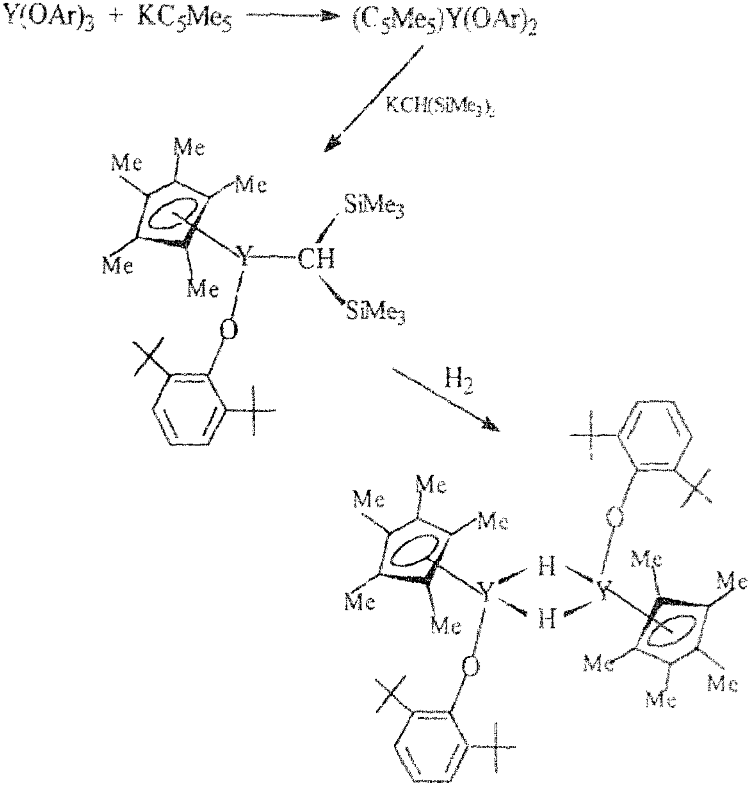

Scheme 10.

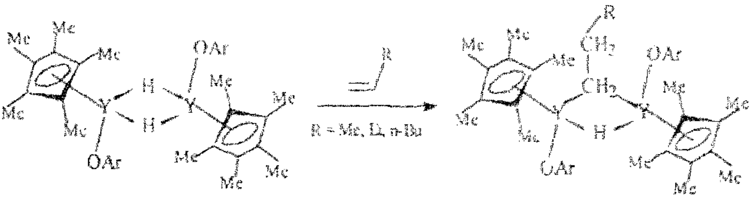

Scheme 11.

The complex consists of isolated ion pairs $[Li(THF)_4]^+$ and $[(^tBuCp)Yb(NPh_2)_3]^-$ (Fig. 16). In the anion, the central Yb atom is surrounded by one ^tBuCp and three diphenylamino groups to form a distorted tetrahedron. The

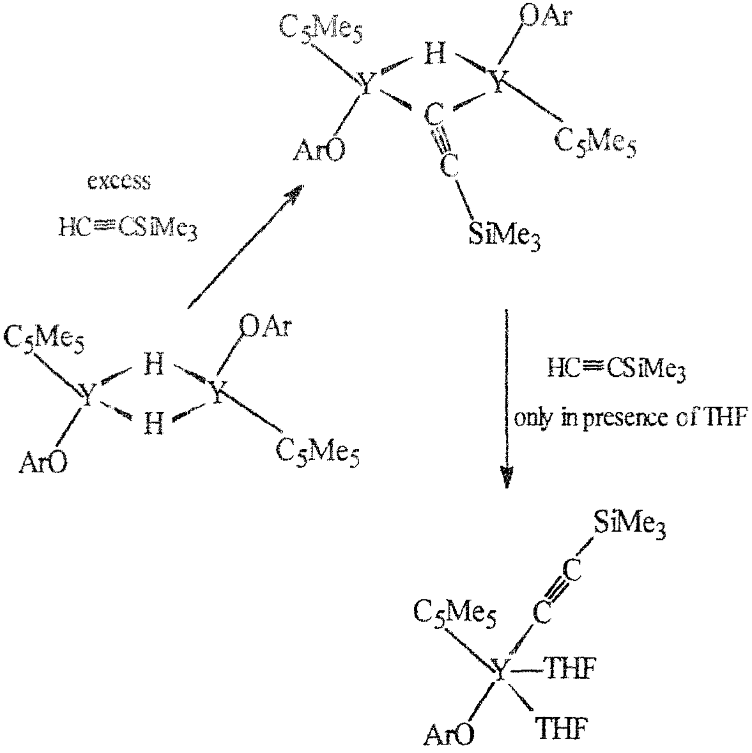

Scheme 12.

average Yb–N distance is 2.264(9) Å. In the cation the lithium is coordinated by four oxygen atoms from four THF molecules, forming a tetrahedral structure with average Li–O distances of 1.935(31) Å.

Taube and Windisch [24] reported the preparation of the monocyclopentadienyl tris(allyl)lanthanate(III) complexes $[Li(C_4H_8O_2)][\eta^5\text{-}Cp'La(\eta^3\text{-}C_3H_5)_3]$ ($Cp'=C_5H_5$, C_5Me_5, C_9H_7, $C_{13}H_9$) by partial protolysis of the $[Li(C_4H_8O_2)_{3/2}][La(\eta^3\text{-}C_3H_5)_4]$ with one equivalent of the corresponding HCp′

$$[Li(C_4H_8O_2)_{3/2}][La(C_3H_5)_4]+HCp' \xrightarrow[2.\ Et_2O\text{-dioxane}]{1.\ THF}$$

$$[Li(C_4H_8O_2)_2][Cp'La(C_3H_5)_3]+C_3H_6$$

2.2.2. *Bis(cyclopentadienyl) complexes*

Shen and Xie [25] prepared seven new organolanthanide complexes ($Cp_4Ln_2L_1L_2$) (Ln = Gd, Tb, Dy, Ho, Er, Tm, Yb; $Cp=C_5H_5$) from Cp_3Ln and

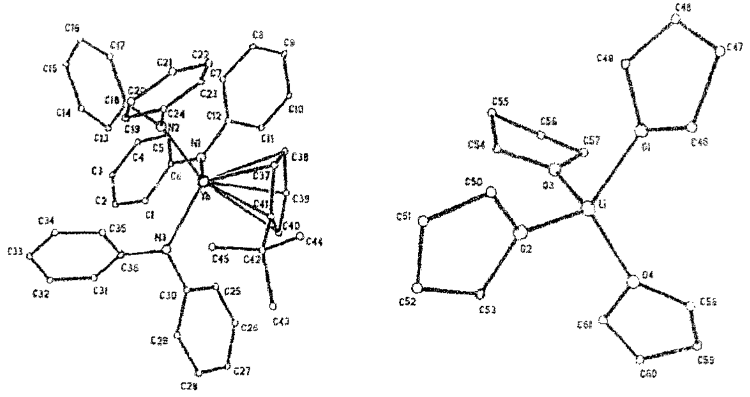

Fig. 16. Molecular structure of [Li(THF)$_4$][(^{t}BuCp)Yb(NPh$_2$)$_3$].

benzophenoneoxime (HL $_1$) or cyclohexanoneoxime (HL $_2$) in THF. The compounds were characterized by elemental analyses, IR and MS spectra. According to the data these complexes were found to be dimers with oxo-bridged bonds.

$$\mathrm{HL}_1 + \mathrm{HL}_2 + 2\mathrm{Cp_3Ln} \xrightarrow[\text{reflux}]{\text{THF}} (\mathrm{Cp_4Ln_2L_1L_2}) + 2\mathrm{C_5H_6}$$

Wu et al. [26] published the synthesis and X-ray crystal structure of bis[acetoneoximatobis(cyclopentadienyl)gadolinium] [Cp$_2$Gd(μ-η^2-ONCMe$_2$)]$_2$. The complex was obtained by the reaction of Cp$_3$Gd with acetone oxime (HONCMe$_2$) in THF. According to the X-ray structure the molecule is asymmetric with the O–N fragment of the oximato-group acting as both a bridging and side-on donating ligand (Fig. 17). The Gd atom has a distorted trigonal-bipyramidal geometry with oxygen and nitrogen atoms in an axial position. The Gd$_2$N$_2$ unit forms a near-parallelogram which contains the rhombic quadrilateral unit Gd$_2$O$_2$. The average Gd–C(Cp) distance is 2.68(2) Å, the Gd–O bond distances range from 2.25(1) to 2.38(1) Å.

Wang et al. [27] reported the synthesis of [Cp$_2$Sm(η^5-C$_6$H$_5$)(THF)] by the reaction of Cp$_2$SmCl with sodium allyloxypropynylide in THF.

$$\mathrm{Cp_2SmCl} + \mathrm{NaC{\equiv}CCH_2OCH_2CH{=}CH_2} \xrightarrow{\text{THF}} [\mathrm{Cp_2Sm}(\eta^5\text{-}\mathrm{C_6H_5})(\mathrm{THF})]$$

According to the X-ray structure the Sm atom in the complex [Cp$_2$Sm(η^5-C$_6$H$_5$)(THF)] has a tetrahedral arrangement (Fig. 18). The ligand η^5-C$_6$H$_5$ is the anionic form of cyclohexen-4-yne. The Sm–X(1c) distance is 2.500 Å (X(1c) represents the plane formed by C(16), C(17), C(18), C(19) and C(20)).

Deacon et al. [28] investigated the regiospecific replacement of fluorine by hydrogen in an aromatic ring induced by YbCp$_2$(dme). The reaction of pentafluorobenzoic acid with Cp$_2$Yb(dme) gave, after hydrolysis, the 2,3,4,5-tetrafluorobenzoic acid.

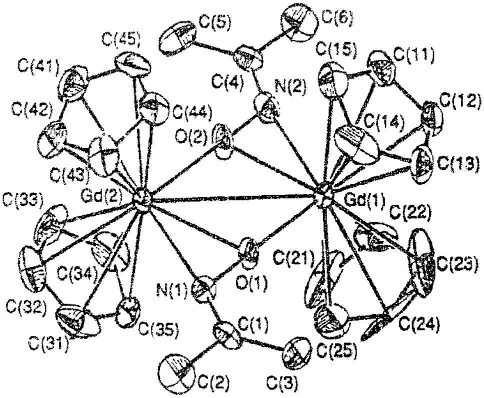

Fig. 17. Molecular structure of $[Cp_2Gd(\mu-\eta^2-ONCMe_2)]_2$.

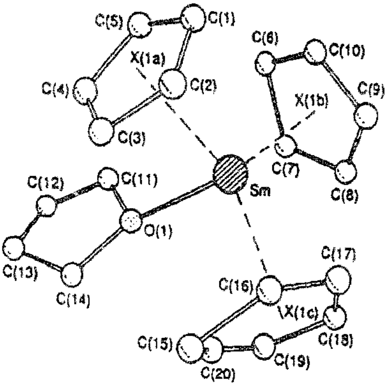

Fig. 18. Molecular structure of $[Cp_2Sm(\eta^5-C_6H_5)(THF)]$.

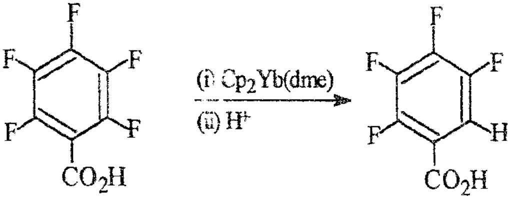

The effects of coreductants Zn, Yb, Mg and activated (by I_2) magnesium were investigated. With activated magnesium as coreductant, near quantitative yields were obtained. The defluorination of *o*-fluorobenzoic and 2,6-difluorobenzoic acid by reaction with $YbCp_2(dme)$, activated magnesium and thallous cyclopentadienide have also been achieved.

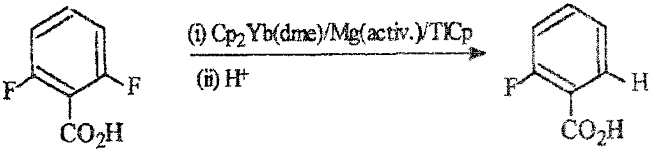

X = H or F

Guan et al. [29] described the synthesis and crystal structure of a bis(cyclopentadienyl)amido complex of neodymium, $[Li(DME)_3][Cp_2Nd(NPh_2)_2]$. The complex was obtained by the reaction of $NdCl_3 \cdot 2LiCl \cdot nTHF$, CpNa and $LiNPh_2$ in THF followed by recrystallization from DME.

$$NdCl_3 \cdot 2LiCl \cdot nTHF + 2CpNa \rightarrow Cp_2NdCl \cdot LiCl \cdot nTHF \xrightarrow{2LiNPh_2}$$

$$[Li(DME)_3][Cp_2Nd(NPh_2)_2] + 2LiCl$$

According to the X-ray structure the complex consists of the anion $[Cp_2Nd(NPh_2)_2]^-$ and the cation $[Li(DME)_3]^+$ (Fig. 19). In the anion the Nd atom has a distorted tetrahedral arrangement. The average Nd–Cp distances are 2.783(8), 2.767(9) Å and the Nd–N distance is 2.428(7) Å.

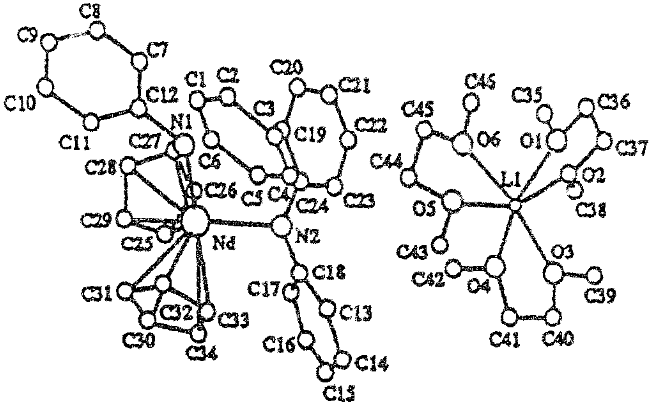

Fig. 19. Molecular structure of $[Li(DME)_3][Cp_2Nd(NPh_2)_2]$.

Qian et al. [30] published the synthesis and X-ray crystal structure of bis[(2-methoxyethyl)cyclopentadienyl)] rare earth metal chlorides. The series of bis[(2-methoxyethyl)cyclopentadienyl)] lanthanide chlorides $(CH_3OCH_2CH_2C_5H_4)_2LnCl$ (Ln = La, Pr, Nd, Sm, Gd, Dy, Ho, Er, Tm, Yb, Lu, Y) were obtained by the reaction of the corresponding $LnCl_3$ with two equivalents of $CH_3OCH_2CH_2C_5H_4Na$.

$$LnCl_3 + 2CH_3OCH_2CH_2C_5H_4Na \rightarrow (CH_3OCH_2CH_2C_5H_4)_2LnCl + 2NaCl$$

All the complexes have been characterized by elemental analyses, MS, IR and NMR spectra. The complexes $(CH_3OCH_2CH_2C_5H_4)_2LnCl$ (Ln = La, Dy, Yb) have also been studied by X-ray diffraction analyses. The structure of $(CH_3OCH_2CH_2C_5H_4)_2LaCl$ is dimeric with two chloride bridges (Fig. 20). Besides two cyclopentadienyl ligands and two chlorine atoms, each lanthanum atom is coordinated by two oxygen atoms from the $CH_3OCH_2CH_2$-groups. The formal coordination number of La is ten and the metal atom has a distorted octahedral arrangement. In contrast, the structures of the Dy and Yb analogues are monomeric. The coordination of the Ln atoms by two Cp-rings, one chlorine atom and two oxygen atoms form distorted trigonal bipyramids. Thus the structures of the complexes depend on the radius of the lanthanide ions.

Qian et al. [31] also reported the syntheses and X-ray crystal structures of bis[(2-methoxyethyl)cyclopentadienyl] rare earth iodides (MeO-

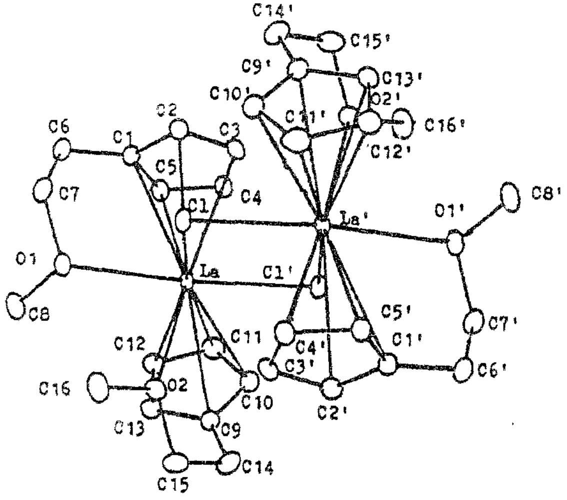

Fig. 20. Molecular structure of $(CH_3OCH_2CH_2-C_5H_4)_2LaCl$.

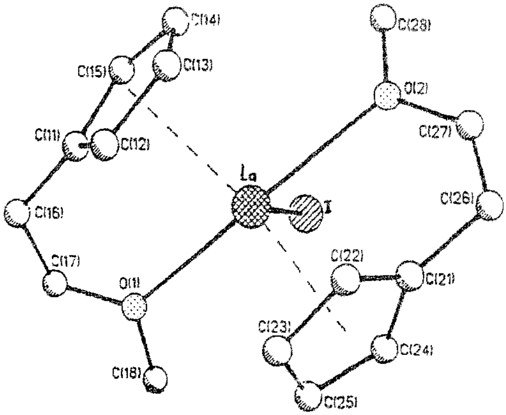

Fig. 21. Molecular structure of $(MeOCH_2CH_2C_5H_4)_2LaI$.

$CH_2CH_2C_5H_4)_2LnI$ (Ln = La or Y). The complexes were obtained according to equation

$$(MeOCH_2CH_2C_5H_4)_2LnCl + NaI \xrightarrow{THF} (MeOCH_2CH_2C_5H_4)_2LnI + NaCl$$

Ln = La, Y

The lanthanum and yttrium complexes are isostructural. In the molecules (Fig. 21) the Ln atom is coordinated by two cyclopentadienyl ligands, one iodine atom and two oxygen atoms. The structure has a trigonal bipyramidal coordination geometry. The most striking feature of these compounds is the formation of the intramolecular coordination bond from the oxygen atom of the ligand to the central rare earth metal.

Zhang et al. [32] prepared the complexes $(C_4H_7OCH_2C_5H_4)_2LnCl$ (Ln = Nd, Gd, Dy, Yb) from the appropriate lanthanide trichlorides and sodium tetrahydrofurfurylcyclopentadienide in THF. The dysprosium derivative $(C_4H_7OCH_2C_5H_4)_2DyCl$ was characterized by X-ray crystallography. The structure has C_2 symmetry about the Dy–Cl axis. The central Dy atom is coordinated by two Cp, two oxygens of tetrahydrofurfuryl and one chlorine to form a distorted trigonal bipyramid. The two oxygen atoms are at both apices, and chlorine, dysprosium and the two Cp-centroids form the equatorial plane.

Deng et al. [33] published the synthesis, spectroscopic and X-ray crystallographic characterization of new early organolanthanide, organoyttrium hydride and organoholmium hydroxide complexes. Bis(2-methoxyethylcyclopentadienyl) hydride complexes of the type $[(MeOCH_2CH_2C_5H_4)_2Ln(\mu\text{-}H)]_2$ (Ln = La, Pr, Ho, Y) were obtained by reaction of the corresponding halide precursors $[(MeOCH_2CH_2C_5H_4)_2Ln(\mu\text{-}Cl)]_2$ with excess NaH in THF.

$$[(MeOCH_2CH_2C_5H_4)_2Ln(\mu\text{-}Cl)]_2 + 2NaH \xrightarrow[-2NaCl]{THF} [(MeOCH_2CH_2C_5H_4)_2Ln(\mu\text{-}H)]_2$$

According to an X-ray structure determination and IR data the complex $[(MeOCH_2CH_2C_5H_4)_2Y(\mu\text{-}H)]_2$ is dimerized via hydrogen-bridges (Fig. 22). In the unit cell there are two dimers which are not identical, but in both dimers each Y atom is coordinated by two cyclopentadienyl ligands, one oxygen from one ether substituent-group and two hydrogen atoms. Thus each Y atom has a distorted trigonal bipyramidal coordination geometry (if the cyclopentadienyl rings are regarded as occupying a single polyhedral vertex). The average lengths of Y–C(Cp) bonds for the two dimers are 2.676, 2.674 Å and 2.674, 2.683 Å.

The product of hydrolysis $[(MeOCH_2CH_2C_5H_4)_2Ho(\mu\text{-}OH)]_2$ of the holmium hydride was also obtained and structurally characterized. The complex forms a dimer with two hydroxyl-bridges. The Ho atom has a distorted trigonal-bipyramidal arrangement with the three oxygen atoms nearly lying in the equatorial plane. The

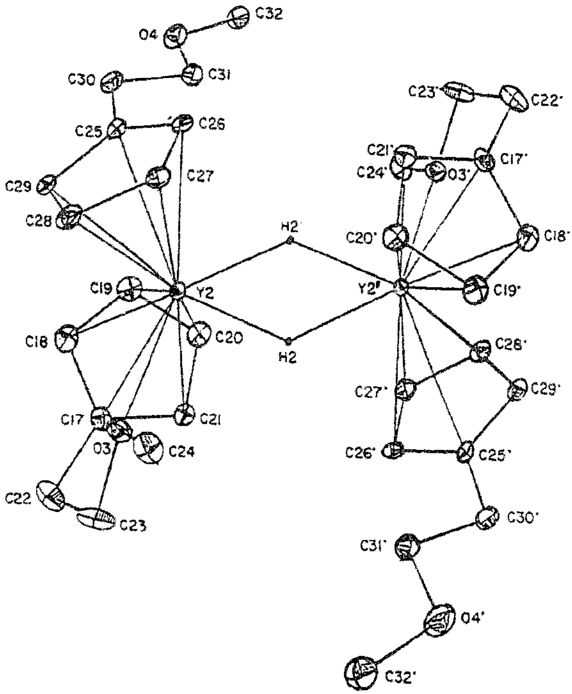

Fig. 22. Molecular structure of $[(MeOCH_2CH_2C_5H_4)_2Y(\mu\text{-}H)]_2$.

average Ho–C(Cp) bonds lengths are 2.694 and 2.711 Å.

$$[(MeOCH_2CH_2C_5H_4)_2Ho(\mu\text{-}H)]_2 \xrightarrow[\text{THF-hexane}]{H_2O} [(MeOCH_2CH_2C_5H_4)_2Ho(\mu\text{-}OH)]_2$$

Deng et al. [34] also described the synthesis of five new bis[(2-methoxyethyl)cyclopentadienyl]lanthanide tetrahydroborates (Ln = La, Pr, Nd, Sm or Gd) from the corresponding $(MeOCH_2CH_2C_5H_4)_2LnCl$ and $NaBH_4$.

$$(MeOCH_2CH_2C_5H_4)_2LnCl + NaBH_4 \xrightarrow{THF} (MeOCH_2CH_2C_5H_4)_2Ln(BH_4) + NaCl$$

Ln = La, Pr, Nd, Sm or Gd

The complexes have been characterized by elemental analyses, MS, ^1H NMR and IR spectra. The praseodymium and neodymium tetrahydroborate complexes have also been structurally characterized. Both complexes are monomeric (Fig. 23) with the metal ions coordinated by two Cp-rings, two $MeOCH_2CH_2$- and one BH_4-groups. Since the hydride ligands cannot be located, the coordination environment about the central metal was difficult to describe. The Pr–B and Nd–B distances are 2.757 Å and 2.664 Å respectively.

The same cyclopentadienyl ligand was used by Deng et al. [35] in the synthesis of organolanthanide complexes $[Ln(C_5H_4CH_2CH_2OMe)_2(THF)][Co(CO)_4]$ (Ln = Sm or Yb, thf = tetrahydrofuran). The complexes were obtained by the reaction of $[Ln(C_5H_4CH_2CH_2OMe)_2I]$ with $K[Co(CO)_4]$ in THF, or by the one-electron

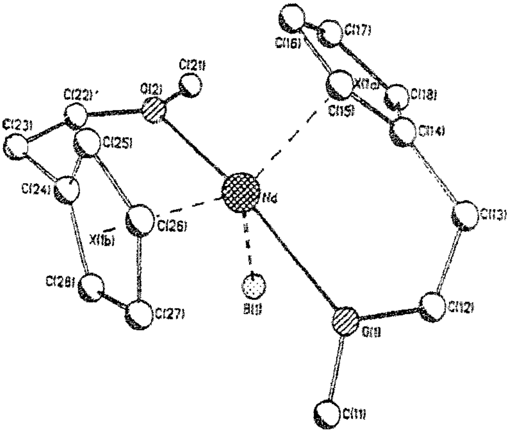

Fig. 23. Molecular structure of $(MeOCH_2CH_2C_5H_4)_2Nd(BH_4)$.

oxidation of $[Ln(C_5H_4CH_2CH_2OMe)_2(THF)]$ with $[Co_2(CO)_8]$ in THF. The X-ray structure of the $[Yb(C_5H_4CH_2CH_2OMe)_2(THF)][Co(CO)_4]$ consists of discrete $[Yb(C_5H_4CH_2CH_2OMe)_2(THF)]^+$ cations and $[Co(CO)_4]^-$ anions. The cation adopts a very distorted trigonal-bipyramidal structure with the two oxygen atoms of the chain on the axis of the trigonal pyramid (Fig. 24). The centroid(1)–Yb–centroid(2) angle is 126.0°, the average Yb–C(ring) bond distance is 2.57(2) Å. The anion has normal distances and angles and is well separated from the cation.

Lin and Wong [36] reported the synthesis and structural characterization of the sodium and ytterbium (diphenylphosphino)cyclopentadienyl complex $[\{(C_6H_5)_2P(\eta^5\text{-}C_5H_4)\}_2Yb(\mu\text{-}Cl)_2Na(C_4H_{10}O_2)_2]$. The complex was obtained from the reaction of anhydrous $YbCl_3$ with $[(C_6H_5)_2P(C_5H_4)Na(C_4H_{10}O_2)]_2$ in THF. The structure (Fig. 25) consists of discrete bimetallic molecules in which $\{(C_6H_5)_2P(\eta^5\text{-}C_5H_4)\}_2Yb$ and Na(DME) fragments are bridged by two Cl^- ligands. The metal geometry of ytterbium and sodium can be described as distorted tetrahedral and distorted octahedral respectively. The Yb–C distances range from 2.611(6) to 2.635(5) Å; the separation between two metal centres is 3.951(1) Å.

Van den Hende et al. [37] published the synthesis and X-ray structures of ytterbocene(II) complexes containing pendant pyridyl groups, $[Yb(Cp^x)_2]$ ($Cp^x = \eta^5\text{-}C_5H_3(R)[CMe_2(CH_2)_nC_5H_4N\text{-}2]\text{-}1,3$; R = H or $SiMe_3$ and $n = 0$ or 1).

$$2KCp^x + YbI_2 \xrightarrow{THF} [Yb(Cp^x)_2]$$

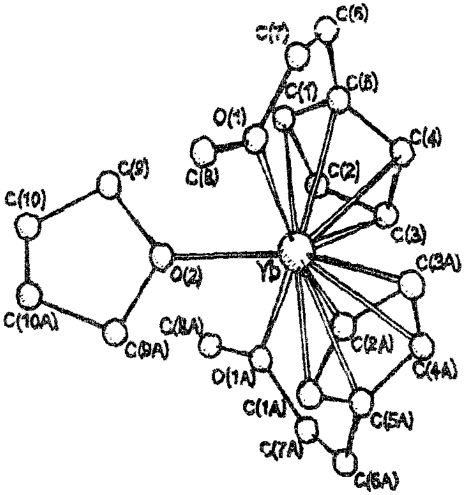

Fig. 24. Structure of cation $[Yb(C_5H_4CH_2CH_2OMe)_2(THF)]^+$.

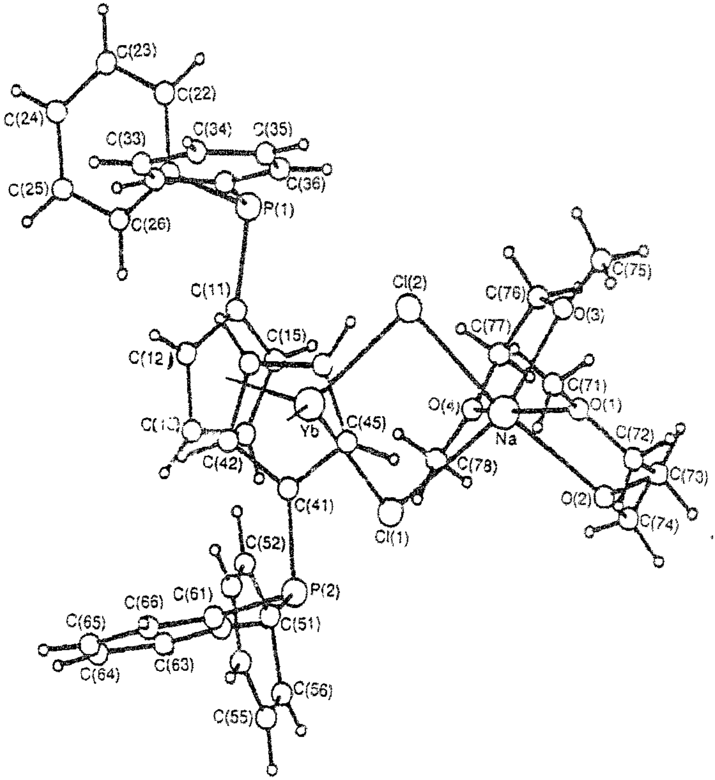

Fig. 25. Molecular structure of $[\{(C_6H_5)_2P(\eta^5\text{-}C_5H_4)\}_2Yb(\mu\text{-}Cl)_2Na(C_4H_{10}O_2)_2]$.

The crystal structures of $[Yb\{\eta\text{-}C_5H_4(CMe_2CH_2C_5H_4N\text{-}2)\}_2]$ (Fig. 26) and $[Yb\{\eta\text{-}C_5H_3(SiMe_3)(CMe_2C_5H_4N\text{-}2)\text{-}1,3\}_2]$ involve a distorted tetrahedral arrangement of the ligands around the metal with the coordination of both the pyridyl groups to the ytterbium.

Beletskaya et al. [38] investigated the reaction of alkyl derivatives of yttrium and lutetium with organic disulphides and diselenides. The series of dimeric bis(t-butylcyclopentadienyl)lanthanide organosulphides or organoselenides $[(^tBuC_5H_4)_2Ln(\mu\text{-}EPh)]_2$ (Ln = Y, E = S, R = Ph, ^{n}Bu, ^{t}Bu or CH_2Ph; Ln = Y, E = Se, R = Ph; Ln = Lu, E = S, R = Ph or CH_2Ph; Ln = Lu, E = Se, R = Ph) were obtained from the appropriate $[(^tBuC_5H_4)_2Ln(\mu\text{-}Me)]_2$ and the corresponding organic disulphides RSSR or diphenylselenide PhSeSePh in benzene.

$$[(^tBuC_5H_4)_2Ln(\mu\text{-}Me)]_2 + 2R_2E_2 \xrightarrow{\text{benzene}} [(^tBuC_5H_4)_2Ln(\mu\text{-}EPh)]_2 + 2MeER$$

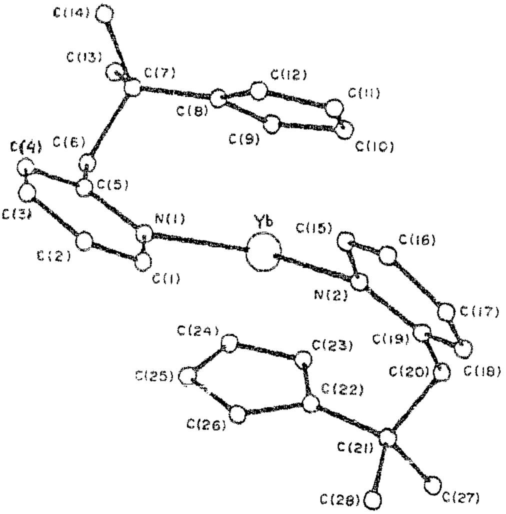

Fig. 26. Molecular structure of $[Yb\{\eta\text{-}C_5H_4(CMe_2CH_2C_5H_4N\text{-}2)\}_2]$.

The structure of $[(^tBuC_5H_4)_2Y(\mu\text{-}SePh)]_2 \cdot C_6H_6$ consists of dimeric molecules with two bridging SePh groups (Fig. 27). The Y_2Se_2 unit is planar, with the Y–Se distances 2.915(1) and 2.912(1) Å. The coordination of the Y atoms is that of a distorted tetrahedron Cp_2YSe_2. Each bridging Se atom is on top of a trigonal pyramid with the two Y atoms and the *ipso*-carbon atom of the phenyl group forming the base.

Piers et al. [39] published the synthesis and study of the permethylscandocene chalcogenolates and chalcogenides. Use of either elemental tellurium or $Te{=}P^nBu_3$ allowed for incorporation of one tellurium atom to form the permethylscandocene tellurolate (Scheme 13). The insertion of elemental selenium into the Sc–C bond of $(C_5Me_5)_2ScCH_2SiMe_3$ gave the analogous selenolate $(C_5Me_5)_2Sc\text{–}SeCH_2SiMe_3$.

The tellurolates are monomeric, as inferred from the X-ray structure of $(C_5Me_5)_2ScTeCH_2C_6H_5$ (Fig. 28). The tellurolate ligand occupies the central position of the metallocene wedge. The ligand features an sp^2-hybridized tellurium atom (Sc–Te–C1 = 121.61(21)°), the Sc–Te bond distance is 2.8337(14) Å.

The reaction of tellurium or selenium with the deuteride $(C_5Me_5)_2ScD$ led to chalcogenide dimers $[(C_5Me_5)_2Sc]_2(\mu\text{-}E)$ (E = Te, Se).

$$(C_5Me_5)_2Sc\text{–}D \xrightarrow[\text{hexane}-D_2]{E\,(0.5\text{ equiv})} (C_5Me_5)_2Sc\text{–}E\text{–}Sc(C_5Me_5)_2$$

$$E = Te, Se$$

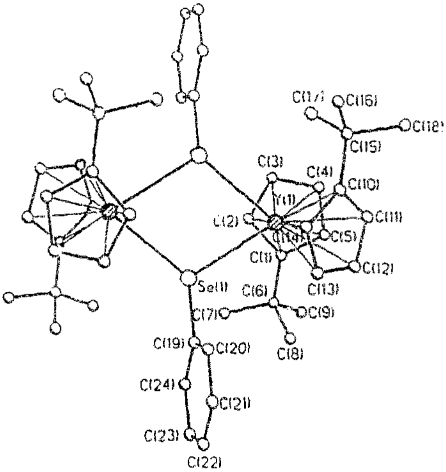

Fig. 27. Molecular structure of $[(^tBuC_5H_4)_2Y(\mu\text{-}SePh)]_2 \cdot C_6H_6$.

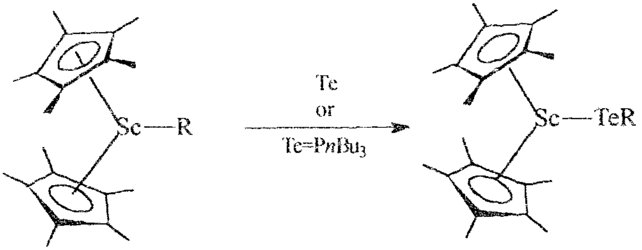

R = $-CH_2SiMe_3$, $-CH_2C_6H_5$, *erythro*-$CH(D)CH(D)\text{-}tC_4H_9$,

$-CH_2CH(D)(CH_2)_2CH{=}CMe_2$, $-C_6H_5$, $-CH_2(c\text{-}C_5H_9)$

Scheme 13.

The telluride dimer $[(C_5Me_5)_2Sc]_2(\mu\text{-}Te)$ was also obtained by the thermal or photochemical extrusion of TeR_2 from the tellurolates $(C_5Me_5)_2ScTeR$. According to X-ray structures the complexes $[(C_5Me_5)_2Sc]_2(\mu\text{-}E)$ are μ-chalcogenide dimers with a slightly distorted D_{2d} symmetry (Fig. 29). The Sc–E bond distances are 2.5425(16) Å for E=Se and 2.7528(12) Å for E=Te; the Sc–E–Sc bridges are nearly linear.

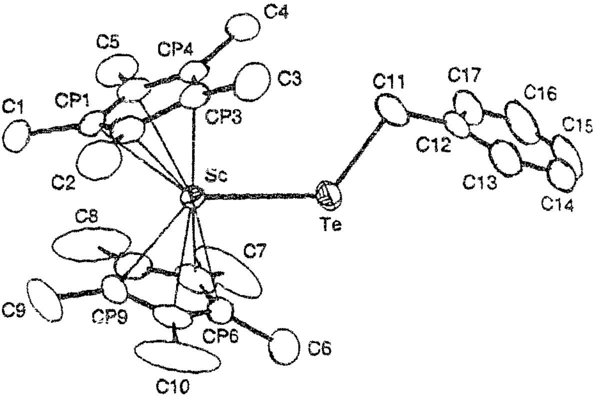

Fig. 28. Molecular structure of $(C_5Me_5)_2ScTeCH_2C_6H_5$.

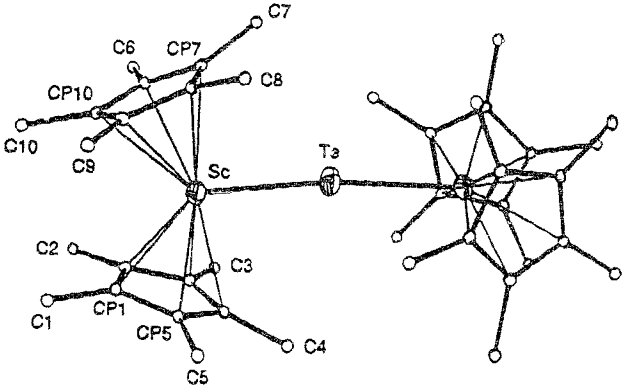

Fig. 29. Molecular structure of $[(C_5Me_5)_2Sc]_2(\mu\text{-}Te)$.

Thermal and photochemical interconversion of the permethylscandocene tellurolates have been studied with a variety of mechanistic experiments (Scheme 14). Experiments utilizing tellurolates indicated that both the thermal and photochemical eliminations of TeR_2 proceeded from a transition state without involving Te–C bond cleavage, leading to $R^{\cdot}$ intermediates.

Using the 1,2-$[^2H_2]$-neohexyl stereochemical probes, Piers [40] has also demonstrated that the extrusion of TeR_2 from permethylscandocene tellurolates proceeds via a concerted transition state (Scheme 15).

Evans et al. [41] described the syntheses and study of the series of organosamar-

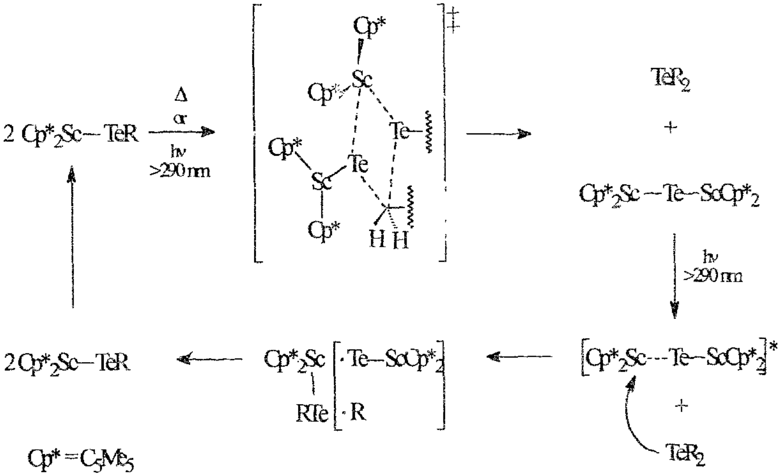

Scheme 14.

ium complexes with Group 16 element anions: $[(C_5Me_5)_2Sm(THF)]_2(\mu\text{-}E)$, $[(C_5Me_5)_2Sm]_2(E_3)(THF)$ (E = S, Se, Te), $[(C_5Me_5)_2Sm]_2(\mu\text{-}\eta^2{:}\eta^2\text{-}Te_2)$ and mixed chalcogenide complexes $[(C_5Me_5)_2Sm]_2(E_aE_b')(THF)$ $(a+b=3)$.

$$2(C_5Me_5)_2Sm(THF)_2 + (1/x)E_x \rightarrow [(C_5Me_5)_2Sm(THF)]_2(\mu\text{-}E)$$

E = Se, Te

$$2(C_5Me_5)_2Sm(THF)_2 + Ph_3P{=}E \rightarrow [(C_5Me_5)_2Sm(THF)]_2(\mu\text{-}E) + Ph_3P$$

E = S, Se

$$2(C_5Me_5)_2Sm(THF)_2 + \text{excess } E_x \rightarrow [(C_5Me_5)_2Sm]_2(E_3)(THF)$$

E = Se, Te

$$2(C_5Me_5)_2Sm(THF)_2 + 3/8S_8 \rightarrow [(C_5Me_5)_2Sm]_2(S_3)(THF)$$

$$[(C_5Me_5)_2Sm]_2(S_3)(THF) + PMe_3 \rightarrow [(C_5Me_5)_2Sm]_2(\mu\text{-}\eta^2{:}\eta^2\text{-}Te_2) + Me_3P{=}Te$$

$$[(C_5Me_5)_2Sm(THF)]_2(\mu\text{-}Te) + Se_x \rightarrow [(C_5Me_5)_2Sm]_2(Se_aTe_b)(THF) + \text{other products}$$

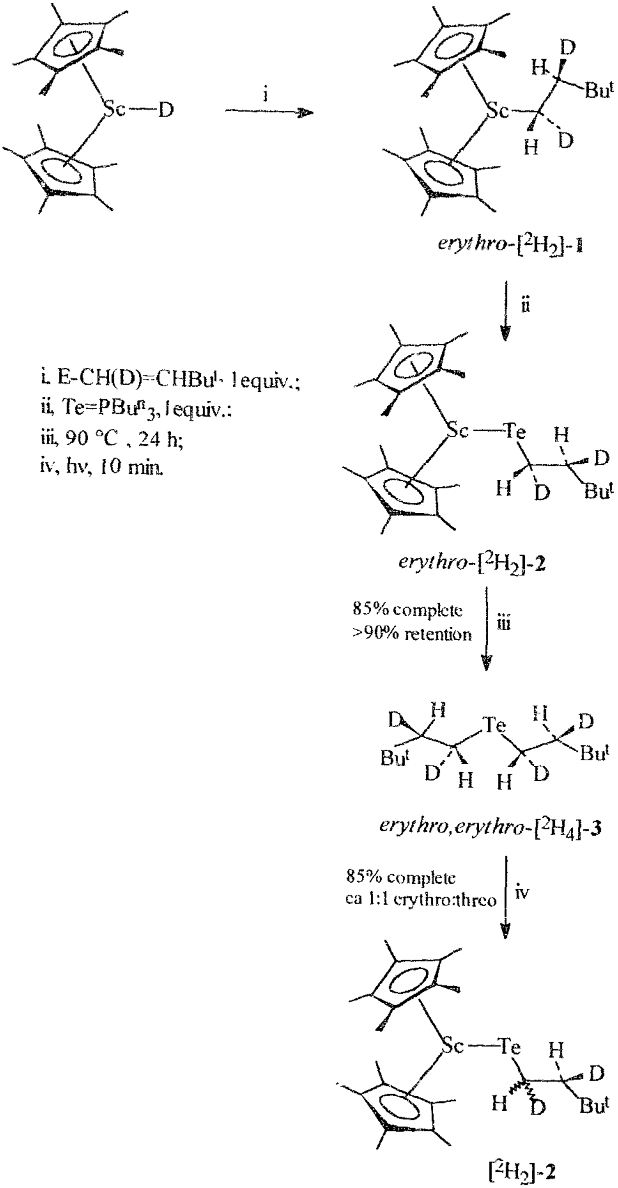

i. E-CH(D)=CHBu^t, 1equiv.;
ii, Te=PBu$^n{}_3$, 1equiv.;
iii, 90 °C, 24 h;
iv, hν, 10 min.

Scheme 15.

Complexes [(C_{5}Me_{5})_{2}Sm]_{2}(E_{3})(THF) can also be interconverted with [(C_{5}Me_{5})_{2}Sm (THF)]_{2}(μ-E).

$$[(C_5Me_5)_2Sm(THF)]_2(\mu\text{-}E) + (2/x)E_x \rightarrow [(C_5Me_5)_2Sm]_2(E_3)(THF)$$

E = Se, Te

$$[(C_5Me_5)_2Sm]_2(E_3)(THF) + 2PPh_3 \rightarrow [(C_5Me_5)_2Sm(THF)]_2(\mu\text{-}E) + Ph_3P{=}E$$

E = S, Se

The complexes $[(C_5Me_5)_2Sm(THF)]_2(\mu\text{-}E)$ (E = S, Se, Te) are isostructural (Fig. 30) and have a formally eight-coordinate local environment around each Sm atom. The Sm–E distances follow a progression consistent with the differences in the radii of the chalcogens (Sm–Te = 2.998(2) Å, Sm–Se = 2.782(1) Å and Sm–S = 2.663(1) Å).

Complex $[(C_5Me_5)_2Sm]_2(Se_3)(THF)$ (Fig. 31) contains two distinct types of Sm atom. Sm(1) is formally nine-coordinate and Sm(2) is formally eight-coordinate. The Sm–Se distances in the molecule (3.007(1), 3.198(1) and 2.917(1) Å) are much longer than the corresponding distances in $[(C_5Me_5)_2Sm(THF)]_2(\mu\text{-}Se)$.

In the structure of $[(C_5Me_5)_2Sm]_2(\mu\text{-}\eta^2{:}\eta^2\text{-}Te_2)$ (Fig. 32), the two bent metallocene units are oriented such that the four pentamethylcyclopentadienyl ring centroids describe a square plane rather than a tetrahedron. The Sm–Te distances are 3.213(1) and 3.204(1) Å. The Te–Te distance of 2.773(1) Å is in the single bond range.

Scholz et al. [42] reported the reactions of $[(C_5Me_5)_2La(\mu\text{-}Cl)_2K(dme)]$ with sodium 2,3-dimethylquinoxaline (Scheme 16) or with sodium phenazine. The reactions led to dimeric complexes which were structurally characterized. The structure

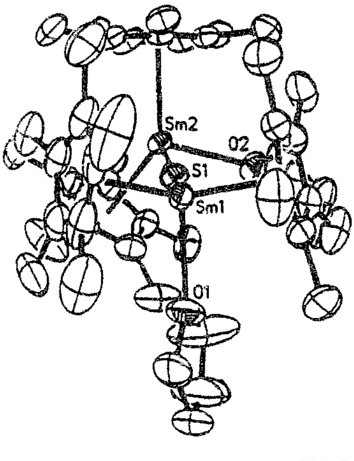

Fig. 30. Molecular structure of $[(C_5Me_5)_2Sm(THF)]_2(\mu\text{-}S)$.

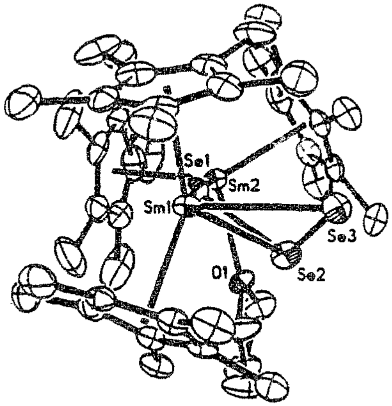

Fig. 31. Molecular structure of $[(C_5Me_5)_2Sm]_2(Se_3)(THF)$.

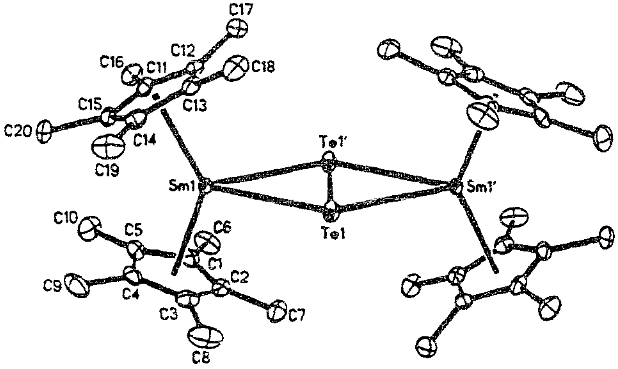

Fig. 32. Molecular structure of $[(C_5Me_5)_2Sm]_2(\mu\text{-}\eta^2\text{:}\eta2\text{-}Te_2)$.

with 2,3-dimethylquinoxaline contains two Cp^*_2La fragments, which are bound by the quinoxaline dianion. The La–N distances are 2.409(4) and 2.444(4) Å. The La–C(dimethylquinoxaline) distances of 2.903(5) and 2.891(5) Å are essentially longer than La–C(Cp*) (from 2.789 to 2.806 Å) or La–C distances in the ion $[La(\eta^3\text{-}C_3H_5)_4]^-$ (La–C_{av} 2.811 Å). The phenazine complex (Fig. 33) has a similar dimeric structure with the La–N(1) and La–C(22) distances being 2.452(2) Å and 2.931(2) Å respectively.

Evans et al. [43] investigated the reactivity of decamethylsamarocene with polycyclic aromatic hydrocarbons. A series of new bimetallic complexes of samarium

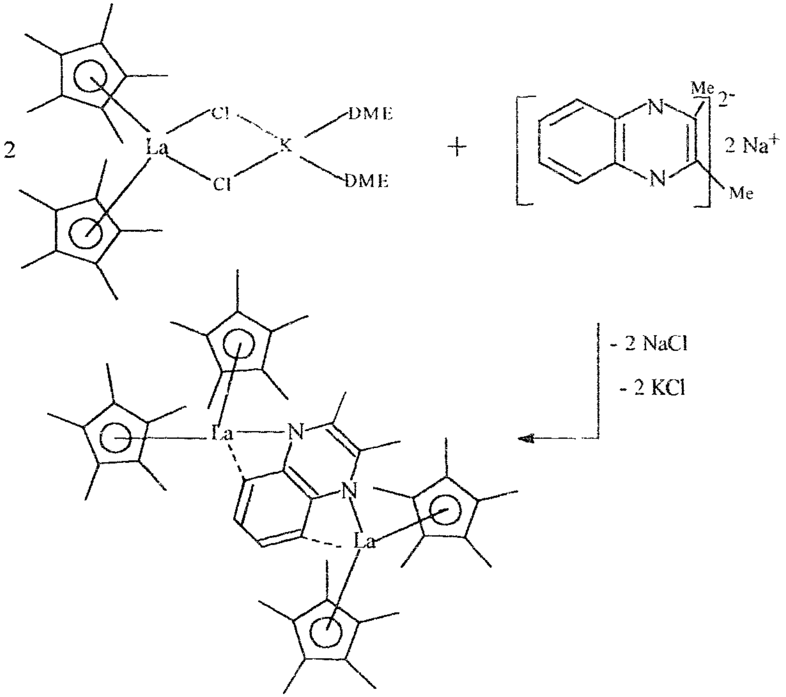

Scheme 16.

was obtained by the reactions of (η^5-C_5Me_5)$_2$Sm with various aromatic hydrocarbons and related nitrogen heterocycles. The reaction with anthracene (Scheme 17) gave the $[(C_5Me_5)_2Sm]_2[\mu$-η^3-η^3-$(C_{14}H_{10})]$.

According to X-ray data (Fig. 34) the planar $C_{14}H_{10}$ unit in the complex is coordinated on each side by the $(C_5Me_5)_2Sm$ groups with the shortest Sm–C(polycyclic ligand) distances of 2.595(4) Å, 2.840(4) Å and 2.791(4) Å for C(9), C(9a), and C(1) carbon atoms (anthracene numbering) respectively.

The analogous reaction (Scheme 18) with pyrene led to the complex $[(C_5Me_5)_2Sm]_2[\mu$-η^3-η^3-$(C_{16}H_{10})]$, which was also structurally characterized. In the

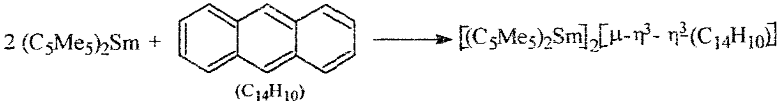

Scheme 17.

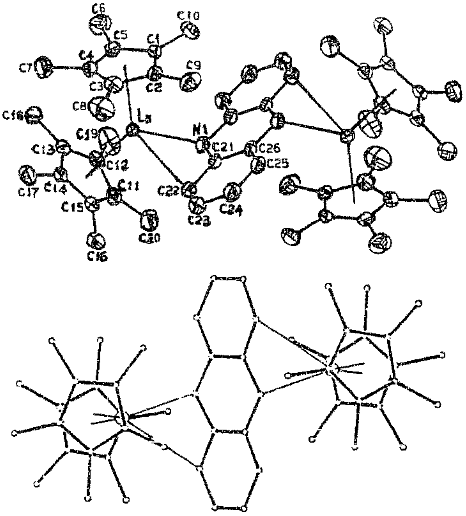

Fig. 33. Molecular structure of $[(C_5Me_5)_2La]_2C_{12}H_8N_2$.

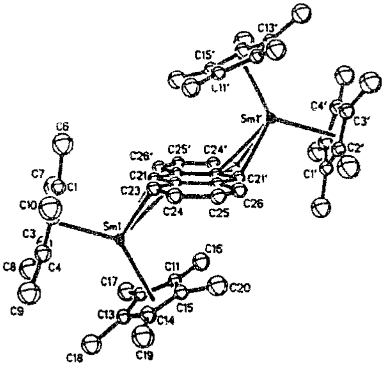

Fig. 34. Molecular structure of $[(C_5Me_5)_2Sm]_2\,[\mu\text{-}\eta^3,\eta^3\text{-}(C_{14}H_{10})]$.

complex, two $(C_5Me_5)_2Sm$ units also coordinated to opposite sides of the planar polycyclic system, but they are on the same end of the tetracyclic unit. The Sm–C(polycyclic ligand) distances range from 2.660 to 2.806(4) Å.

$(C_5Me_5)_2Sm$ was also found to react in a similar manner with 2,3-benzanthracene, 9-methylanthracene, acenaphthylene and phenazine to give $[(C_5Me_5)_2Sm]_2[\mu\text{-}\eta^3\text{-}\eta^3\text{-}$

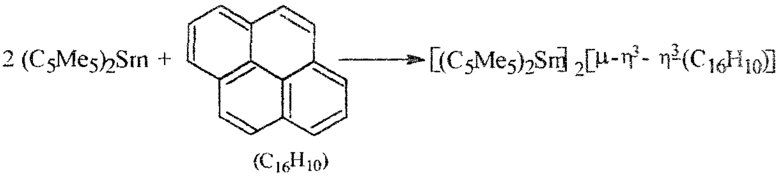

Scheme 18.

$(C_{18}H_{12})]$, $[(C_5Me_5)_2Sm]_2(C_{15}H_{12})$, $[(C_5Me_5)_2Sm]_2(C_{12}H_8)$, and $[(C_5Me_5)_2Sm]_2$-$[\mu$-η^3-η^3-$(C_{12}H_8N_2)]$ respectively. The complexes $[(C_5Me_5)_2Sm]_2[\mu$-η^3-η^3-$(C_{18}H_{12})]$ and $[(C_5Me_5)_2Sm]_2[\mu$-η^3-η^3-$(C_{12}H_8N_2)]$ were also structurally characterized.

The reaction of $(C_5Me_5)_2Sm$ with azulene produced $(C_5Me_5)_3Sm$, and another product which was not fully established. A similar reaction with acridine $(C_{13}H_9N)$ led to the complex $[(C_5Me_5)_2Sm]_2[\mu$-η^3-η^3-$(C_{13}H_9N)_2]$ (Scheme 19) which, according to X-ray diffraction, contains nonplanar $C_{13}H_9N$ units. The Sm–N distance is 2.380(5) Å. The polycyclic ligand in the complex $[(C_5Me_5)_2Sm]_2[\mu$-η^3-η^3-$(C_{13}H_9N)_2]$ exhibits a larger deviation from planarity (±0.26 Å) than any of the previously described complexes.

Arduengo et. al. [44] described the synthesis and structures of new lanthanide carbene complexes. 1,3,4,5-Tetramethylimidazol-2 ylidene reacted with bis(pentamethylcyclopentadienyl)samarium according to Scheme 20 giving the samarium(II) carbene complexes.

Schumann et al. [45] reported the synthesis of new carbene complexes of divalent samarium and ytterbium. The (imidazol-2-ylidene)lanthanide (Sm, Yb) complexes were obtained from 1,3,4,5-tetramethyl-imidazol-2-ylidene or 1,4-diisopropyl-2,3-dimethylimidazol-2-ylidene and the corresponding bis(cyclopentadienyl) complexes of Sm(II) and Yb(II) (Scheme 21).

The molecular structure of the ytterbium carbene complex $(C_5H_3^tBu_2)_2Yb$–$\overline{CN(Me)CMe{=}CMeN}(Me)$ was studied by X-ray diffraction (Fig. 35). In the

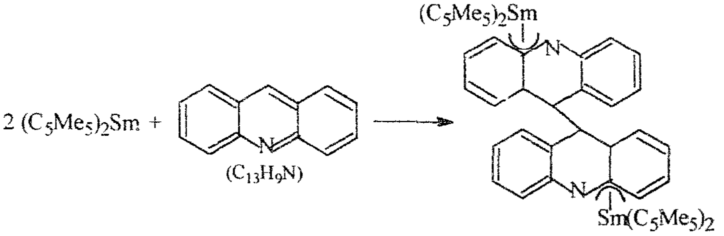

$[(C_5Me_5)_2Sm]_2[\mu$-η^3- $\eta^3(C_{13}H_9N)_2]$

Scheme 19.

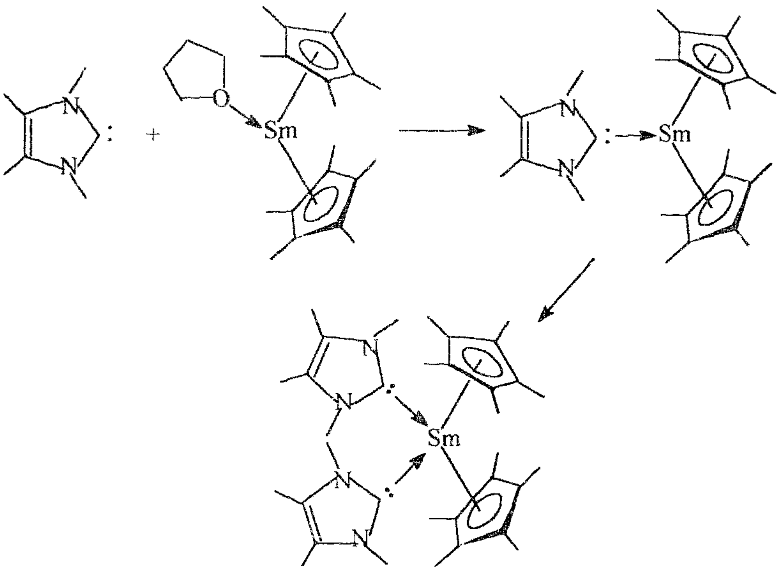

Scheme 20.

structure the seven-coordinated Yb atom has a pseudo-trigonal ligand-arrangement. The Yb–C27 distance is 2.598(3) Å.

Tilley and coworkers [46] prepared lanthanide–tungsten heterobimetallic complexes via σ-bond metathesis. Reaction of $[W(C_5H_5)_2H_2]$ with $[\{Ln(C_5Me_5)_2H\}_2]$ (Ln = Y, Sm) in toluene at room temperature (Scheme 22) led to the metallated cyclopentadienyl derivative $[(C_5Me_5)_2Ln(\mu\text{-}\eta^1,\eta^5\text{-}C_5H_4)(\mu\text{-}H\}_2W(C_5H_5)]$. The molecular structure of the samarium complex consists of two metallocene fragments linked by a Sm–C(C_5H_4) bond (Fig. 36). The Sm–W distance (3.402(1) Å) is greater than the sum of the atomic radii for Sm and W, suggesting the absence of a direct Sm–W bond. The overall conformation of the molecule implied the presence of bridging hydride ligands.

Radu and Tilley [47] also reported about σ-bond metathesis reactions involving lanthanide–silicon and lanthanide–hydrogen bonds. The lanthanide silyl complexes $Cp^*_2LnSiH(SiMe_3)_2$ (Ln = Sm, Nd, Y; $Cp^* = \eta^5\text{-}C_5Me_5$) were obtained by reaction of the appropriate $Cp^*_2LnCH(SiMe_3)_2$ with $SiH_2(SiMe_3)_2$.

$$\begin{array}{ccc} Cp^*_2LnCH(SiMe_3)_2 & & Cp^*_2LnSiH(SiMe_3)_2 \\ + & \longrightarrow & + \\ SiH_2(SiMe_3)_2 & & CH_2(SiMe_3)_2 \end{array}$$

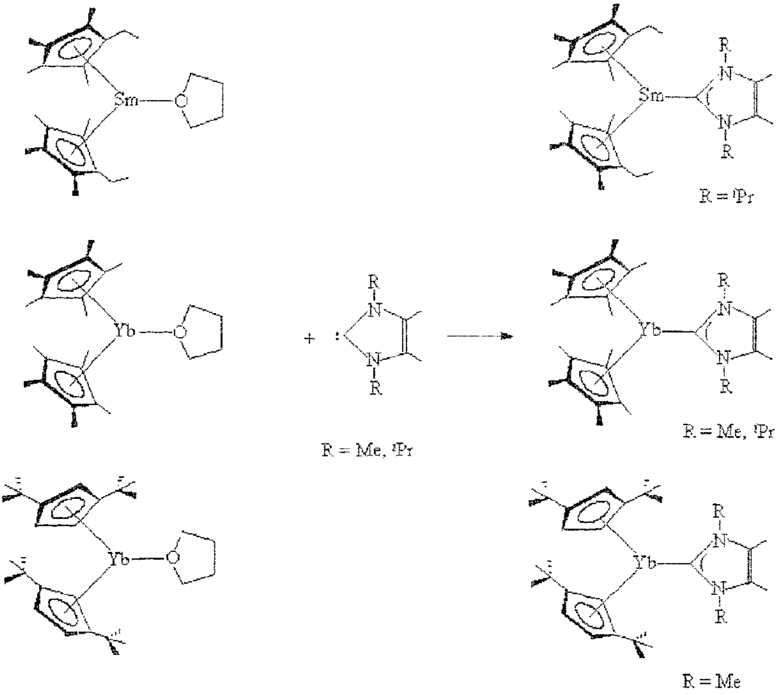

Scheme 21.

The silyl complexes $Cp_2^*LnSiH(SiMe_3)_2$ are monomeric in pentane solution but in the solid state they contain an intermolecular $Ln\cdots CH_3{-}Si$ interaction. The σ-bond metathesis reaction proceeds via a second-order autocatalytic process catalysed by $[Cp_2^*LnH]_2$. The above-mentioned reactions of $[\{Ln(C_5Me_5)_2H\}_2]$ (Ln = Y, Sm) with $[W(C_5H_5)_2H_2]$ (Scheme 22) were also discussed in the work. The borohydride complexes $Cp_2^*Ln(\eta^2\text{-}H_2BMes_2)$ (Mes = mesityl, Ln = Sm, Y) were synthesized from $[Cp_2^*LnH]_2$ and $[HBMes_2]_2$.

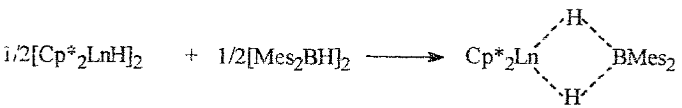

$$1/2[Cp^*_2LnH]_2 + 1/2[Mes_2BH]_2 \longrightarrow Cp^*_2Ln(\mu\text{-}H)_2BMes_2$$

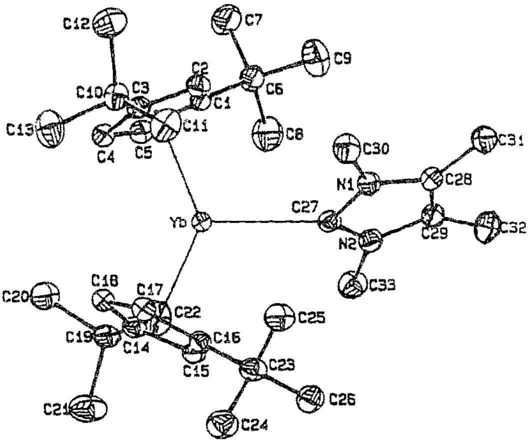

Fig. 35. Molecular structure of $(C_5H_3^tBu_2)_2Yb\text{-}\overline{CN(Me)CMe{=}CMeN}(Me)$.

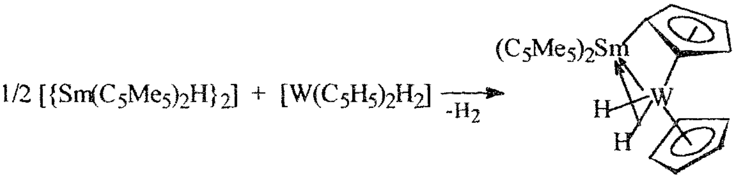

Scheme 22.

Teuben and coworkers [48] reported the synthesis and properties of $Cp_2^*Y(2\text{-pyridyl})$ ($Cp^* = C_5Me_5$). The complex was obtained from $[Cp_2^*YH]_2$ and pyridine.

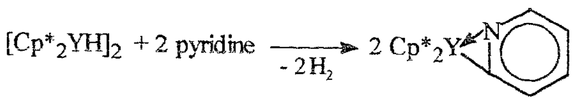

This compound reacts with hydrogen and Lewis bases (THF, Et_2O, pyridine) as well as with alkenes, alkynes and carbon monoxide (Scheme 23).

The structure of the CO insertion complex $[Cp_2^*Y]_2[\mu\text{-}\eta^2{:}\eta^2\text{-}OC(NC_5H_4)_2]$ (Fig. 37) consists of two normal bent Cp_2^*Y units that are bridged by a $\mu\text{-}\eta^2{:}\eta^2$-dipyridyl ketone fragment. The product of ethylene insertion $Cp_2^*YCH_2CH_2(2\text{-}NC_5H_4)$ gave σ-bond metathesis with pyridine to form

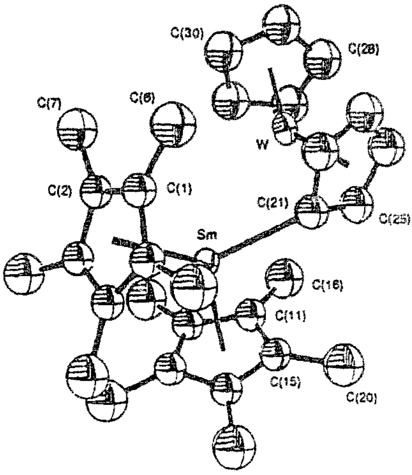

Fig. 36. Molecular structure of $[(C_5Me_5)_2Ln(\mu\text{-}\eta^1,\eta^5\text{-}C_5H_4)(\mu\text{-}H)_2W(C_5H_5)]$.

2-ethylpyridine and Cp^*_2Y(2-pyridyl). The complex $Cp^*_2YCH_2CH_2(2\text{-}NC_5H_4)$ decomposes to the isomers $Cp^*_2Y[2\text{-}NC_5H_3(6\text{-}Et)]$ and $Cp^*_2YCHMe(2\text{-}NC_5H_4)$ at 80 °C.

Marks and coworkers [49] investigated the bis(polymethylcyclopentadienyl)lanthanide hydrocarbyl complexes $Cp'_2LnCH(SiMe_3)_2$ and $Me_2SiCp''_2LnCH(SiMe_3)_2$ ($Cp' = \eta^5\text{-}(CH_3)_5C_5$; $Cp'' = \eta^5\text{-}(CH_3)_4C_5$; Ln = La, Ce, Nd, Sm, Lu) by relativistic ab initio and DV-Xα calculations and gas-phase UV photoelectron spectroscopy. The investigations revealed that the lanthanide–ligand bonding interactions are dominated by the metal 5d orbitals. The metal 4f orbitals are only marginally involved in the bonding. The ionization from the Ln–C bonding orbital represents the lowest-energy, nearly constant PE feature followed by Ln–Cp ionization in the He I spectra. Metal f^1 ionizations, observed in the He II spectra of the Ce, Nd, Sm and Lu complexes, were interpreted on the basis of the states generated upon ionization of the f^n ground states. They had either the form of low intensity onset features for Ce, Nd and Sm complexes, or of intense structures in the 16–17 eV range in the spectrum of the Lu compound. Trends in the $4f^1$ ionizations are consistent with a gradual energetic stabilization of 4f orbitals across the lanthanide series. Metal 4f orbitals appear core-like in character in the f^{14} Lu complex.

2.2.3. *Tris(cyclopentadienyl) complexes*

Chen et al. [50] published the syntheses and crystal structures of $(\eta^5\text{-}C_5H_5)_3Ln(THF)$ (Ln = Ce, Er). The reaction of $(NH_4)_2Ce(NO_3)_6$ with C_5H_5Na in THF led to the Ce(III) complex $(C_5H_5)_3Ce(THF)$. The authors also made an attempt to obtain a cyclooctadienyl bis(cyclopentadienyl)erbium complex by the reaction

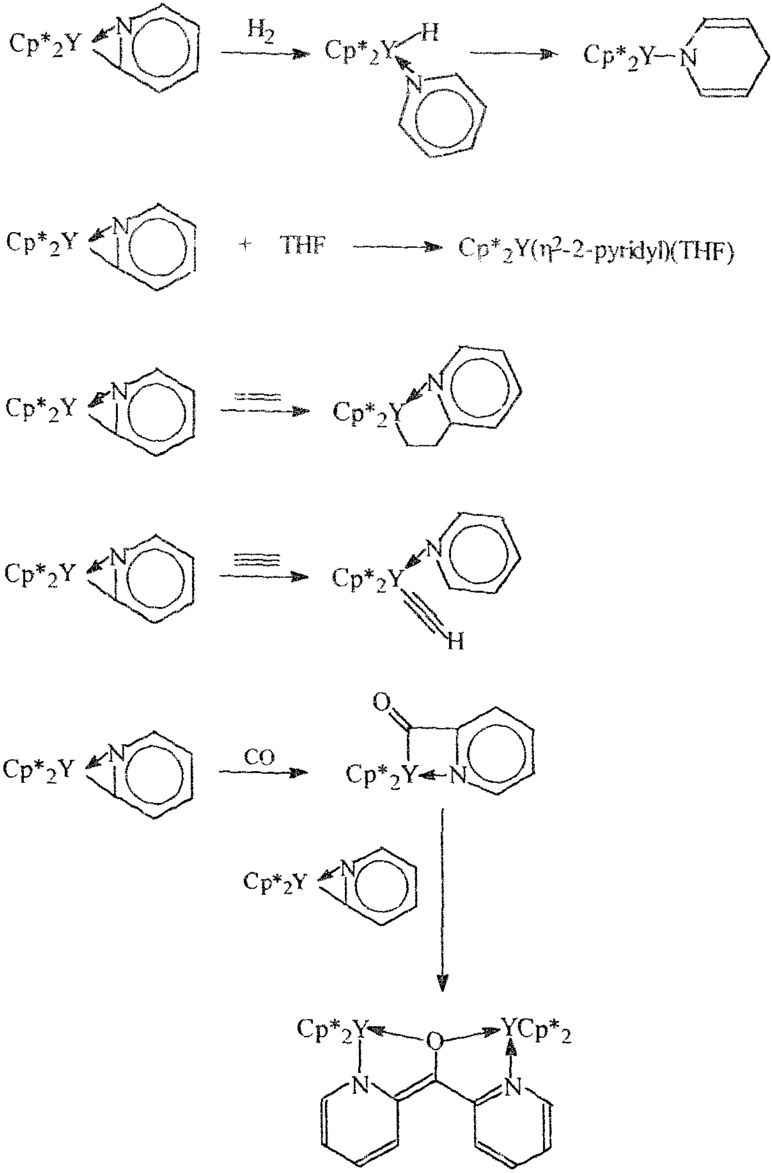

Cp*₂Y
N
H₂
Cp*₂Y
H
N
Cp*₂Y
N
+ THF
Cp*₂Y(η²-2-pyridyl)(THF)
CO
O
Cp*₂Y
N
YCp*₂

Scheme 23.

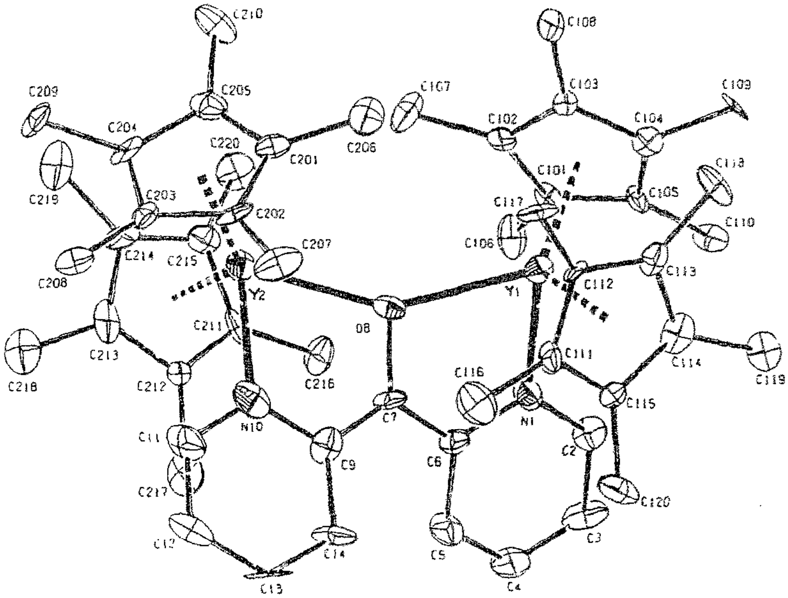

Fig. 37. Molecular structure of $[\mathrm{Cp}^{\ddagger}_{2}\mathrm{Y}]_2[\mu\text{-}\eta^2{:}\eta^2\text{-OC(NC}_5\mathrm{H}_4)_2]$.

of $\mathrm{ErCl_3 \cdot 4THF}$ with $\mathrm{C_8H_{11}K}$ and with $\mathrm{C_5H_5Na}$. but the reaction gave $\mathrm{(C_5H_5)_3Er(THF)}$ only. The complex $(\eta^5\text{-}\mathrm{C_5H_5})_3\mathrm{Ce(THF)}$ and the analogous erbium complex are not isostructural, but $(\eta^5\text{-}\mathrm{C_5H_5})_3\mathrm{Er(THF)}$ is isostructural with known $(\eta^5\text{-}\mathrm{C_5H_5})_3\mathrm{Ln(THF)}$ (Ln = La, Pr, Nd, Gd, Dy, Y and Lu).

Wang et al. [51] reported the formation and molecular structure of $(\eta^5\text{-}\mathrm{C_5H_5})_3\mathrm{Sm(THF)}$. The complex was obtained from the reaction of $(\eta^5\text{-}\mathrm{C_5H_5})\mathrm{SmCl_2(THF)_3}$ with $\mathrm{NaC{\equiv}CCH_2OCH_2CH{=}CH_2}$ in THF.

$$3\mathrm{CpSmCl_2(THF)_3} + 6\mathrm{NaC{\equiv}CCH_2OCH_2CH{=}CH_2} \xrightarrow{\mathrm{THF}}$$

$$\{3[\mathrm{CpSm(C{\equiv}CCH_2OCH_2CH{=}CH_2)_2}]\} + 6\mathrm{NaCl}$$

$$\{3[\mathrm{CpSm(C{\equiv}CCH_2OCH_2CH{=}CH_2)_2}]\} \xrightarrow{\mathrm{THF}} (\eta^5\text{-}\mathrm{C_5H_5})_3\mathrm{Sm(THF)}$$

$$+ 2\mathrm{Sm(C{\equiv}CCH_2OCH_2CH{=}CH_2)_3}$$

The molecular structure of $(\eta^5\text{-}\mathrm{C_5H_5})_3\mathrm{Sm(THF)}$ has a coordination sphere of three η^5-cyclopentadienyl ligands and one tetrahydrofuran to form a distorted tetrahedron around the Sm atom.

This structure, as well as the structure of $(C_5H_5)_3Dy(THF)$, was also reported by Wu et al. [52]. The complexes were obtained by refluxing $[Cp_2SmO(CH_2)_4CH_3]_2$ and $[Cp_2DyS(CH_2)_4CH_3]_2$ $(Cp = C_5H_5)$ in THF.

$$3[Cp_2Ln(\mu\text{-}L)]_2 \xrightarrow[\text{reflux}]{\text{THF}} 4Cp_3Ln + 2LnL_3$$

$$Ln = Sm,\ L = O(CH_2)_4CH_3;\ Ln = Dy,\ L = S(CH_2)_4CH_3$$

The complexes are isostructural with the known complexes $Cp_3Ln(THF)$ $(Ln = La, Pr, Nd, Gd$ and $Lu)$.

Knjazhansky et al. [53] reported the synthesis and structure of the complex $[AlH_2(OC_4H_8)_4][(\eta^5\text{-}C_5H_5)_3Yb(\mu\text{-}Na)Yb(\eta^5\text{-}C_5H_5)_3]$, which was obtained by the reaction of $Na[(C_5H_5)_3Yb]$ with aluminium hydride in THF.

$$2Na[(C_5H_5)_3Yb] + 2AlH_3 \cdot THF \rightarrow$$
$$[AlH_2(OC_4H_8)_4][(\eta^5\text{-}C_5H_5)_3Yb(\mu\text{-}Na)Yb(\eta^5\text{-}C_5H_5)_3] + NaAlH_4$$

The structure (Fig. 38) consists of the anion $[(\eta^5\text{-}C_5H_5)_3Yb(\mu\text{-}Na)Yb(\eta^5\text{-}C_5H_5)_3]^-$ and the cation $[AlH_2(OC_4H_8)_4]^+$. In the cation the Al atom has an

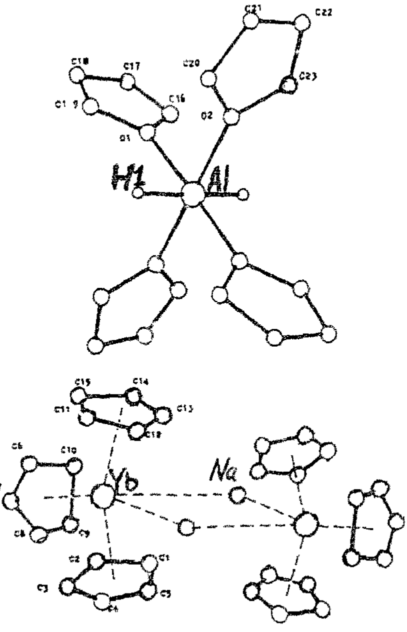

Fig. 38. Molecular structure of $[AlH_2(OC_4H_8)_4][(\eta^5\text{-}C_5H_5)_3Yb(\mu\text{-}Na)Yb(\eta^5\text{-}C_5H_5)_3]$.

octahedral environment with bond angles close to 90°. The anion contains two $[(\eta^5\text{-C}_5\text{H}_5)_3\text{Yb}]^-$ fragments and the Na^+ ion bound by ionic interactions. The Yb···Na distance (3.54(1) Å) is sufficiently large that the interaction can be considered as a purely ionic one.

Depaoli et al. [16] described the europium-151 Mössbauer spectra of several organoeuropium(III) compounds including $(\eta^5\text{-C}_5\text{H}_5)_3\text{Eu(THF)}$. The europium-151 Mössbauer spectrum of $(\eta^5\text{-C}_5\text{H}_5)_3\text{Eu(THF)}$ revealed a weak but definite covalent interaction between the 4f orbitals of Eu(III) and the ligands.

Ren et al. [54] reported the synthesis and X-ray structure of an organolanthanum complex $[(^t\text{BuCp})_3\text{LaClLi(THF)}_3]$. The compound was obtained by the reaction of $\text{LaCl}_3 \cdot 2\text{LiCl}$ with two equivalents of $^t\text{BuCpNa}$ in THF. In the structure the central La^{3+} is coordinated to three $^t\text{BuCp}$ groups and one chloride to form a distorted tetrahedron (Fig. 39). The two units $(^t\text{BuCp})_3\text{La}$ and Li(THF)^- are connected by a single chloride bridge.

2.2.4. *Bridged cyclopentadienyl complexes*

Sun et al. [55] published the synthesis and crystal structure of $[\text{Me}_4\text{C}_2\text{Cp}_2\text{SmCl(THF)}]_2$. The complex was synthesized by the reaction of SmCl_3 with the $\text{Me}_4\text{C}_2(\text{C}_5\text{H}_4\text{MgCl})_2\text{(THF)}$ in THF. The structure of $[\text{Me}_4\text{C}_2\text{Cp}_2\text{SmCl(THF)}]_2$ is dimeric (Fig. 40). Two Sm atoms are bridged by two chlorine atoms to form two unsymmetrical Sm–Cl bonds (Sm–Cl distance is 2.78, 2.84 Å). The two Cp rings are in eclipsed conformation.

Paolucci et al. [56] reported the synthesis of new bis(cyclopentadienyl)lanthanide chlorides (Scheme 24). The compounds were characterized by elemental analyses, IR, MS, ^{1}H NMR and X-ray photoelectron spectroscopy. The reaction of two equivalents of $\text{PrCl}_3\text{(THF)}_x$ and three equivalents of $\text{Na}_2[2,6\text{-(CH}_2\text{C}_5\text{H}_4)_2\text{C}_5\text{H}_3\text{N}]$

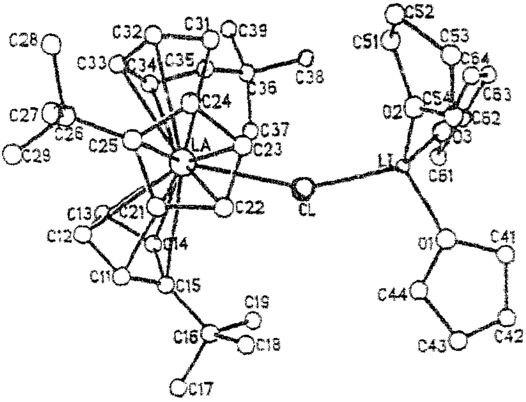

Fig. 39. Molecular structure of $[(^t\text{BuCp})_3\text{LaClLi(THF)}_3]$.

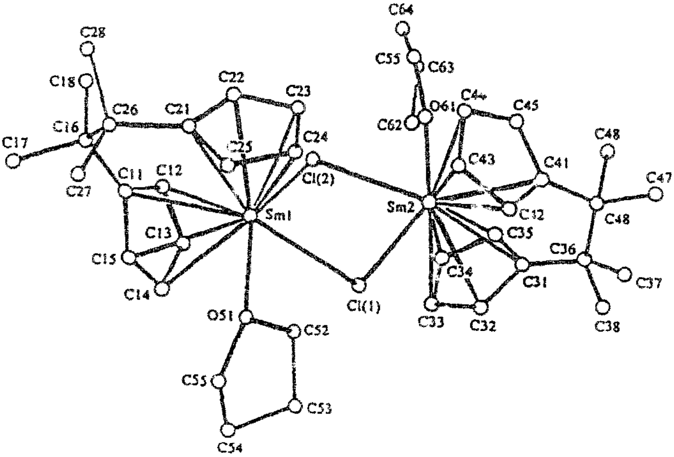

Fig. 40. Molecular structure of $[Me_4C_2Cp_2SmCl(THF)]_2$.

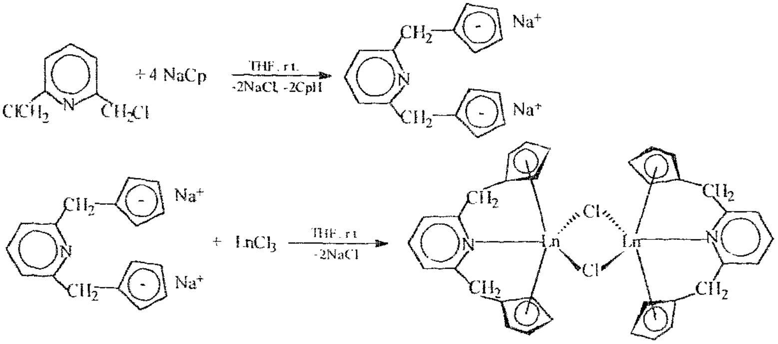

Ln = Y, Pr, Nd, Sm, Dy, Er, Yb, or Lu.

Scheme 24.

led to the complex, which according to elemental analysis, has the formula $[(2,6\text{-}(CH_2C_5H_4)_2C_5H_3N)_3Pr_2]$. Some preliminary studies of the catalytic properties of the bis(cyclopentadienyl)lanthanide chlorides in the reduction of hex-1-ene by $LiAlH_4$ were also carried out.

Gräper et al. [57] described the new lanthanocenophanes $[\{OMe_2SiC_5H_4)_2\}PrCl(THF)]_x$ ($x=1$ or 2) and $[\{OMe_2SiC_5H_4)_2\}YbCl]_2$. The complexes were synthesized by the reaction of the potassium salt of 1,1,3,3-tetramethyl-1,3-dicyclopentadienyl disiloxane with $PrCl_3$ or $YbCl_3$. According to the X-ray structure determination the complex $[\{OMe_2SiC_5H_4)_2\}YbCl]_2$ is a Cl-bridged dimer. In the molecule of $[\{OMe_2SiC_5H_4)_2\}YbCl]_2$ the ring-bridging $-Me_2SiOSiMe_2$-group is positioned asymmetrically with respect to the Cl–Yb–Cl′ plane. The Yb–Cp(cent.) distances are 229.0(7) and 228.1(7) Å.

Qian and Zhu [58] published the synthesis of a series of furan-bridged bis(cyclopentadienyl) lanthanide (Yb, Sm or Nd) and yttrium (Scheme 25) complexes.

The compounds were characterized by elemental analyses, MS, IR and ^1H NMR. The reactivity of organolanthanide hydrides generated in situ from the $[Ln(C_5H_5)_2Cl]$–NaH system was studied. The authors come to the conclusion that the reactivity can be tuned not only by varying the ligands but also by taking advantage of the lanthanide contraction. The goal of acquiring more reactive organolanthanide hydrides can be achieved by selecting the appropriate ligands and using the early lanthanide metals.

Piers et al. [59] investigated the insertion of elemental tellurium into the scandium–carbon bonds of the *ansa*-scandocene alkyl{*meso*-$(CH_3)_2Si[(t\text{-}C_4H_9)C_5H_3]_2$} $Sc(CH_2SiMe_3)$(DpScR). The chemical procedures are summarized in Scheme 26.

The dimeric telluride DpSc–Te–ScDp was characterized by X-ray analysis as the benzene solvate of its bis(trimethylphosphine) adduct $DpSc(PMe_3)$–Te–$Sc(PMe_3)Dp$ (Fig. 41). The asymmetric unit of the complex consists of two independent half-molecules (the Te atom is on an inversion centre), which differ only slightly in conformation. The Sc–Te–Sc coordination is, as a consequence, precisely linear, with a mean Sc–Te bond distance of 2.875(5) Å.

Schumann et al. [60] reported the synthesis and characterization of the $[(^tBuC_5H_3)SiMe_2(C_5Me_4)]Ln(\mu\text{-}Cl)_2Li(OEt_2)_2$ (Ln = La, Lu) (Scheme 27) and the chiral tris(cyclopentadienyl) complexes $[(^tBuC_5H_3)SiMe_2(C_5Me_4)]Ln(C_5Me_4H)$(THF) (Ln = La, Nd) (Scheme 27).

According to X-ray analysis, in the structure of $[(^tBuC_5H_3)SiMe_2(C_5Me_4)]$-$La(C_5Me_4H)$(THF) the La atom adopts a distorted tetrahedral arrangement, which is formed by the three cyclopentadienyl rings and one THF molecule (Fig. 42). This complex, as well as the other complexes, were characterized also by their ^1H and ^{13}C NMR and MS spectra.

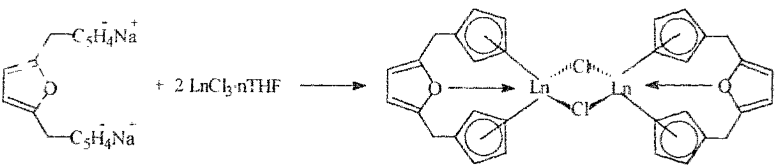

Ln = Y, Yb, Sm or Nd

Scheme 25.

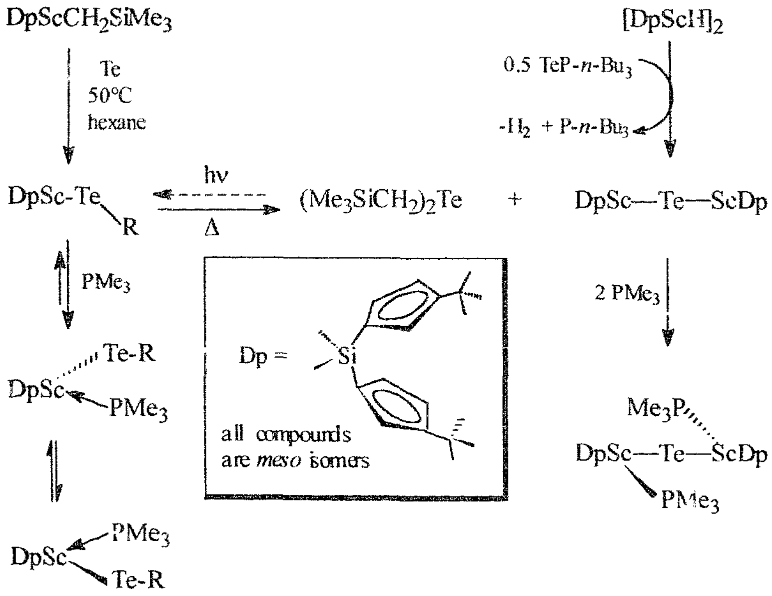

Scheme 26.

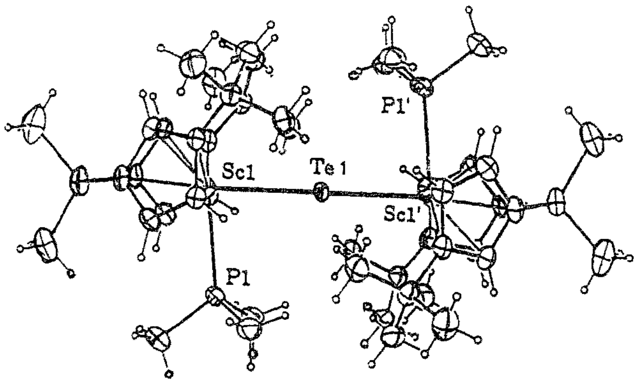

Fig. 41. Molecular structure of $DpSc(PMe_3)$–Te–$Sc(PMe_3)Dp$ (Dp = {*meso*-$(CH_3)_2Si[(t\text{-}C_4H_9)\text{-}C_5H_3]_2\}^{2-}$).

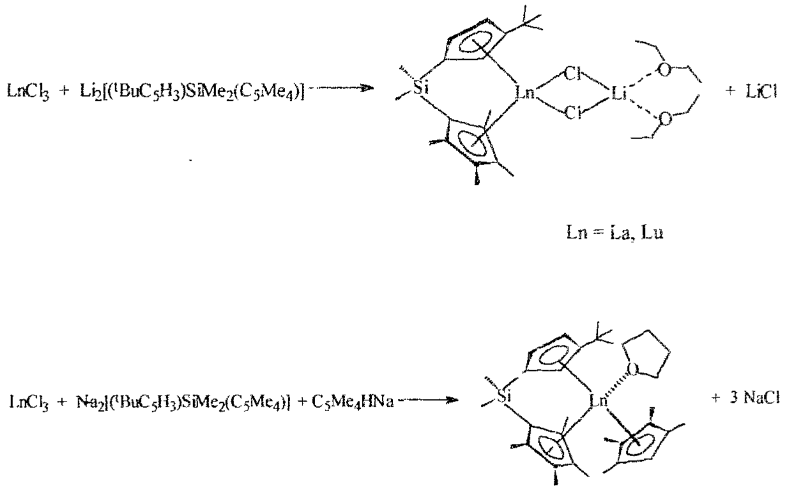

Ln = La, Lu

Scheme 27.

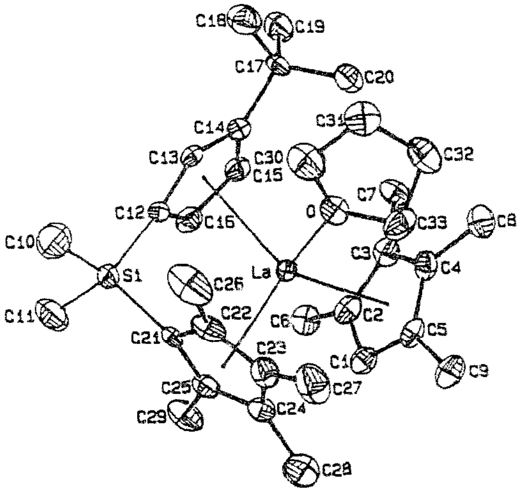

Fig. 42. Molecular structure of $[(^tBuC_5H_3)SiMe_2(C_5Me_4)]La(C_5Me_4H)(THF)$.

Hajela and Bercaw [61] reported that the reaction of permethylscandocene complex $OpSc(H)(PMe_3)$ ($Op = \{(\eta^5\text{-}C_5Me_4)_2SiMe_2\}$) with isobutene produced $OpSc\{(CH_2CH(CH_3)_2\}(PMe_3)$, which slowly decomposed to afford the $OpSc(CH_3)(PMe_3)$ along with isobutene, 2-methylpentane, isobutene, 2-methyl-1-pentene, propane and *n*-pentane (Scheme 28).

A transient observed in the reaction sequence has been unambiguously characterized as $OpSc(CH_2CH_2CH_3)(PMe_3)$. The two C_6 products, 2-methylpentane, 2-methyl-1-pentene and *n*-pentane, were formed according to Eqs. (1)–(10).

$$OpSc\{(CH_2CH(CH_3)_2\}(PMe_3) \rightarrow [OpScCH_2CH(CH_3)_2] + PMe_3 \tag{1}$$

$$[OpScCH_2CH(CH_3)_2] \rightarrow [OpScCH_3] + CH_2{=}CHCH_3 \tag{2}$$

$$[OpScH] + CH_2{=}CHCH_3 \rightarrow [OpScCH_2CH_2CH_3] \tag{3}$$

$$[OpScCH_2CH_2CH_3] + CH_2{=}CHCH_3 \rightarrow [OpScCH_2CH(CH_3)CH_2CH_2CH_3] \tag{4}$$

$$[OpScCH_2CH(CH_3)CH_2CH_2CH_3] \rightarrow [OpScH] + CH_2{=}C(CH_3)CH_2CH_2CH_3 \tag{5}$$

$$[OpScCH_2CH(CH_3)CH_2CH_2CH_3] + PMe_3 \rightarrow OpScCH_2PMe_2 + CH_3CH(CH_3)CH_2CH_2CH_3 \tag{6}$$

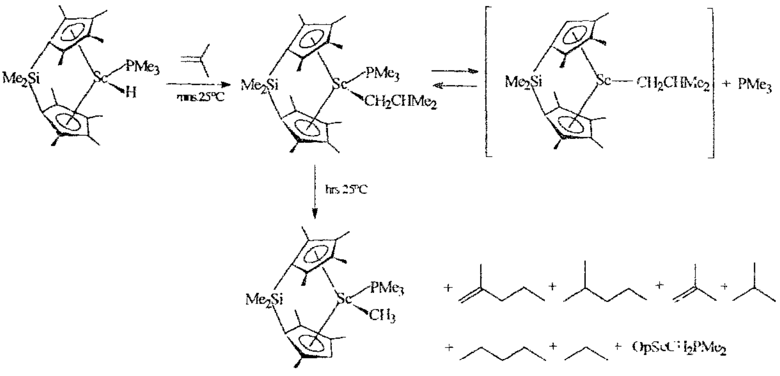

Scheme 28.

$$[\mathrm{OpScCH_2CH(CH_3)CH_2CH_2CH_3}] \rightarrow \qquad (7)$$
$$[\mathrm{OpScCH_3}] + \mathrm{CH_2{=}CHCH_2CH_2CH_3}$$

$$[\mathrm{OpScCH_3}] + \mathrm{PMe_3} \rightarrow \mathrm{OpSc(CH_3)(PMe_3)} \qquad (8)$$

$$[\mathrm{OpScH}] + \mathrm{CH_2{=}CHCH_2CH_2CH_3} \rightarrow [\mathrm{OpScCH_2CH_2CH_2CH_2CH_3}] \qquad (9)$$

$$[\mathrm{OpScCH_2CH_2CH_2CH_2CH_3}] + \mathrm{PMe_3} \rightarrow \qquad (10)$$
$$\mathrm{OpScCH_2PMe_2} + \mathrm{CH_3CH_2CH_2CH_2CH_3}$$

β-Ethyl migration is not observed for the derivative $\mathrm{OpSc\{CH_2CH(C_2H_5)CH_2CH_3\}(PMe_3)}$, obtained from reaction of 2-ethyl-1-butene with $\mathrm{OpSc(H)(PMe_3)}$.

Marks and coworkers [62] described the synthesis, characterization, and configurational interconversions of chiral, C_1-symmetric organolanthanide halides, amides, and hydrocarbyls. The $\mathrm{Me_2Si(Cp''H)(R^*CpH)}$ ancillary ligands and the corresponding dilithium derivatives were obtained according to the Scheme 29. The chiral $\mathrm{Me_2SiCp''(R^*Cp)Ln(\mu\text{-}Cl)_2Li(ether)_2}$ complexes were synthesized by transmetalation of $\mathrm{Me_2SiCp''(R^*Cp)Li_2}$ with the appropriate lanthanide trichloride.

$$\mathrm{Me_2SiCp''(R^*Cp)Li_2} + \mathrm{LnCl_3} \xrightarrow[\text{2. Et}_2\text{O}]{\text{1. THF}}$$
$$\mathrm{Me_2SiCp''(R^*Cp)Ln(\mu\text{-}Cl)_2Li(Et_2O)_2} + \mathrm{LiCl}$$

R* = (+)-neomenthyl, Ln = La, Nd, Sm, Y, Lu;

R* = (−)-menthyl, Ln = Sm, Y, Lu;

R* = (−)-phenylmenthyl, Ln = Y

The mono-DME adducts can be prepared by the analogous reaction in the presence of DME. Diastereomers produced are epimeric with respect to the orientation of the chiral auxiliary on the Cp group relative to the lanthanide centre (**G**, **H**):

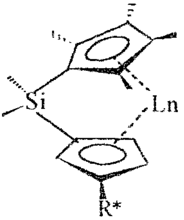

G(*S*)

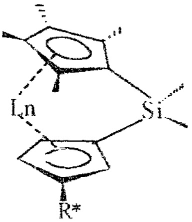

H(*S*)

The molecular structure of (*R*)-$\mathrm{Me_2SiCp''[(+)\text{-}neomenthylCp]Lu(\mu\text{-}Cl)_2Li(ether)_2}$ is shown in Fig. 43. The X-ray diffraction analysis reveals a single

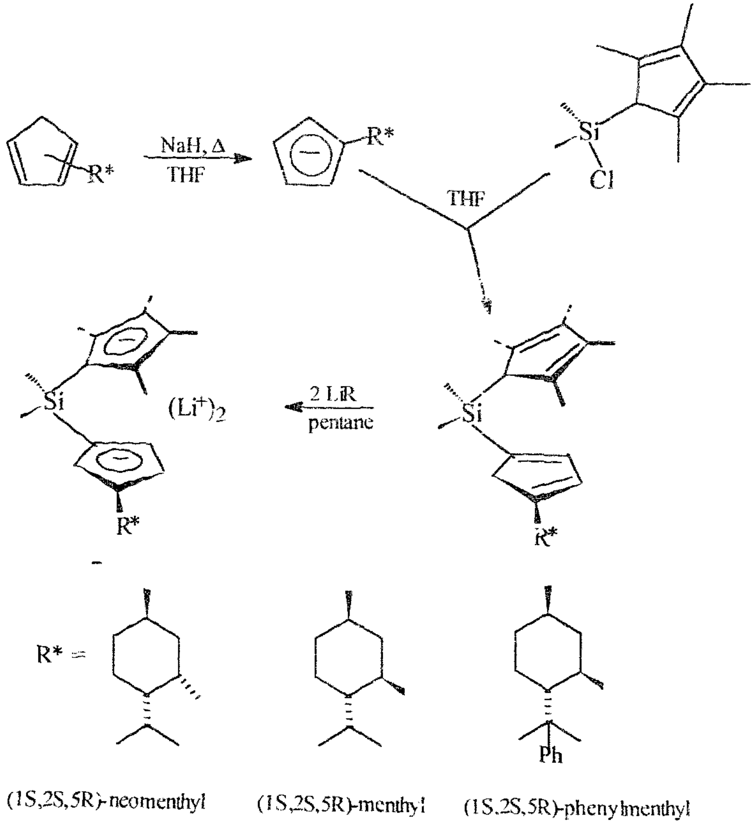

Scheme 29.

planar chiral configuration of the diastereotopic, chirally substituted Cp group, i.e. the (*R*)-configuration. Chiral organolanthanide hydrocarbyls and amides were prepared according to the following equations:

$$\mathrm{Me_2SiCp''(R^*Cp)Ln(\mu\text{-}Cl)_2Li(S)_2 + LiCH(TMS)_2 \xrightarrow[\text{2. pentane}]{\text{1. toluene}}}$$

$$\mathrm{Me_2SiCp''(R(Cp)LnCH(TMS)_2 + 2LiCl}$$

$$\mathrm{Me_2SiCp''(R^*Cp)Ln(\mu\text{-}Cl)_2Li(S)_2 + MN(TMS)_2 \xrightarrow[\text{2. pentane}]{\text{1. toluene}}}$$

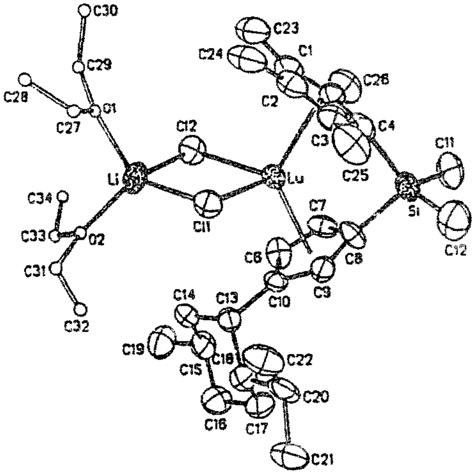

Fig. 43. Molecular structure of (*R*)-Me_2SiCp''[(+)-neomenthylCp]Lu(μ-Cl)$_2$Li(ether)$_2$.

$Me_2SiCp''(R^*Cp)LnN(TMS)_2 + MCl + 2LiCl$

R^* = (+)-neomenthyl, Ln = La, Nd, Sm, Y, Lu;

R^* = (−)-menthyl, Ln = Sm, Y, Lu;

R^* = (−)-phenylmenthyl, Ln = Y

The spectroscopic data supported solution structures **I**, **J** and **K**, **L** for the pair of hydrocarbyl and amido complexes respectively:

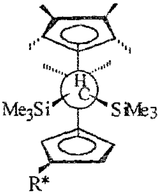

I

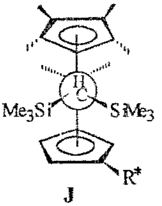

J

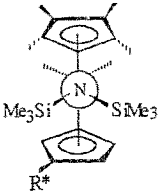

K

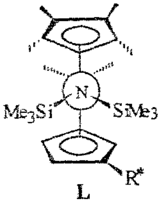

L

The reactions of (*R*)-Me_2SiCp'[(+)-neomenthylCp]Lu(μ-Cl)$_2$Li(ether)$_2$ with the other alkylating reagents were also investigated.

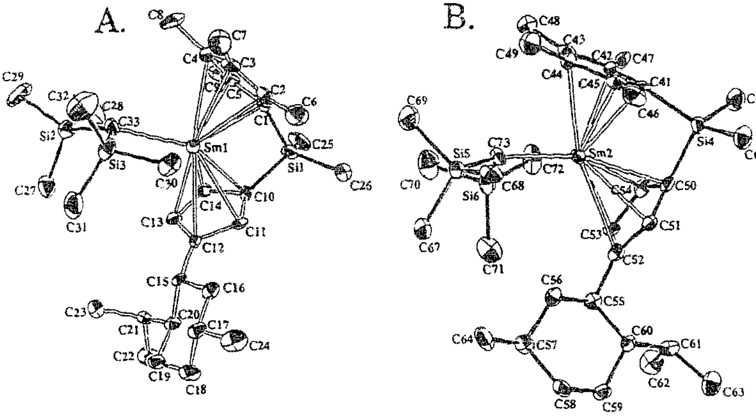

Fig. 44. Structure of (R)-$Me_2SiCp''[(-)\text{-menthylCp}]SmCH(TMS)_2$.

$$Me_2SiCp''[(+)\text{-neomenthylCp}]Lu(\mu\text{-}Cl)_2Li(ether)_2 + Li(2\text{-}C_6H_4CH_2NMe_2)$$
$$\xrightarrow[\text{2. pentane}]{\text{1. toluene}} Me_2SiCp''[(+)\text{-neomenthylCp}]Lu(\eta^2\text{-}2\text{-}C_6H_4CH_2NMe_2) + LiCl$$

$$Me_2SiCp''[(+)\text{-neomenthylCp}]Lu(\mu\text{-}Cl)_2Li(ether)_2 + Li(CH_2)_2PMe_2$$
$$\xrightarrow[\text{2. pentane}]{\text{1. toluene}} Me_2SiCp''[(+)\text{-neomenthylCp}]Lu(\eta^2\text{-}(CH_2)_2PMe_2) + LiCl$$

Low-temperature single crystal X-ray structural determinations were carried out on selected hydrocarbyl (E=CH) and amide (E=N) complexes to establish the absolute configuration (**Q**(S) and **R**(R)):

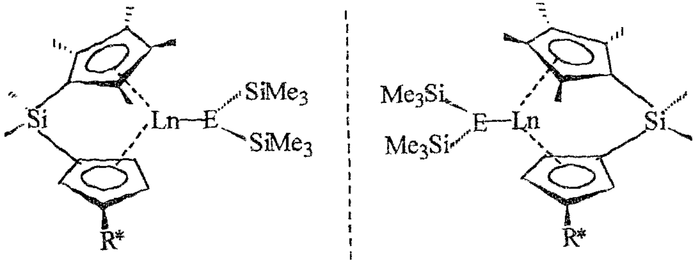

Q(S) **R**(R)

X-ray analyses of (R)-$Me_2SiCp'[(-)\text{-menthylCp}]LnCH(TMS)_2$ complexes (Ln=Y, Sm) showed that each unit cell contains two crystallographically independent molecules (**A** and **B**) with the same planar chiral (R)-configurations (Fig. 44).

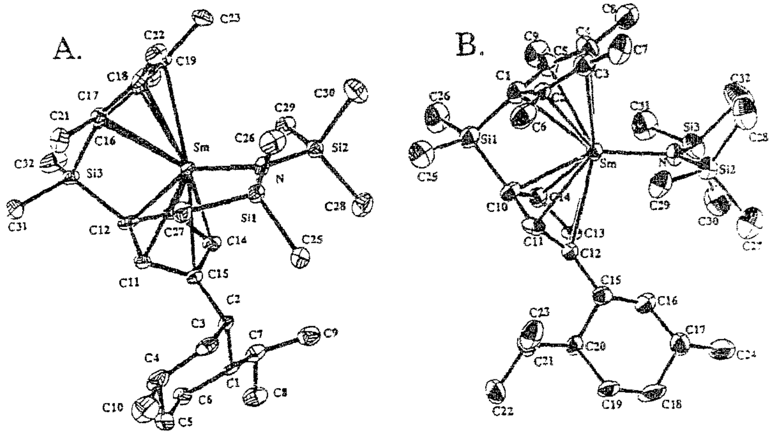

Fig. 45. Molecular structures of (*S*)-Me_2SiCp''[(+)-neomenthylCp]$SmN(TMS)_2$ (A) and (*S*)-Me_2SiCp''[(−)-menthylCp]$SmN(TMS)_2$ (B)

Diffraction analyses of (*S*)-Me_2SiCp'[(+)-neomenthylCp]$SmN(TMS)_2$ (**A**) and (*S*)-Me_2SiCp''[(−)-menthylCp]$SmN(TMS)_2$ (**B**) indicate the (*S*)-configuration in both complexes (Fig. 45), while analysis of Me_2SiCp''[(−)-menthylCp]$YN(TMS)_2$ indicated the (*R*)-configuration in the two independent molecules.

The hydrocarbyl and amide complexes $Me_2SiCp'(R^*Cp)LnR$ ($R = CH(SiMe_3)_2$, $N(SiMe_3)_2$, η^2-2-$C_6H_4CH_2NMe_2$, η^2-$(CH_2)_2PMe_2$) are protolyzed by alkylamines, presumably forming organolanthanide amide–amine adducts.

$$Me_2SiCp''(R^*Cp)LnR + 2H_2NR' \rightarrow Me_2SiCp''(R^*Cp)Ln(NHR')(NH_2R') + RH$$

The $Me_2SiCp'(R^*Cp)LnCH(SiMe_3)_2$ complexes also undergo hydrogenolysis of the $E(TMS)_2$ group, affording $CH_2(SiMe_3)_2$ and a hydrido complex.

$$Me_2SiCp''(R^*Cp)LnCH(SiMe_3)_2 + 2H_2 \rightarrow$$
$$[Me_2SiCp''(R^*Cp)LnH]_2 + 2CH_2(SiMe_3)_2$$

Thus the work has presented the first systematic study of the synthetic, spectroscopic and structural properties of chiral organolanthanides.

2.3. *Cyclopentadienyl-like complexes*

2.3.1. *Indenyl and fluorenyl complexes*

Evans et al. [63] published the synthesis and structures of indenyl and fluorenyl complexes of Sm(II), which were prepared by the reactions between the

$SmI_2(THF)_2$ and the corresponding potassium salts in THF.

$$SmI_2(THF)_2 + 2KC_9H_7 \rightarrow (C_9H_7)_2Sm(THF) + 2KI$$

$$SmI_2(THF)_2 + 2KC_{13}H_9 \rightarrow (C_{13}H_9)_2Sm(THF)_2 + 2KI$$

After crystallization of $(C_9H_7)_2Sm(THF)$ from THF, crystals of the trisolvate $(C_9H_7)_2$ $Sm(THF)_3$ were obtained. The crystallographic data for the latter complex were not complete owing to decomposition of the crystal during the X-ray diffraction experiment.

According to the X-ray structure the fluorenyl complex $(C_{13}H_9)_2Sm(THF)_2$ is an eight-coordinate disolvated complex (Fig. 46). The average Sm–C(ring) distance is 2.90(7) Å. Several bond distances and angles in the $(C_{13}H_9)_2$ $Sm(THF)_2$ suggest that the effective steric bulk of the fluorenyl ligand is less than that provided by the C_5Me_5 ligand.

2.3.2. *Heterocycles*

Jubb and Gambarotta [64] described the preparation of a low-valent samarium macrocyclic complex and its reaction with dinitrogen to form a tetralithium hydrazide salt (Scheme 30).

The X-ray crystal structure determination of $[(THF)_2Li(OEPG)Sm]_2(N_2Li_4)$ has shown a dimeric complex where two $(THF)_2Li(OEPG)Sm$ units are bridged by a planar N_2Li_4 moiety placed on a symmetry centre (Fig. 47). The crystal structure indicated that the molecule arises from the aggregation of two $(THF)_2Li(OEPG)Sm$ units, formally containing Sm(III), with an N_2Li_4 unit. The magnetic moment of 2.72 μ_B per dimeric complex was also as expected for a Sm(III) species.

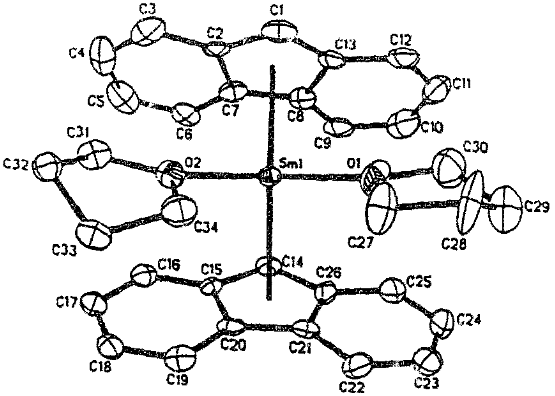

Fig. 46. Molecular structure of $(C_{13}H_9)_2Sm(THF)_2$.

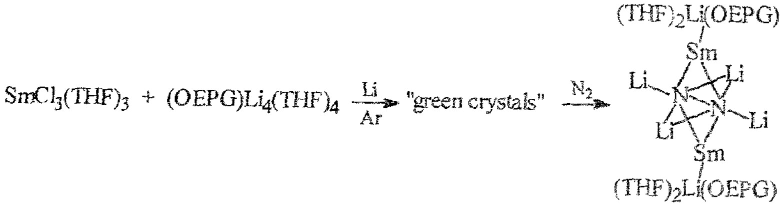

(OEPG = octaethylporphyrinogen)

Scheme 30.

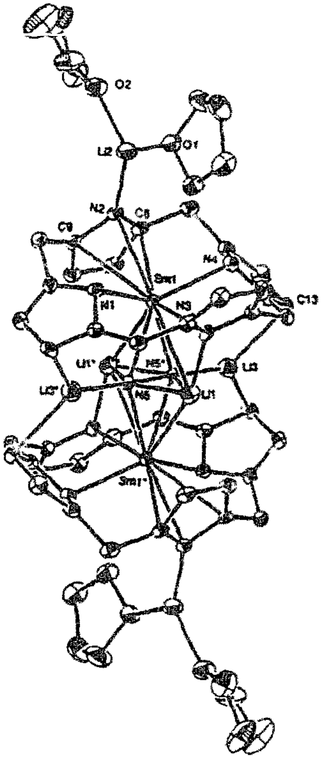

Fig. 47. Structure of $[(THF)_2Li(OEPG)Sm]_2(N_2Li_4)$ (OEPG = octaethylporphyrinogen).

2.4. Complexes with cyclooctatetraenyl ligands

Mashima et al. [65] published a preparation of monocyclooctatetraenyl-lanthanide complexes from metallic lanthanides and oxidants. The iodo(cyclooctatetraenyl) complexes of lanthanides $LnI(\eta^8\text{-cot})(THF)_n$ (cot = C_8H_8; Ln = La, Ce, Pr, $n=3$; Ln = Nd, $n=2$; Ln = Sm, $n=1$) have been prepared by the one-pot reaction of metallic lanthanides with cyclooctatetraene in the presence of an equimolar amount of iodine in THF.

$$Ln(metal) + C_8H_8 + 1SMOVER2I_2 \rightarrow LnI(C_8H_8)(THF)_n$$

$$Ln = La, Ce, Pr, n=3; Ln = Nd, n=2; Ln = Sm, n=1$$

Bromo- and chloro-bridged binuclear complexes of samarium, $[Sm(\mu\text{-}X)(cot)(THF)_2]_2$ (X = Br, Cl), were also prepared by the reaction of samarium metal with cyclooctatetraene in the presence of 1,2-dibromoethane or Ph_3PCl_2.

$$2Sm + 2C_8H_8 + Ph_3PCl_2 \rightarrow [Sm(\mu\text{-}Cl)(C_8H_8)(THF)_2]_2$$

Reaction among Sm, COT, and diphenyl disulphide in THF in the presence of a catalytic amount of iodine afforded $[Sm(\mu\text{-}SPh)(COT)(THF)_2]_2$. Similarly, $[Sm(\mu\text{-}SC_6H_2Me_3\text{-}2,4,6)(COT)(THF)_2]_2$ and $[Sm(\mu\text{-}SC_6H^i_2Pr_3\text{-}2,4,6)(COT)(THF)]_2$ were prepared. A benzeneselenolate complex $[Sm(\mu\text{-}SePh)(COT)(THF)_2]_2$ was also prepared by the same procedure.

$$2Sm + 2C_8H_8 + 12ArEEAr \rightarrow 12[Sm(\mu\text{-}EAr)(C_8H_8)(THF)_n]_2$$

$$EAr = SC_6H_5, n=2; EAr = SC_6H_2Me_3, n=2$$

$$EAr = SC_6H^i_2Pr_3, n=1; EAr = SeC_6H_5, n=2$$

The molecular structure of $[Sm(\mu\text{-}SePh)(COT)(THF)_2]_2$ was studied by X-ray diffraction (Fig. 48). The samarium atom has a pseudo square pyramidal and four-legged piano-stool geometry coordinated by one planar C_8H_8 ring, two bridging selenium atoms, and two oxygen atoms of THF. The Sm_2Se_2 unit is exactly planar, and two bridging selenium ligands are in a distorted trigonal-planar geometry. The Sm–Se bond distances are 3.015(2) and 3.174(2) Å.

Edelmann and coworkers [66] prepared $[Li(THF)_4][Ce(COT)_2]$ and $(THF)_3Na(\mu\text{-}COT)Ce(COT)$ (COT = η^8-cyclooctatetraenyl(2-)) complexes. The complex $[Li(THF)_4][Ce(COT)_2]$ was obtained as a by-product from $[(COT)Ce(\mu\text{-}Cl)(THF)_2]_2$ and $LiCH(SiMe_3)_2$ in THF. The structure consists of separated ions' pairs (Fig. 49). In the anion $[Ce(COT)_2]^-$ the central Ce atom is coordinated by two η^8-cyclooctatetraenyl rings to form a sandwich. The Ce(1)–COT(centroid) distance is 204.3(4) Å. In the cation $[Li(THF)_4]^+$ the Li has tetrahedral arrangement, which is formed by the coordination of four THF molecules.

The complex $(THF)_3Na(\mu\text{-}COT)Ce(COT)$ was separated from the reaction of $[(COT)Ce(\mu\text{-}Cl)(THF)_2]_2$ with ${}^tBuN{=}CH{-}CH{=}N^tBu$ in THF. In the structure of $(THF)_3Na(\mu\text{-}COT)Ce(COT)$ (Fig. 50), cerium and sodium are bound by the bridg-

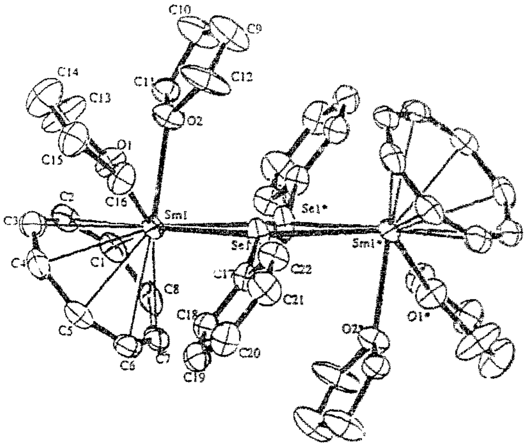

Fig. 48. Molecular structure of $[Sm(\mu\text{-}SePh)(COT)(THF)_2]_2$.

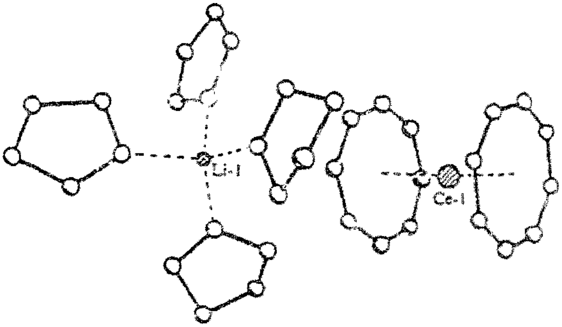

Fig. 49. Structure of $[Li(THF)_4][Ce(COT)_2]$.

ing μ-η^8:η^8-cyclooctatetraenyl ligand to give a linear (COT)Ce(μ-COT)Na arrangement. The distances Ce(1)–COT(1)(centroid) and Ce(1)–COT(2)(centroid) are 201.8(1) and 208.1(1) Å, the Na(1)–COT(2)(centroid) distance is 224.6(2) Å.

The same authors [67] also published the synthesis and studies of cyclooctatetraenyl lanthanide complexes with triflate and iodide ligands. Reaction between the anhydrous triflates $Ln(O_3SCF_3)_3$ (Ln = Ce, Pr, Nd, Sm) and K_2COT gave the dimeric complexes $[(COT)Ln(\mu\text{-}O_3SCF_3)(THF)_2]_2$.

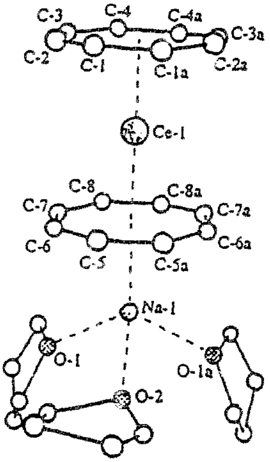

Fig. 50. Structure of $(THF)_3Na(\mu\text{-}COT)Ce(COT)$.

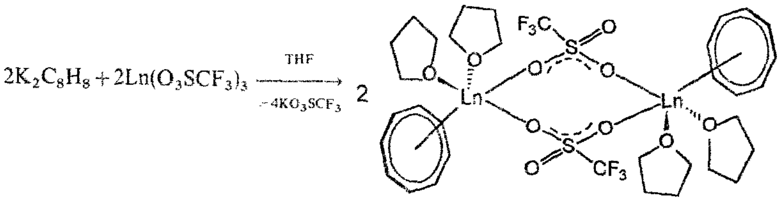

$$2K_2C_8H_8 + 2Ln(O_3SCF_3)_3 \xrightarrow[-4KO_3SCF_3]{THF} 2$$

The structure of $[(COT)Nd(\mu\text{-}O_3SCF_3)(THF)_2]_2$ consists of dimeric molecules with two bridging triflate-anions between two Nd atoms (Fig. 51). The Nd(1)–COT(1)(centroid) distance is 193.5(2) pm, the average Nd–O distance for triflate ligands is 248.6(3) pm.

The monomeric iodides $(COT)Ln(I)(THF)_3$ ($Ln = Nd$, Sm) were synthesized by the reaction of lanthanide triiodides with K_2COT:

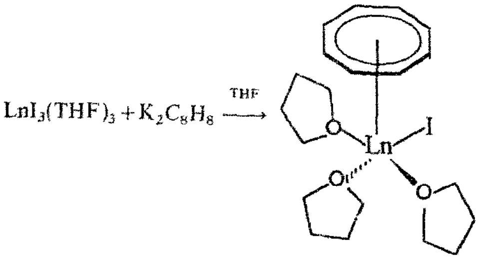

$$LnI_3(THF)_3 + K_2C_8H_8 \xrightarrow{THF}$$

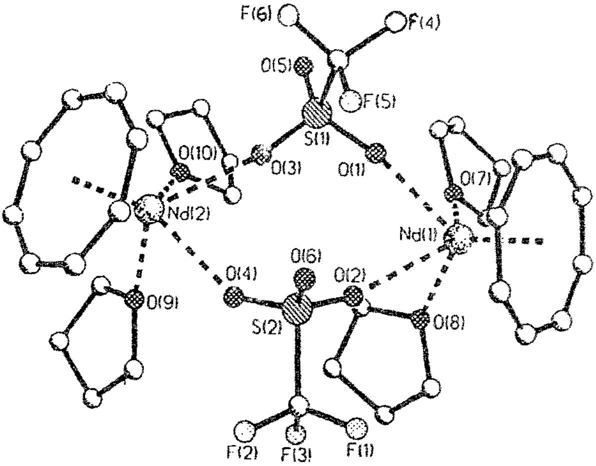

Fig. 51. Molecular structure of $[(COT)Nd(\mu\text{-}O_3SCF_3)(THF)_2]_2$.

The neodymium derivative $(COT)Nd(I)(THF)_3$ is isostructural with the previously described $(COT)Ce(I)(THF)_3$. The Nd–I distance is 328.7(1) pm.

Kilimann and Edelmann [68] also reported the synthesis of some yttrium half-sandwich cyclooctatetraenyl complexes. The complex $[(COT)Y(\mu\text{-}O_3SCF_3)(THF)]_2$ was obtained from $Y(O_3SCF_3)_3$ and K_2COT in THF. Reaction of $[(COT)Y(\mu\text{-}O_3SCF_3)(THF)]_2$ with pyrazolylborate anions gave the monomeric half-sandwich complexes $(COT)Y(HBpz_3)$ and $(COT)Y[HB(3,5\text{-}Me_2pz)_3]$. The yttrium benzamidinates $(COT)Y[MeOC_6H_4C(NSiMe_3)_2]THF$ and $(COT)Y[CF_3C_6H_4C(NSiMe_3)_2](THF)$ were prepared similarly. The treatment of $[(COT)Y(\mu\text{-}O_3SCF_3)(THF)]_2$ with $Li[Ph_2P(NSiMe_3)_2]$ led to the yttrium phosphazene derivative $(COT)Y[Ph_2P(NSiMe_3)_2](THF)$. All synthetic procedures are shown in the Scheme 31. The new organoyttrium complexes have been characterized by elemental analyses and spectroscopic methods, including ^{89}Y NMR spectroscopy.

Zhang et al. [69] published the synthesis and crystal structure of $[(C_8H_8)Dy\{\mu\text{-}OCH_2(CH_2)_2CH{=}CH_2\}(THF)]_2$. The complex $[(C_8H_8)Dy\{\mu\text{-}OCH_2(CH_2)_2CH{=}CH_2\}(THF)]_2$ was synthesized by the reaction of $DyCl_3$ and $K_2C_8H_8$ in THF, followed by the addition of $NaOCH_2(CH_2)_2CH{=}CH_2$.

$$DyCl_3 + K_2C_8H_8 \rightarrow (C_8H_8)DyCl(THF)_n + NaOCH_2(CH_2)_2CH{=}CH_2 \rightarrow$$

$$[(C_8H_8)Dy\{\mu\text{-}OCH_2(CH_2)_2CH{=}CH_2\}(THF)]_2 + KCl$$

The complex has a dimeric structure (Fig. 52). Each dysprosium is coordinated by one C_8H_8 ligand, one THF and two bridging $OCH_2(CH_2)_2CH{=}CH_2$ groups. The average Dy–C(C_8H_8 ring) distance is 2.593(6) Å.

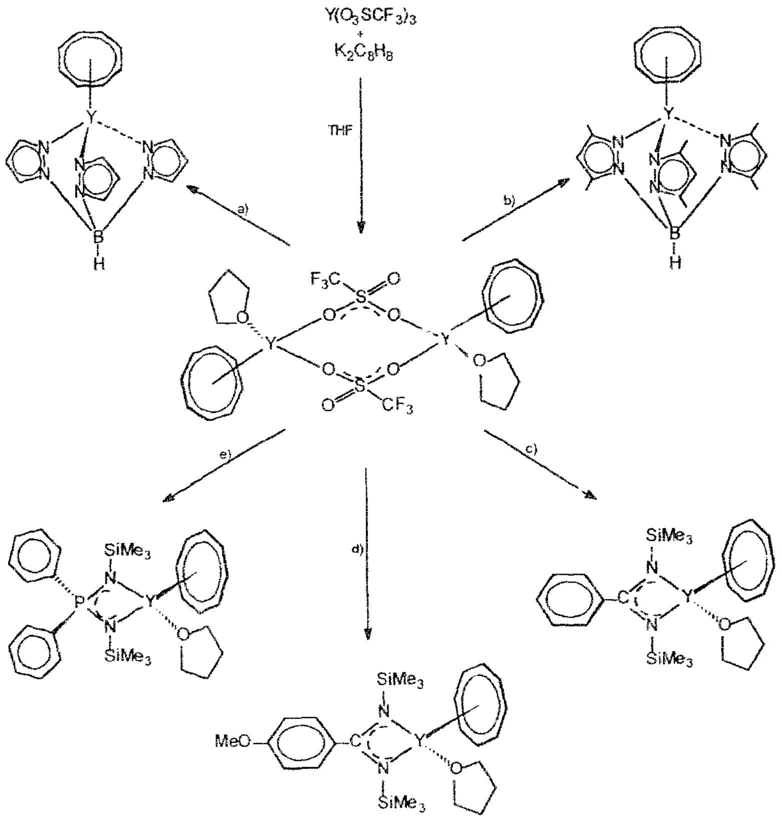

(a) $K[HBpz_3]$, (b) $K[HB(3,5\text{-}Me_2pz)_3]$, (c) $Li[MeOC_6H_4C(NSiMe_3)_2]$,

(d) $Li[CF_3C_6H_4C(NSiMe_3)_2]$, (e) $Li[Ph_2P(NSiMe_3)_2]$.

Scheme 31.

Kilimann et a.. [70] published the synthesis of some Ce(III), Ce(IV) and U(IV) cycloctatetraenyl complexes. The reaction of the dilithium salt of 1,4-bis(trimethylsilyl)cyclooctatetraene with anhydrous cerium trichloride led to the anionic sandwich complex, which was immediately converted to the neutral Ce(IV) derivative by oxidation with excess of silver iodide (Scheme 32).

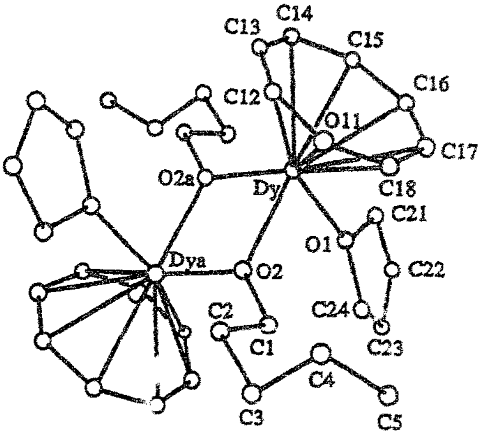

Fig. 52. Molecular structure of $[(C_8H_8)Dy\{\mu\text{-}OCH_2(CH_2)_2CH{=}CH_2\}(THF)]_2$.

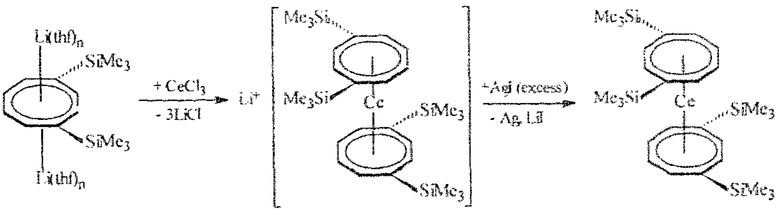

Scheme 32.

One more Ce(IV) sandwich complex was prepared by the reaction between the dipotassium salt of the 1,3,6-tris(trimethylsilyl)cyclooctatetraene and cerium triflate followed by oxidation of the ionic intermediate by AgI (Scheme 33).

The structure of the latter complex was studied by X-ray diffraction. In the structure (Fig. 53) the two annulene rings are η^8-coordinated to the Ce atom. The Ce1–C distances range from 267.0 to 275.1 pm. The two C_8-rings are not coplanar; the ring-centroid–Ce–ring-centroid angle is 176.1°.

A redox reaction of $[\{1,4\text{-}(Me_3Si)_2C_8H_6\}_2Ce]$ with cobaltocene afforded a novel Ce(III) ionic complex, in which both the cation and the anion are sandwich complexes (Scheme 34).

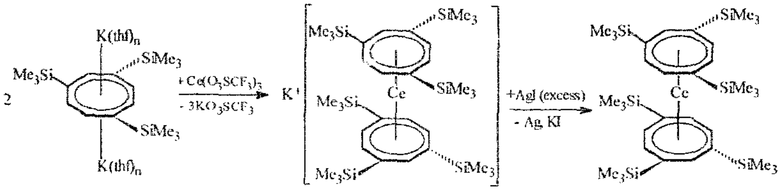

Scheme 33.

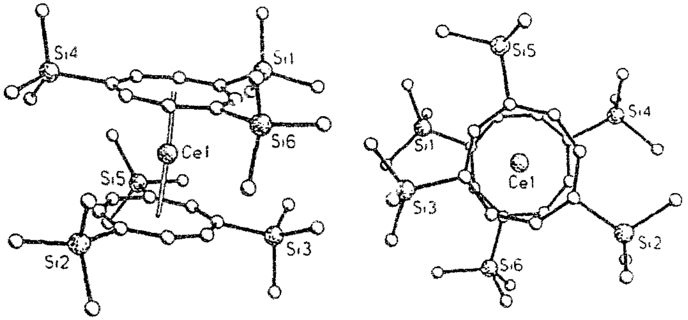

Fig. 53. Molecular structure of $[\{1,3,6\text{-}(Me_3Si)_3C_8H_5\}_2Ce]$.

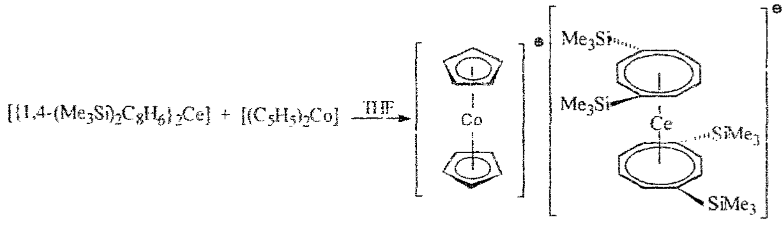

Scheme 34.

2.5. *Organolanthanide catalysis*

Li et al. [71] showed that the complex $(\eta^5\text{-}Me_5C_5)_2SmCH(TMS)_2$ serves as a precatalyst for the efficient and regiospecific hydroamination/cyclization of aliphatic and aromatic aminoalkynes $RC{\equiv}C(CH_2)_nNH_2$ to yield the corresponding heterocycles (Scheme 35).

Marks and coworkers [72] investigated the C_1-symmetric $Me_2Si(Me_4C_5)(C_5H_3R)\text{–}LnE(SiMe_3)_2$ (Ln = La, Nd, Sm, Y, Lu; E = N, CH;

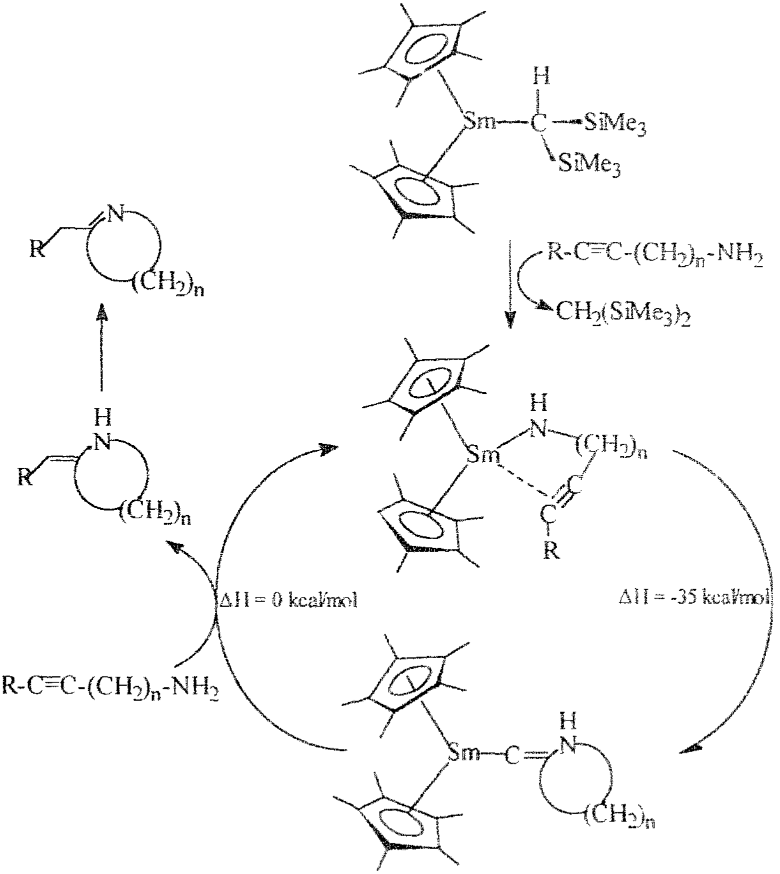

Scheme 35.

R* = chiral auxiliary) complexes as precatalysts for the efficient regio- and enantioselective hydroamination/cyclization of the aminoolefins 1-aminopent-4-ene, 2-aminohex-5-ene, 2,2-dimethyl-1-aminopent-5-ene, and 2,2-dimethyl-1-aminohex-5-ene to yield the corresponding heterocycles (Scheme 36).

The (+)-neomenthyl precatalysts (Ln = Nd, Sm) effect the cyclization of 2-aminohex-5-ene to *trans*-2,5-dimethylpyrrolidine in greater than 95% diastereoselectivity at 25 °C (Scheme 37).

The authors supposed that the basic mechanism for the present asymmetric aminoolefin hydroamination/cyclization by the chiral organolanthanides is ana-

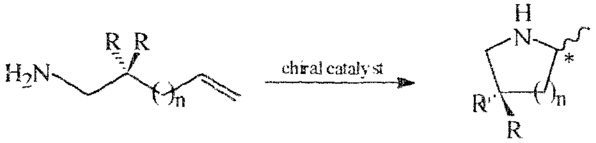

R = H, n=1; R = CH$_3$, n=1, 2.

Scheme 36.

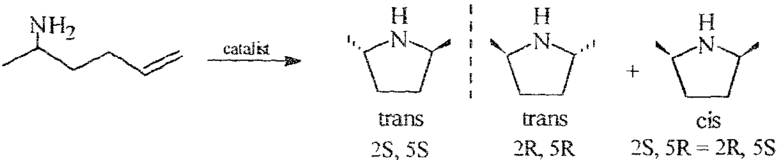

Scheme 37.

logous to the mechanism proposed for the achiral Cp'_2Ln-catalysed process (Scheme 38).

Yang et al. [73] reported on efforts to broaden the scope of polymerization/copolymerization using efficiently prepared methylenecyclopropane and organolanthanide catalysts of the type $[(\eta^5\text{-}C_5Me_5)_2LnH]_2$ (Ln = Lu, Sm). The homopolymerization of methylenecyclopropane in the presence of $[(\eta^5\text{-}C_5Me_5)_2LuH]_2$ proceeds cleanly to afford ring-opened, *exo*-methylene product. However, polymer yields are low and the polymerization process ceases before monomer consumption is complete. The larger Sm^{+3} ion effects catalytic methylenecyclopropane dimerization to yield the known 1,2-dimethylene-3-methylcyclopentane.

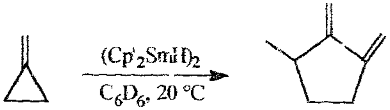

A probable mechanism for the reaction invokes β-H elimination and the intermediacy of a 1,3-diene fragment (Scheme 39).

Evans and Katsumata investigated the polymerization of ε-caprolactone [74] and copolymerization of ethylene carbonate and ε-caprolactone [75] by samarium complexes. Some characteristics of the catalysts are shown in Tables 1 and 2.

A variety of Sm(II) complexes generate a ring-opening polymerization system with ε-caprolactone in reactions which initially involve oxidation of the metal. The $(C_5Me_5)_2$–$Sm(THF)_x$ reaction has been shown to be an active polymerization system which maintains activity after all of the initial batch of monomer is consumed [74].

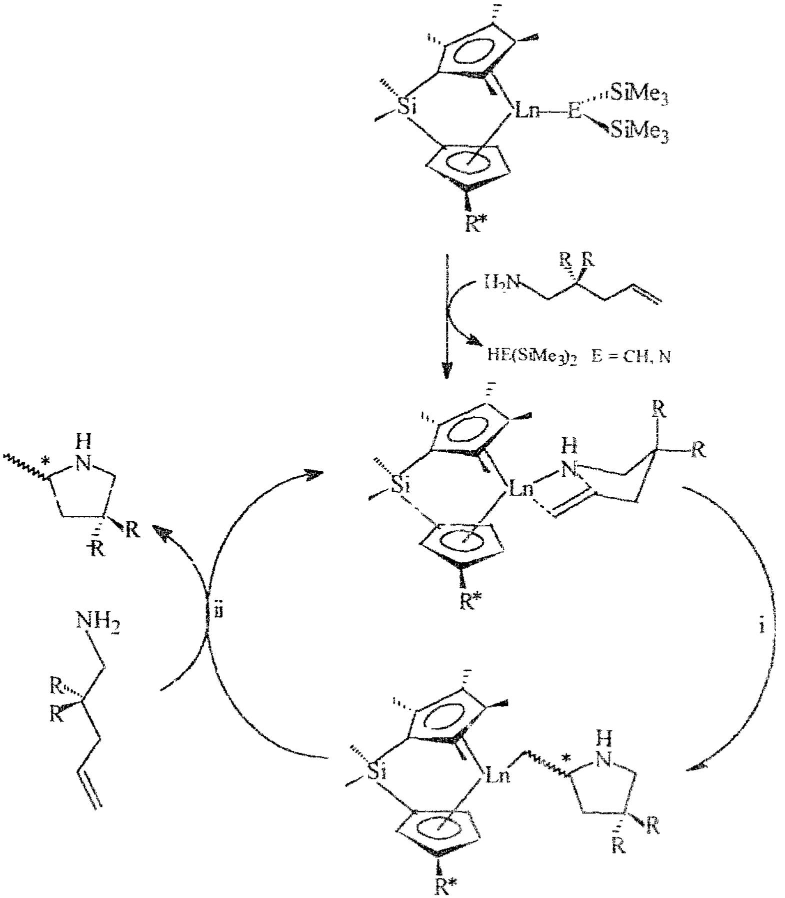

Scheme 38.

Ethylene carbonate can be incorporated into a caprolactone polymer using a Sm(II) catalyst precursor to form rubbery polymer with up to 22% ethylene carbonate content [75].

Taube and Windisch [24] reported the catalysis of butadiene polymerization by the complexes $[Li(C_4H_8O_2)][\eta^5\text{-}Cp'La(\eta^3\text{-}C_3H_5)_3]$ ($Cp' = C_5H_5$, C_5Me_5, C_9H_7) in toluene under standard conditions with moderate activity and high trans selectivity. The results are presented in Table 3.

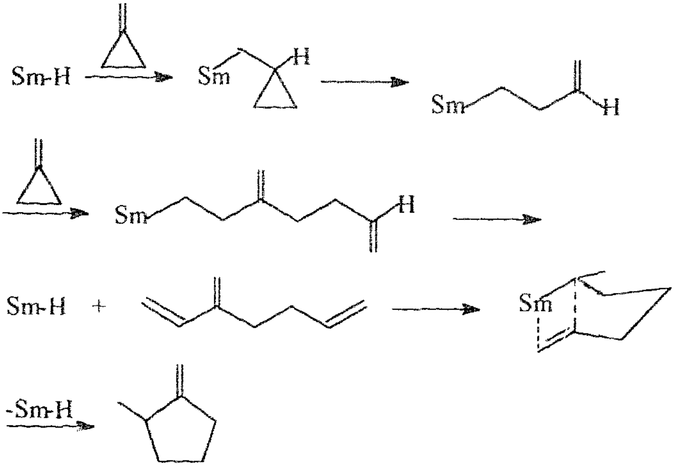

Scheme 39.

Table 1
Polymerization of ϵ-caprolactone by divalent samarium complexes [74]

Sm(II) complex	Solvent	Time	Yield (wt.%)	M_n	M/M_n
$(C_5Me_5)_2Sm(THF)_x$	toluene	1 min	15	9000	1.4
		5 min	61	18000	1.7
		1 h	99	63000	1.4
		6 h	98	29000	2.5
	THF	5 min	70	31000	1.5
	THF	1 h	98	56000	1.3
$(C_5Me_5)_2Sm$	toluene	5 min	55	17000	1.5
$(C_9H_7)_2Sm(THF)_x$	THF	5 min	98	30000	1.7
$(C_{13}H_9)_2Sm(THF)_2$	THF	5 min	94	24000	1.6
$[(Me_3Si)_2N]_2Sm(THF)_2$	toluene	1 min	99	17000	3.0

Onozawa et al. [76] revealed that a wide variety of aldehydes are efficiently dimerized to esters by a catalytic amount of $(C_5Me_5)_2LnCH(SiMe_3)_2$ (Ln = Nd, La).

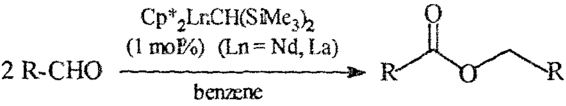

Table 2
Ethylene carbonate (EC)/ε-caprolactone (CL) copolymerization by divalent samarium complexes [75]

Catalyst	Solvent	EC/CL	Time (h)	Yield (wt.%)	GPC		EC content (mol%)	
					M_n	M_w/M_n	Calc.	Found
$(C_5Me_5)_2Sm(THF)_x$	toluene	100/100	1	12	6000	1.9		22
			6	54	43000	2.0		22
			24	68	82000	1.9	21	22
			48	70	82000	1.8	23	22
		40/160	24	94	95000	1.9	13	11
	THF	100/100	6	30	19000	1.7		12
			24	59	34000	1.9		
$(C_9H_7)_2Sm(THF)_{1.5}$	THF	100/100	6	14	18000	1.9		10
$(C_{13}H_9)_2Sm(THF)_2$	THF	100/100	6	63	28000	2.3	13	14
$[(Me_3Si)_2N]_2Sm(THF)_2$	toluene	100/100	1	30	7000	4.7		23

Table 3
Results of butadiene polymerization catalyzed by the complexes $[Li(C_4H_8O_2)][\eta^5\text{-}Cp'La(\eta^3\text{-}C_3H_5)_3]$ ($Cp' = C_5H_5$ (1), C_5Me_5 (2), C_9H_7 (3))

Catalyst	1	1	1	2	3
Temperature (°C)	25	50	50	50	50
Time of the reaction (h)	14	3	4	4	4
Yield (%)	71	43	25	57	74
Turnover number (mol C_4H_6 (mol La)$^{-1}$ h^{-1}	102	284	308	284	368
1,4-*trans*-Polybutadiene (%)	73	74	74	82	56
1,4-*cis*-Polybutadiene (%)	11	19	18	12	30
1,4-Polybutadiene (%)	16	7	8	6	14

The neodymium catalyst was applied to polyester synthesis starting with dialdehydes.

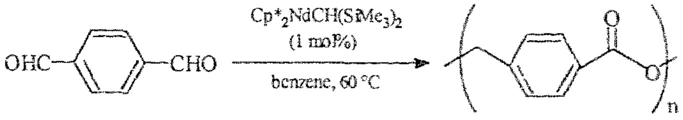

A stoichiometric reaction of the lanthanum complex with benzaldehyde indicated the intermediacy of alkoxo complexes in the catalysis.

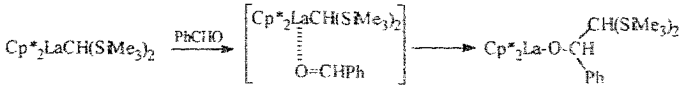

The same authors [77] also reported the hydrosilylation of dienes catalysed by $Cp_2^*NdCH(SiMe_3)_2$ (Scheme 40).

Two different catalytic cycles are possible for the hydrosilylation: one involving a hydridometal species as a key intermediate and the other being based on silylmetal species (Cycles A and B, Scheme 41).

In contrast, hydrosilylation of 1,5- and 1,6-dienes proceeded through intramolecular C–C bond formation to give (silylmethyl)cyclopentanes.

Qian et al [78] published the regioselective acylative cleavage of cyclic ethers catalysed by 1% Cp_2YCl or 10% $LnCl_3$ (Ln = Y, Yb, Er, Gd, Pr, Ce, La). Heavy rare earth trichlorides were much more catalytically active than the lighter ones.

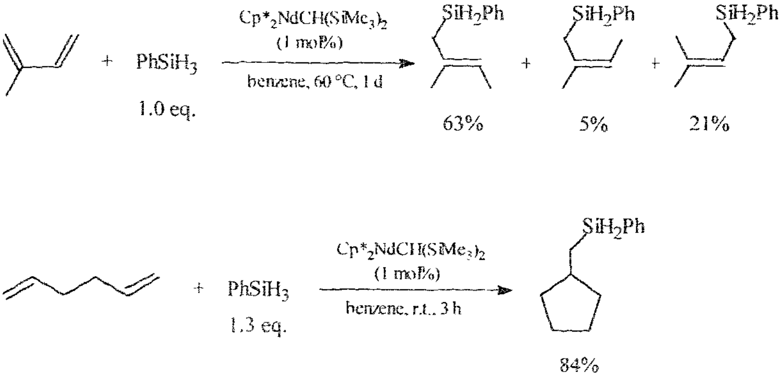

Scheme 40.

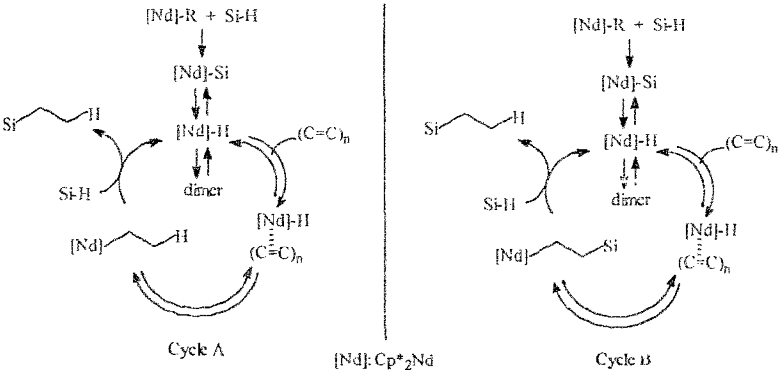

Scheme 41.

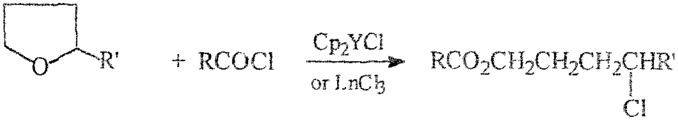

Yasuda [79] reported the preparation of lactone polymers at low temperature by ring-opening polymerization of lactones using the cyclopentadienyl complexes $(C_5R_5)_aLnX_b$ ($R = H$, Alk, $SiMe_3$; Ln = Sc, Y, La, Ce, Pr, Nd, Pm, Sm, Eu, Gd, Tb, Dy, Ho, Er, Tm, Yb, Lu); X = Cl, Br, I; $a + b = 3$) as catalysts.

Geerts [80] patented a catalytic system consisting of $Cp_nYX_{4-n} \cdot ML_x$ ($Cp = C_5H_5$ or C_5Me_5; X = halogen; M = alkali metal; L = electron donor ligand; $n = 1,2$) and an alkali or alkaline earth metal alkyl as cocatalyst. For example, ethylene was polymerized by using $(Me_5C_5)_2Y(\mu\text{-}Cl)_2K(THF)_2$ as catalyst and BuLi as cocatalyst in the presence of H_2.

Yokota [81] published catalysts containing organoaluminium compounds, Lewis bases and (substituted) dicyclopentadienyl lanthanides for preparation of polyolefins with controlled molecular weight. The polymerization of ethylene at 3 atm in PhMe in the presence of bis(pentamethylcyclopentadienyl)lutetium tetramethylaluminate and THF–trimethylaluminium complex produced polyethylene with $M_w = 2670$ and $M_w/M_n = 2.17$.

Schaverien [21,22] reported the α-olefin and diene polymerization catalysed by the yttrium complexes $[Y(C_5Me_5)(OC_6H_3^tBu_2)(\mu\text{-}H)]_2$ and $[Y(C_5Me_5)(OAr)]_2$-$(\mu\text{-}H)(\mu\text{-}CH_2CH_2R)$. The compounds are single-component catalysts for the polymerization of α-olefins. Dissolution of $[Y(C_5Me_5)(OC_6H_3^tBu_2)(\mu\text{-}H)]_2$ in 1-hexene led to slow polymerization to yield poly(1-hexene) with $M_w = 15\,700$, $M_n = 9400$, $M_w/M_n = 1.67$. The complex also cyclopolymerized the nonconjugated diene 1,5-hexadiene to afford poly(methylene-1,3-cyclopentane).

Hajela and Bercaw [61] investigated the model Ziegler–Natta olefin polymerization system $[Me_2Si(\eta^5\text{-}C_5Me_4)_2]Sc\{CH_2CH(CH_3)_2\}(PMe_3)$. The authors reported the competitive chain transfer by β-hydrogen and β-methyl elimination for the system.

Woo et al. [82,83] carried out nonlocal density functional (DF) calculations on the insertion of ethylene into the metal–CH_3 bond of Kaminsky-type metallocenes including Cp_2ScCH_3 . The DF calculations revealed that the insertion into the bis-Cp systems proceeds with 14 kJ mol^{-1} for Cp_2ScCH_3. This barrier is marginally influenced by going from the charged species $Cp_2ZrCH_3^+$ to the neutral d^0 system Cp_2ScCH_3.

Bierwagen et al. [84] reported investigations of the geometries of the isoelectronic model complexes X_2M–R including the complexes where M = Sc, X = Cl or $(\eta^5\text{-}C_5H_5)$ and R = H, CH_3, SiH_3. The Sc compounds strongly prefer a planar configuration that is related to the electronic configuration of Sc $(4s)^2(3d)^1$. The results suggested that $[(\eta^5\text{-}C_5H_4)CMe_2(\eta^5\text{-fluorenyl})]Sc$–R would not catalyse syndiotactic polymerization under these conditions.

3. Actinides

3.1. *Actinides complexes without supporting cyclopentadienyl ligands*

3.1.1. *Alkyl complexes*

Domingos et al. [85] published the synthesis of the tetravalent uranium hydrocarbyl compounds $UCl_2[CH(SiMe_3)_2]L^*$ ($L^* = HB(3,5\text{-}Me_2pz)_3$) and $UCl_{3-x}[CH_2(SiMe_3)_x]L^*$ by salt metathesis from $UCl_3L^*(THF)$ and the appropriate lithium alkyls:

$$UCl_3L^*(THF) + xLiR \rightarrow UCl_{3-x}R_xL^* + xLiCl$$

$$R = CH(SiMe_3)_2,\ x = 1;\ R = CH_2SiMe_3,\ x = 1,2,3$$

Reaction of $UCl_2(CH_2SiMe_3)L^*$ with stoichiometric amounts of ketones gave tertiary alkoxide derivatives as a result of insertion of the ketone into the U–C bond:

$$UCl_2(CH_2SiMe_3)L^* + OCR_2 \rightarrow UCl_2[OC(R)_2CH_2SiMe_3]L^*$$

$$R = Me, Et$$

Reaction of $UCl_2(CH_2\ SiMe_3)L^*$ with acetaldehyde and benzaldehyde led to the corresponding $UCl_2[OC(H)(R)CH_2SiMe_3]L^*$ (R = Me, Ph).

$$UCl_2(CH_2SiMe_3)L^* + RCHO \rightarrow UCl_2[OC(H)(R)CH_2SiMe_3]L^*$$

$$R = Me, Ph$$

When $UCl_2(CH_2\ SiMe_3)L^*$ reacted with two equivalents of aldehydes the reaction gave some different products:

$$UCl_2(CH_2SiMe_3)L^* + 2RCHO \rightarrow \overline{UCl_2[OC(H)(R)NN}C_5H_7]L^* + unidentified products$$

$$R = Me,Ph$$

The molecular structure of $UCl_2[OC(H)(Me)CH_2SiMe_3]L^*$ consists of monomeric units with the uranium atom in a distorted-octahedral environment (Fig. 54). The U–O distance is 2.05(2) Å, the average U–Cl and U–N bond distances are 2.61(1) Å and 2.48(2) Å respectively.

The structures of $\overline{UCl_2[OC(H)(R)NN}C_5H_7]L^*$ (R = Me (Fig. 55), Ph) and $\overline{UCl_2[OC(Me)_2NN}C_5H_7]L^*$ consist of discrete molecules. In the structures the uranium atom is seven-coordinate and displays capped-octahedral geometry.

3.1.2. *Complexes with phosphine ligands*

Edwards et al. [86] studied the reaction of $Th[P(CH_2CH_2PMe_2)_2]_4$ with carbon monoxide, which led to the compound $Th\{OC[P(CH_2CH_2PMe_2)_2]_2\}_2$. The molecule contains ten-coordinate thorium bonded to two di-anionic diphospha-secondary alkoxy ligands generated as a result of CO insertion (Fig. 56). Only two CO molecules

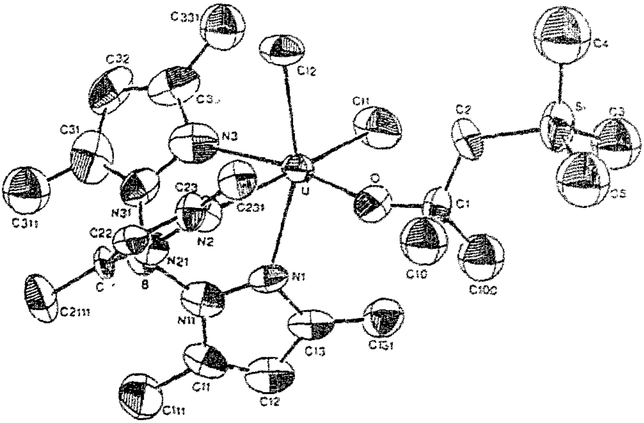

Fig. 54. Molecular structure of $UCl_2[OC(H)(Me)CH_2SiMe_3]L^*$ ($L^* = HB(3,5\text{-}Me_2pz)_3$).

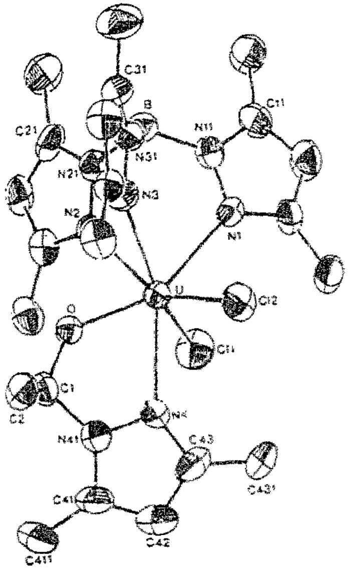

Fig. 55. Molecular structure of $\overline{UCl_2[OC(H)(Me)N}NC_5H_7]L^*$ ($L^* = HB(3,5\text{-}Me_2pz)_3$).

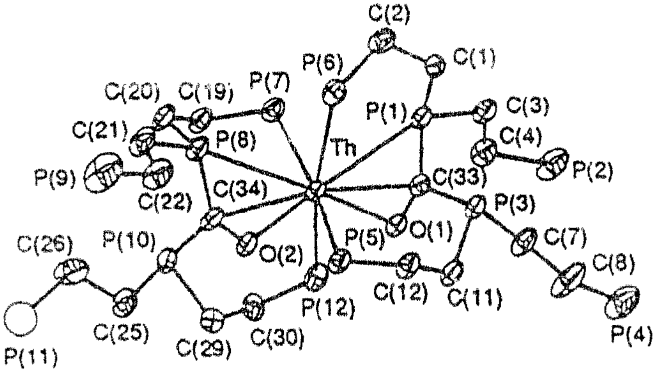

Fig. 56. Molecular structure of $Th\{OC[P(CH_2CH_2PMe_2)_2]_2\}_2$.

have inserted, each between two metal phosphide bonds, thereby coupling two phosphido phosphorus atoms at each CO carbon atom generating two new tertiary phosphines with concomitant formal reduction of the CO bond order from 3 to 1. Each P_2CO unit is η^3-bonded to the thorium atom with one of the phosphorus atoms coordinated to thorium. Although the geometry of the ten-coordinate thorium atom cannot be described in terms of any idealized polyhedron, if each η^3-PCO unit is considered to occupy one coordination site then the geometry is distorted trans-octahedral.

3.2. *Cyclopentadienyl complexes*

3.2.1. *Mono- and bis(cyclopentadienyl complexes)*

Gradós et al. [87] prepared several mono- and bis(pentamethylcyclopentadienyl) borohydrides of uranium (Scheme 42).

The complex $[U(C_5Me_5)_2(BH_4)_2]$ has been characterized by an X-ray crystal structure analysis (Fig. 57). The molecule adopts a pseudo-tetrahedral bent-sandwich configuration. The U–B and the average U–C bond distances are 2.58(3) Å and 2.74(3) Å respectively.

England et al. [88] reported new syntheses of $Cp^*_2ThPh_2$ and $Cp^*_2Th(Me)(aryl)$ derivatives. The complex $Cp^*_2ThPh_2$ was obtained from $Cp^*_2ThCl_2$ and PhMgBr in the presence of *p*-dioxane.

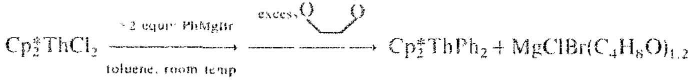
$$Cp^*_2ThCl_2 \xrightarrow[\text{toluene, room temp}]{\sim 2\text{ equiv PhMgBr}} \xrightarrow{\text{excess } C_4H_8O_2} Cp^*_2ThPh_2 + MgClBr(C_4H_8O)_{1,2}$$

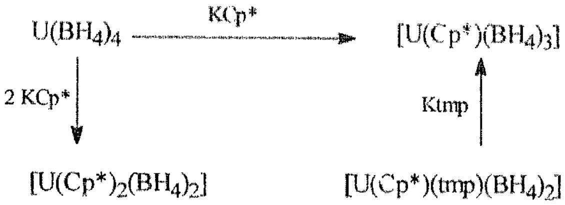

Cp* = C_5Me_5; tmp = C_4Me_4P

Fig. 42.

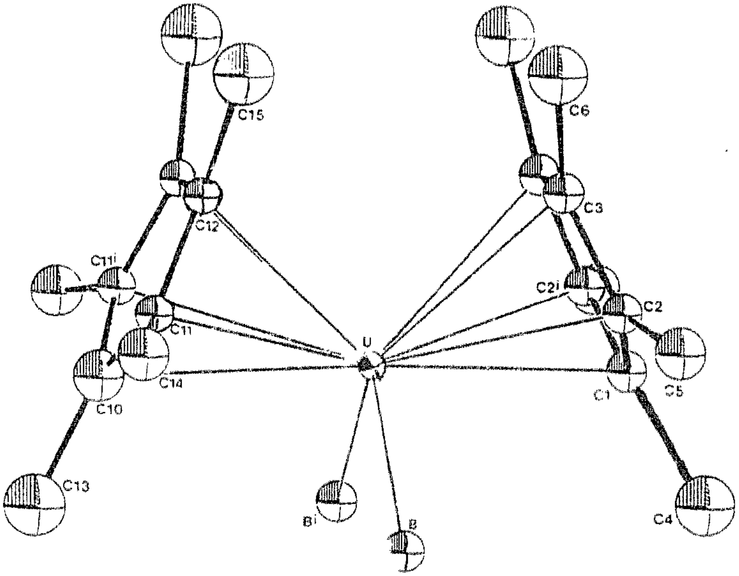

Fig. 57. Molecular structure of $[U(C_5Me_5)_2(BH_4)_2]$.

The aryl-halide intermediates and the respective methyl-aryl complexes $Cp_2^*Th(Me)(o\text{-}Ar)$ ($o-Ar = o\text{-}MeOC_6H_4$, $o\text{-}MeC_6H_4$ and $2.5\text{-}Me_2C_6H_3$ were prepared according to Scheme 43.

The tolyl and xylyl derivatives exits as pairs of rotamers in solution. The halide exchange was observed in the preparation of the aryl-halide complexes when arylmagnesium bromides were employed.

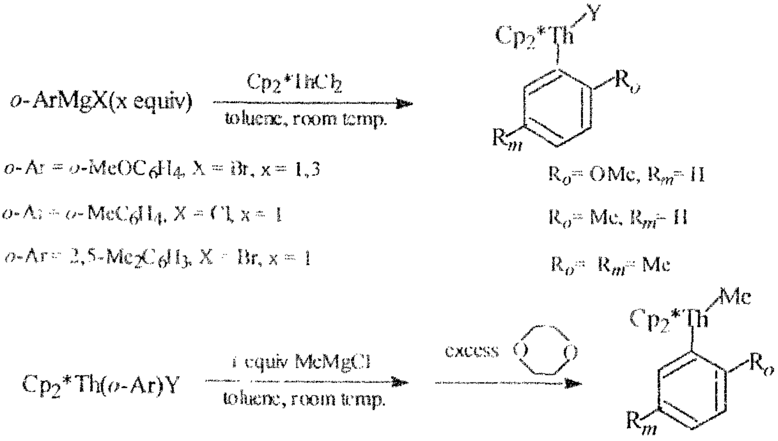

Scheme 43.

Jia et al. [89] reported the synthesis and properties of the cationic metallocene complex $Cp^*_2ThCH_3^+\{^tBuCH_2CH[B(C_6F_5)_2]_2H\}^-$ ($Cp^* = \eta^5$-C_5Me_5). The complex was obtained by the protolytic reaction of the $[HN^nBu_3]^+\{^tBuCH_2CH[B(C_6F_5)_2]_2H\}^-$ with $Cp^*_2Th(CH_3)_2$.

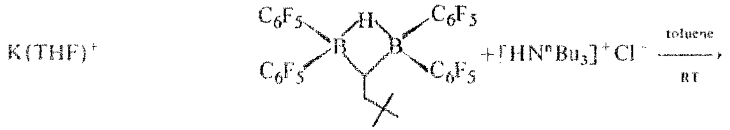

$[HN^nBu_3]^+[^tBuCH_2CH\{B(C_6F_5)_2\}H]^- + KCl$

$$Cp^*_2Th(CH_3)_2 + [HN^nBu_3]^+[^tBuCH_2CH\{B(C_6F_5)_2\}_2H]^- \xrightarrow[25\ ^\circ C]{toluene}$$

$$[Cp^*_2ThCH_3]^+[^tBuCH_2CH\{B(C_6F_5)_2\}_2H]^-$$

The mono-THF adduct $[Cp^*_2Th(CH_3)THF]^+[^tBuCH_2CH\{B(C_6F_5)_2\}_2H]^-$ has been characterized by X-ray diffraction. The complex consists of well-separated $Cp^*_2Th(CH_3)THF^+$ and $^tBuCH_2CH\{B(C_6F_5)_2\}_2H^-$ ions (Fig. 58). The cation adopts a 'bent metallocene' geometry with the angle Cp*ThCp* = 137.1° and with the distances Th–C(1) = 2.433(7), Th–O(1) = 2.455(4), $Th-C_{ring}$(av.) = 2.486 Å. The dinuclear anion contains an essentially planar four-membered ring with significant steric screening of the μ-H functionality. The average B–C(aryl) distance of 1.62 Å in the cation is shorter than in typical $CH_3B(C_6F_5)_3^-$ complexes (1.64–1.66 Å).

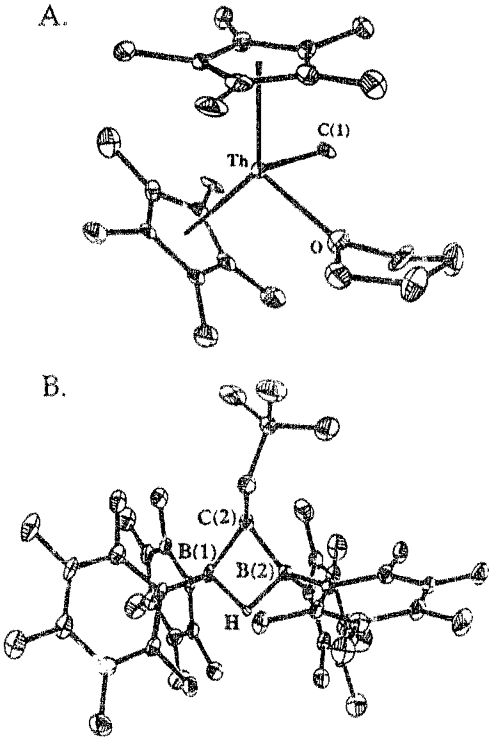

Fig. 58. Structure of $[Cp^*_2Th(CH_3)(THF)]^+[{}^tBuCH_2CH\{B(C_6F_5)_2\}_2H]^-$.

3.2.2. *Tris(cyclopentadienyl) complexes*

Cloke et al. [90] reported the synthesis of tris(tetramethylcyclopentadienyl) derivatives of the uranium and thorium $[MCl(\eta\text{-}C_5Me_4H)_3]$ (M = U, Th) from $[Li(C_5Me_4H)]$ and the appropriate MCl_4 in THF. The products have been characterized by variable-temperature NMR studies and the uranium complex by X-ray crystallography. In the molecular structure of $[UCl(\eta\text{-}C_5Me_4H)_3]$ (Fig. 59) the U–Cl vector lies on a crystallographic three-fold axis; the average U–C(Cp) lengths are 2.79 Å.

Ephritikhine and coworkers [91] reported the reaction of saturated ketones $RCOCH_2R'$ with the trivalent uranium complex $Cp_3U(THF)$ ($Cp = \eta\text{-}C_5H_5$) (Scheme 44). The reaction gave an equimolar mixture of the complexes Cp_3U–$OCHR(CH_2R')$ and Cp_3U–$OCR(=CHR')$. The hydrolysis of the compounds with deuterium oxide afforded respectively the O-deuterated pinacolyl alcohol and the pinacolone.

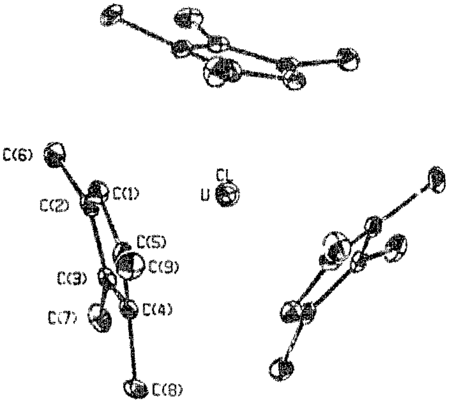

Fig. 59. Molecular structure of [UCl(η-$C_5Me_4H)_3$].

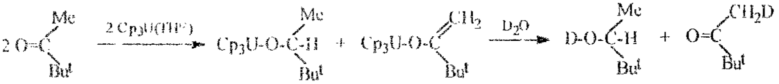

Scheme 44.

Ephritikhine and coworkers [92] also calculated the 'absolute' bond disruption enthalpies [D(U–S)], neglecting solvent effects and possible U–U interaction in L_3U from the oxidative addition reaction by batch-titration solution calorimetry in toluene.

$$UL_3(L = Cp', Cp^* \text{ or } Ind^*) + 1/2EtSSEt \rightarrow UL_3SEt \; \Delta H_{ox}$$

$$U(Cp^*)_3 + 1/2{}^tBuSS^tBu \rightarrow U(Cp^*)_3S^tBu \qquad \Delta H_{ox}$$

$$D[UL_3-SX] = 1/2D[XS-SX] - \Delta H_{ox}$$

The disruption enthalpy of the sulphur–sulphur bond was given by the expression:

$$D[XS-SX] = 2\Delta H_f^0(XS)_g + \Delta H_f^0(XS-SX)_g$$

The derived values were as follows (kJ mol^{-1}): 252 ± 8 (Cp′, Et); 266 ± 9 (Cp*. Et); 158 ± 8 (Cp*. ^{t}Bu) and 158 ± 8 (Ind*, Et).

Baudry et al. [93] investigated the reactivity of U–H and U–C bonds in electron-poor cyclopentadienyluranium complexes. The organouranium complexes [$(C_5H_4PPh_2 \cdot BH_3)_3UX$] (X = Cl, Me) were synthesized according to Scheme 45 ((i) addition of borane and subsequent reaction of the intermediate borane adduct with Na[$HBEt_3$] or LiMe; (ii) addition of three equivalents of borane to the methyl derivative or to the hydride [$(C_5H_4PPh_2)_3UH$]).

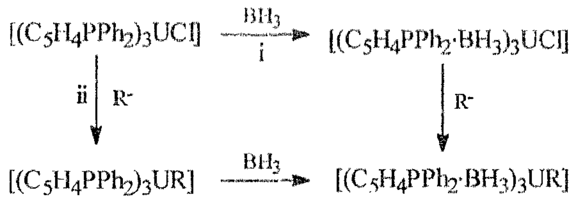

Scheme 45.

The complexes $[(C_5H_4PPh_2)_3UX]$ (X = Me, H) were converted finally into the complex $[(C_5H_4PPh_2 \cdot BH_3)_3UBH_4]$ according to Scheme 46.

The complexes $[(C_5H_4PPh_2 \cdot BH_3)_3UCl]$ and $[(C_5H_4PPh_2 \cdot BH_3)_3UBH_4]$ were easily reduced by sodium amalgam to afford the neutral complex $[(C_5H_4PPh_2 \cdot BH_3)_3U]$.

3.2.3. *Cyclopentadienyl-like complexes*

Arliguie et al. [94] published the ionic complexes $[K(18\text{-crown-6})][(NEt_2)_3U(\mu\text{-}\eta^7,\eta^7\text{-}C_7H_7)U(NEt_2)_3]$ and $[U(BH_4)_2(OC_4H_8)_5][(BH_4)_3U(\mu\text{-}\eta^7,\eta^7\text{-}C_7H_7)U(BH_4)_3]$. The $[(NEt_2)_3U(\mu\text{-}\eta^7,\eta^7\text{-}C_7H_7)U(NEt_2)_3]^-$ anion was formed by treatment of the amide complex $[U(NEt_2)_4]$ with $K[C_7H_9]$. Subsequent treatment of the product with 18-crown-6 leads to $[K(18\text{-crown-6})][(NEt_2)_3U(\mu\text{-}\eta^7,\eta^7\text{-}C_7H_7)U(NEt_2)_3]$.

The reaction between $[U(BH_4)_4]$ and $K[C_7H_9]$ gave $K[(BH_4)_3U(\mu\text{-}\eta^7,\eta^7\text{-}C_7H_7)U(BH_4)_3]$ and the concomitant product $[U(BH_4)_3]$. Recrystallization of the mixture from THF–pentane led to the crystals of $[U(BH_4)_2(OC_4H_8)_5][(BH_4)_3U(\mu\text{-}\eta^7,\eta^7\text{-}C_7H_7)U(BH_4)_3]$. The structure is composed of discrete cation–anion pairs. In the anion (Fig. 60) each uranium atom has a distorted tetrahedral environment formed by the bridging C_7H_7 ligand and three BH_4 groups. In the cation $[U(BH_4)_2(OC_4H_8)_5]^+$ the U atom is in a quite perfect pentagonal-bipyramidal arrangement with the tridentate borohydride ligands in apical position.

Grados et al. [87] also published the syntheses of mono- and bis(tetramethylphospholyl)uranium complexes $[U(tmp)Cl_3(L)_2]$ (tmp = C_4Me_4P, L = THF or L2 = dimethoxyethane), $[U(tmp)X_3]$ (X = BH_4, CH_2Ph), $[U(tmp)_2X_2]$ (X = Cl, BH_4, alkyl) or alkoxide) (Scheme 47).

The complex $[U(tmp)Cl_3(DME)]$ was characterized by X-ray crystallography. In

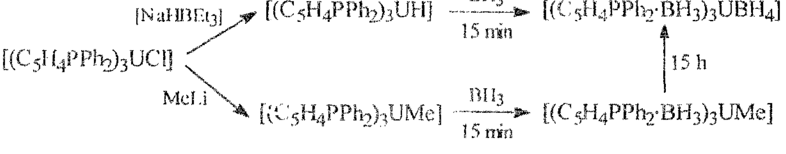

Scheme 46

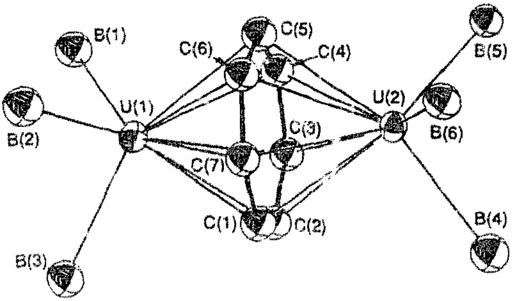

Fig. 60. Structure of anion $[(BH_4)_3U(\mu\text{-}\eta^7,\eta^7\text{-}C_7H_7)U(BH_4)_3]^-$.

$$\begin{tikzcd}
UCl_4 \arrow[r, "\text{1 Ktmp, 1 DME in toluene}"] \arrow[d, "\text{1 Ktmp, 2 THF in toluene}"'] & {[U(tmp)Cl_3(DME)]} \\
{[U(tmp)Cl_3(THF)_2]} & {[U(tmp)_2Cl_2]} \arrow[l, "\text{UCl}_4\text{ in THF}"'] \arrow[u, "\text{UCl}_4\text{ in DME}"']
\end{tikzcd}$$

$$[U(tmp)(BH_4)_3] + LiCH_2Ph \rightarrow [U(tmp)(CH_2Ph)_3] + 3LiBH_4$$

$$[U(tmp)_2(BH_4)_2] + 2LiR \rightarrow [U(tmp)_2(R)_2] + 2LiBH_4$$

Scheme 47.

the structure of $[U(tmp)Cl_3(DME)]$ (Fig. 61) the coordination geometry around uranium is mer pseudo-octahedral with the tmp-ligand and one oxygen atom of the DME molecule in trans axial positions, while the other oxygen and three chlorine atoms, which are coplanar within ±0.07(1) Å, constitute the equatorial plane.

The tetramethylphospholyl complexes were compared with their above-mentioned pentamethylcyclopentadienyl analogues (Scheme 42). Although the structures of tetramethylphospholyl uranium(IV) complexes and their pentamethylcyclopentadienyl counterparts are quite similar, the different electronic effects of C_5Me_5 and tmp ligands are manifested in the coordinating and redox properties of the complexes.

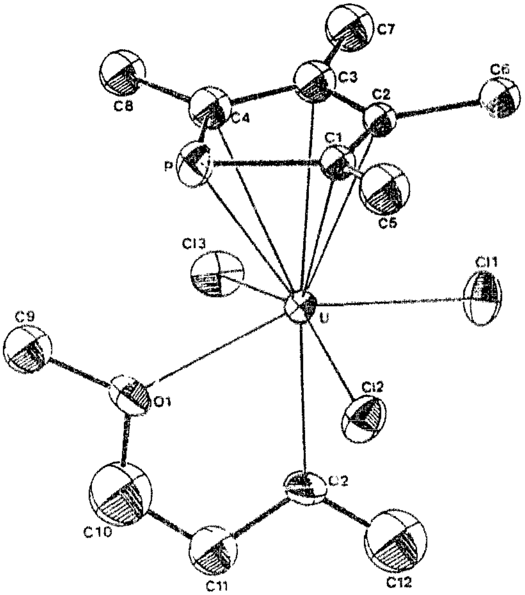

Fig. 61. Molecular structure of [U(tmp)Cl_3(DME)] (tmp = C_4Me_4P).

3.3. Complexes with cyclooctatetraenyl ligands

Leverd et al. [95] described the complexes [U(COT)$(SR)_2$] (R = ^{n}Bu, ^{i}Pr, ^{t}Bu), which were obtained by treating [U(COT)$(BH_4)_2$] with an excess of the corresponding thiol RSH or NaSR in toluene. The complex [U(COT)$(S^iPr)_2$] is built up of two monomeric units which are bridged by four S^{i}Pr groups (Fig. 62). Each uranium atom is five-coordinate in a quite perfect square-pyramidal arrangement, if COT is considered as a monodentate ligand. The U–S^{i}Pr distances range from 2.806(3) to 2.895(3) Å. The reaction of the [U(COT)$(BH_4)_2$] with NaS^{t}Bu led to the anionic species [U(COT)$(S^tBu)_3$]$^-$, for example [Na(thf)][U(COT)$(S^tBu)_3$].

Edelmann and coworkers [70] reported a uranium sandwich complex with the 1,3,6-$(Me_3Si)_3C_8H_5^{2-}$ ligand, which was obtained by the reaction of UCl_4 with two equivalents of the dipotassium salt of the ligand (Scheme 48).

3.4. Organoactinide catalysis

Jia et al. [89] reported the highly active catalyst for ethylene polymerization and 1-hexene hydrogenation $[Cp^*_2ThCH_3]^+[^tBuCH_2CH\{B(C_6F_5)_2\}_2H]^-$ (Cp* = η^5-

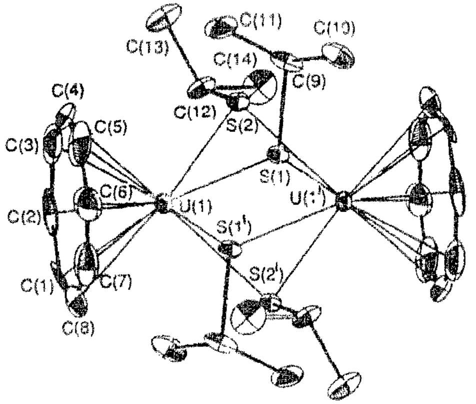

Fig. 62. Molecular structure of $[U(COT)(S^iPr)_2]$.

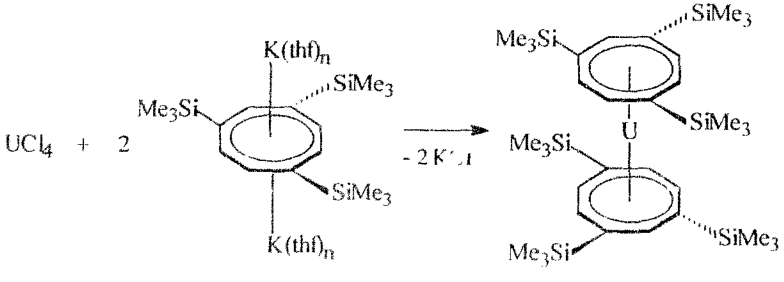

Scheme 48.

C_5Me_5). At 25°C, the activity of the compound was $5.8(1.1) \times 10^6$ g of linear polyethylene (mol Th)$^{-1}$ h^{-1} atm^{-1}; $Nt \approx 58(11)$ s^{-1}.

Samsel [96] patented actinide metallocene catalysts for the chain growth reaction of an α-olefin on an aluminium alkyl. A mixture of 15 mg $(\eta^5\text{-}C_5Me_5)_2ThCl_2$, 200 μl undecene, 5 ml Et_3Al and 5 ml PhMe was charged with ethylene to 100 psig, was heated 10 min at 70°C, then reacted with 1 ml Me-aluminoxane for 30 min; 2 ml Me-aluminoxane was added to the mixture in two portions to give an Al alkyl with C_{4-22} alkyl groups.

References

[1] C. Eaborn, P.B. Hitchcock, K. Izod and J.D. Smith, A monomeric solvent-free bent lanthanide dialkyl and a lanthanide analogue of a Grignard reagent. Crystal structures of $Yb\{C(SiMe_3)_3\}_2$ and $[Yb\{C(SiMe_3)_3\}I \cdot OEt_2]_2$. J. Am. Chem. Soc., 116 (1994) 12071-12072.

[2] K. Mashima, H. Sugiyama and A. Nakamura, Diene complex of lanthanum: the crystal structure of a diene-bridged dilanthanum complex, $[LaI_2(thf)_3(\mu\text{-}\eta^4{:}\eta^4\text{-}PhCH{=}CHCH{=}CHPh)LaI_2(thf)_3]$, J. Chem. Soc. Chem. Commun., (1994) 1581–1582.

[3] J.K. Perry and W.A. Goddard, III, Trends in Sc^+-alkyl bond strengths, J. Am. Chem. Soc., 116 (1994) 5013–5014.

[4] K.C. Crellin, S. Geribaldi and J.L. Beauchamp, Site selective σ-bond metathesis reactions of $Sc(CD_3)_2^+$ with $[2,2\text{-}D_2]$propane, $[1,1,1,4,4,4,\text{-}D_6]$-*n*-butane and [2-D]isobutane, Organometallics, 13 (1994) 3733–3736.

[5] B.H. Lipshutz, C. Lindsley, R. Susfalk and T. Gross, A convenient preparation of triisopropylsilyl acyl silanes, Tetrahedron Lett., 35 (1994) 8999–9002.

[6] M. Murakami and Y. Ito, Carbon–carbon bond forming reactions via new organosamarium(III) intermediates, J. Organomet. Chem., 473 (1994) 93–99.

[7] H. Liang, Q. Shen, J. Guan and Y. Lin, A new method for the synthesis of $Ln(\eta^6\text{-}C_6Me_6)(AlCl_4)_3$ (Ln = Nd, Sm, Gd, Yb), and the X-ray crystal structure of $Yb(\eta^6\text{-}C_6Me_6)(AlCl_4)_3 \cdot MeC_6H_5$, J. Organomet. Chem., 474 (1994) 113–116.

[8] B. Boje and J. Magull, Zur Reaction von 2,2-Dilithiumbiphenyl mit $SmBr_3$. Die Struktur von $[(C_{24}H_{16})SmBr(thf)_2]_2 \cdot [C_{24}H_{14}]$, Z. Anorg. Allg. Chem., 620 (1994) 703–706.

[9] H.H. Karsch, G. Ferazin and P. Bissinger, High phosphine coordination numbers of the lanthanoids: σ- and π-type coordination in $[Sm\{CH(PMe_2)_2\}_3]_2$, J. Chem. Soc. Chem. Commun., (1994) 505–506.

[10] S. Hao, J. Song, H. Aghabozorg and S. Gambarotta, Diphenylphosphino-methanide complexes of chromium(II) and samarium(III): preparation and characterization of the dinuclear $[Cr\{Ph_2PC(H)PPh_2\}_2](\mu\text{-}Cl)[\mu\text{-}C(H)(PPh_2)_2][Cr\{Ph_2PC(H)PPh_2\}]$ and mononuclear pseudo-allylic $Sm[\eta3\text{-}Ph_2PC(H)PPh_2]_2$, J. Chem. Soc. Chem. Commun., (1994) 157–158.

[11] D.M. Barnhart, D.L. Clark, J.C. Gordon, J.C. Huffman, R.L. Vincent, J.G. Watkin and B.D. Zwick, Synthesis, properties, and X-ray structures of the lanthanide η^6-arene-bridged aryloxide dimers $Ln_2(O\text{-}2,6\text{-}i\text{-}Pr_2C_6H_3)_6$ and their Lewis base adducts $Ln(O\text{-}2,6\text{-}i\text{-}Pr_2C_6H_3)_3(THF)_2$ (Ln = Pr, Nd, Sm, Gd, Er, Yb, Lu), Inorg. Chem., 33 (1994) 3487–3497.

[12] P. Biagini, G. Lugli and L. Abis, Alkylation of lanthanide alkoxides: synthesis of $[Ln(\mu\text{-}O^tBu)_3(\mu\text{-}Me)_3(AlMe_2)_3]$ (Ln = Pr, Nd or Y), J. Organomet. Chem., 474 (1994) C16–C18.

[13] N. Greeves, L. Lyford and J.E. Pease, Ligand effects on diastereoselective addition of organocerium reagents to aldehydes and cyclic ketones, Tetrahedron Lett., 35 (1994) 285–288.

[14] C. Capp, T.D. Wood, A.G. Marshall and J.V. Coe, High-pressure toluene extraction of $La@C_n$ for even *n* from 74 to 90, J. Am. Chem. Soc., 116 (1994) 4987–4988.

[15] X. Zhou, Z. Wu, H. Ma, Z. Xu and X. You, Synthesis and structure of monocyclopentadienylyttrium(III) dichloride tris(tetrahydrofuran), Polyhedron, 13 (1994) 375–378.

[16] G. Depaoli, U. Russo, G. Valle, F. Grandjean, A.F. Williams and G.J. Long, 4f Orbital covalence in $(\eta^5\text{-}C_5H_5)_3Eu(THF)$ as revealed by europium-151 Mössbauer spectroscopy, J. Am. Chem. Soc., 116 (1994) 5999–6000.

[17] W.J. Evans, J.L. Shreeve and J.W. Ziller, Synthesis and characterisation of the first pentamethylcyclopentadienyl complex of trivalent europium: $[(C_5Me_5)Eu(OCMe_3)(\mu\text{-}OCMe_3)]_2$, Organometallics, 13 (1994) 731–733.

[18] M. Rieckoff, M. Noltemeyer and F.T. Edelmann, Ein alter Ligand in neuer Umgebung: Dreifach verbrückendes *O,O'*-Dimethyldithiophosphat im Organosamarium-Komplex $[(C_5Me_5)Sm\{S_2P(OMe)_2\}_2]_2$, J. Organomet. Chem., 469 (1994) C19–C21.

[19] P.J. Shapiro, W.D. Cotter, W.P. Schaefer, J.A. Labinger and J.E. Bercaw, Model Ziegler–Natta α-olefin polymerisation catalysts derived from $[\{(\eta^5C_5Me_4)SiMe_2(\eta^1\text{-}NCMe_3)\}(PMe_3)Sc(\mu_2\text{-}H)]_2$ and $[\{(\eta^5\text{-}C_5Me_4)SiMe_2\text{-}(\eta^1\text{-}NCMe_3)\}Sc(\mu_2\text{-}CH_2CH_2CH_3)]_2$. Synthesis, structures and kinetic and equilibrium investigations of the catalytically active species in solution, J. Am. Chem. Soc., 116 (1994) 4623–4640.

[20] X. Shen, Y. Xie, H. Jiang and Q. Li, Synthesis and characterization of cyclopentadienyl lanthanide complexes with benzophenoneoximato and 8-quinolinolato ligands, Pol. J. Chem., 68 (1994) 1303–1307.

[21] C.J. Schaverien, Alkoxides as ancillary ligands in organolanthanide chemistry: synthesis of, reactivity of, and olefin polymerization by the μ-hydride μ-alkyl compounds $[Y(C_5Me_5)(OC_6H_3^tBu_2)]_2(\mu\text{-}H)(\mu\text{-}alkyl)$, Organometallics, 13 (1994) 69–82.

[22] C.J. Schaverien, Alkoxides as ancillary ligands in organolanthanide chemistry: synthesis, reactivity, α-olefin and diene polymerization by $[Y(C_5Me_5)(OC_6H_3^tBu_2)(\mu\text{-}H)]_2$, J. Mol. Catal., 90 (1994) 177–183

[23] L. Mao, Q. Shen and S. Jin, Synthesis and crystal structure of $[Li(THF)_4][(^tBuCp)Yb(NPh_2)_3]$, Polyhedron, 13 (1994) 1023–1025.

[24] R. Taube and H. Windisch, XLIV. Darstellung und Charakterisierung von Monocyclopentadienyl-triallyl)lanthanat(III)-Komplexen und ihre Eignung zur Katalyse der stereospezifischen Butadienpolymerisation, J. Organomet. Chem., 472 (1994) 71–77.

[25] X. Shen and Y. Xie, Synthesis and characterization of cyclopentadienyl lanthanide complexes containing mixed oximato ligands, Synth. React. Inorg. Met. Org. Chem., 24 (1994) 267–276.

[26] Z. Wu, X. Zhou, W. Zhang, Z. Xu, X. You and X. Huang, A novel bonding mode of oximato ligand to a metal; synthesis and X-ray crystal structure of bis[acetone oximatobis(cyclopentadienyl)gadolinium] $[\{(C_5H_5)_2Gd(\mu\text{-}\eta^2\text{-}ONCMe_2)\}_2]$, J. Chem. Soc. Chem. Commun., (1994) 813–814.

[27] S. Wang, Y. Yu, Z. Ye, Ch. Qian and X. Jin, Synthesis of an organolanthanoid complexes with a novel high-strain anionic cyclohexen-4-yne ligand and crystal structure of $[(\eta^5\text{-}Cp)_2Sm(\eta^5\text{-}C_6H_5)(thf)]$, J. Chem. Soc. Chem. Commun., (1994) 1097–1098.

[28] G. Deacon, G.M. Forsyth and J. Sun, Regiospecific replacement of fluorine by hydrogen in an aromatic ring induced by a rare earth organometallic, Tetrahedron Lett., 35 (1994) 1095–1098.

[29] J. Guan, Q. Shen, S. Jin and Y. Lin, Synthesis and crystal structure of bis(cyclopentadienyl)amido complex of neodymium, $[Li(DME)_3][(\eta^5\text{-}C_5H_5)_2\,Nd(NPh_2)_2]$, Polyhedron, 13 (1994) 1695–1699.

[30] Ch. Qian, B. Wang, D. Deng and J. Hu, Studies on organolanthanide complexes. 53. Effect of rare earth metal radius on the molecular structure: synthesis and X-ray crystal strucure of bis(2-methoxyethyl)cyclopentadienyl) rare earth metal chlorides, Inorg. Chem., 33 (1994) 3382–3388.

[31] C. Qian, X. Zheng, B.Wang, D. Deng and J. Sun, Studies on organolanthanide complexes LIV. Syntheses and X-ray crystal structures of bis(2-methoxyethyl cyclopentadienyl) rare earth iodides $(MeOCH_2CH_2C_5H_4)_2LnI$ (Ln = La or Y), J. Organomet. Chem., 466 (1994) 101–105.

[32] S. Zhang, X. Zhuang, G. Wei and W. Chen, Syntheses of $(C_4H_7OCH_2C_5H_4)_2LnCl$ (Ln = Nd, Gd, Dy, Yb) and crystal structure of $(C_4H_7OCH_2C_5H_4)_2DyCl$, Polyhedron, 13 (1994) 2867–2871.

[33] D. Deng, Y. Jiang, Ch. Qian, G. Wu and P. Zheng, Studies on organolanthanide complexes. LXIII. Synthesis, spectroscopic and X-ray crystallographic characterization of new early organolanthanide, organoyttrium hydride and organoholmium hydroxide complexes, J. Organomet. Chem., 470 (1994) 99–107.

[34] D. Deng, X. Zheng, C. Qian, J. Sun and L. Zhang, Studies on organolanthanide complexes XLVII. Syntheses of bis(2-methoxyethylcyclopentadienyl)lanthanide tetrahydroborates (Ln = La, Pr, Nd, Sm or Gd); crystal structures of bis(2-methoxyethylcyclopentadienyl) praseodymium and neodymium tetrahydroborates, J. Organomet. Chem., 466 (1994) 95–100.

[35] D. Deng, X. Zheng, Ch. Qian, J. Sun, A. Dormond, D. Baudry and M. Visseaux, Synthesis, fluxional behaviour in solution and crystal structure of the organolanthanide complexes $[Ln(C_5H_4CH_2CH_2OMe)_2(thf)][Co(CO)_4]$ (Ln = Sm or Yb, thf = tetrahydrofuran), J. Chem. Soc. Dalton Trans., (1994) 1665–1669.

[36] G. Lin and W.-T. Wong, Synthesis and structural characterization of sodium (diphenylphosphino)-cyclopentadienyl and derived heterobimetallic complex $[\{(C_6H_5)_2P(\eta^5\text{-}C_5H_4)\}_2Yb(\mu\text{-}Cl)_2Na(C_4H_{10}O_2)_2]$, Polyhedron, 13 (1994) 3027–3030.

[37] J.R. van den Hende, P.B. Hitchcock and M.F. Lappert, The synthesis and X-ray structures of ytterbocene(II) complexes containing pendant pyridyl groups, $[Yb(Cp_x)_2]$ $\{Cp_x = \eta^5\text{-}C_5H_3(R)[CMe_2(CH_2)_nC_5H_4N\text{-}2]\text{-}1,3$; R = H or $SiMe_3$ and $n = 0$ or 1}, J. Organomet. Chem., 472 (1994) 79–85

[38] I.P. Beletskaya, A.Z. Voskoboynikov, A.K. Shestakova, A.I. Yanovsky, G.K. Fukin, L.N. Zacharov, Yu.T. Struchkov and H. Schumann, The reaction of alkyl derivatives of yttrium and lutetium with organic disulphides and diselenides: the molecular structure of $\{(^tBuC_5H_4)_2Y(\mu\text{-}SePh)\}_2 \cdot C_6H_6$, J. Organomet. Chem., 468 (1994) 121–124.

[39] W.E. Piers, D.J. Parks, L.R. MacGillivray and M.J. Zaworotko, Mechanistic aspects of the permethylscandocene tellurolates and tellurides. X-ray structures of $(C_5Me_5)_2ScTeCH_2C_6H_5$, $[(C_5Me_5)_2Sc]_2(\mu\text{-}Te)$, and $[(C_5Me_5)_2Sc]_2(\mu\text{-}Se)$, Organometallics, 13 (1994) 4547–4558.

[40] W.E. Piers, Evidence for concerted extrusion of TeR_2 from permethylscandocene tellurolates, J. Chem. Soc. Chem. Commun., (1994) 309–310.

[41] W.J. Evans, G.W. Rabe, J.W. Ziller and R.J. Doedens, Utility of organosamarium(II) reagents in the formation of polyatomic Group 16 element anions: synthesis and structure of $[(C_5Me_5)_2Sm]_2(E_3)(THF)$, $[(C_5Me_5)_2Sm(THF)]_2(E)$, and related species (E = S, Se, Te), Inorg. Chem., 33 (1994) 2719–2726.

[42] J. Scholz, A. Scholz, R. Weimann, C. Janiak and H. Schumann, N-Heteroaren-Dianionen als antiaromatiche Brückenliganden zwischen zwei Lanthanocen-Einheiten, Angew. Chem., 106 (1994) 1221–1223.

[43] W.J. Evans, Sh.L. Gonzales and J.W. Ziller, Reactivity of decamethylsamarocene with polycyclic aromatic hydrocarbons, J. Am. Chem. Soc., 116 (1994) 2600–2608.

[44] A.J. Arduengo, III, M. Tamm, S.J. McLain, J.C. Calabrese, F. Davidson and W.J. Marshall, Carbene–lanthanide complexes, J. Am. Chem. Soc., 116 (1994) 7927–7928.

[45] H. Schumann, M. Glanz, J. Winterfeld, H. Hemling, N. Kuhn and T. Kratz, Metallorganische Verbindungen der Lanthanoide, 91. – Carben-Addukte des zweiwertigen Samariums und Ytterbiums, Chem. Ber. [illegible] (1994) 2369–2372.

[46] N.S. Radu, P.K. Gantzel and T.D. Tilley, Lanthanide–tungsten heterobimetallic complexes via σ-bond methathesis, J. Chem. Soc. Chem. Commun., (1994) 1175–1176.

[47] N.S. Radu and T.D. Tilley, Sigma-bond metathesis reaction involving lanthanide–silicon and lanthanide–hydrogen bonds, Phosphorus, Sulfur, and Silicon, 87 (1994) 209–218.

[48] B.J. Deelman, W.M. Stevels, J.H. Teuben, M.T. Lakin and A.L. Spek, Insertion chemistry of $Cp^{\ddagger}_2Y(2\text{-}pyridyl)$ and molecular structure of the unexpected CO insertion product $(Cp^{\ddagger}_2Y)_2(\mu\text{-}\eta^2{:}\eta^2\text{-}OC(NC_5H_4)_2)$, Organometallics, 13 (1994) 3881–3891.

[49] S. Di Bella, A. Gulino, G. Lanza, I. Fragalà, D. Stern and T.J. Marks, Photoelectron spectroscopy of f-element organometallic complexes. 12. A comparative investigation of the electronic structure of lanthanide bis(polymethylcyclopentadienyl)hydrocarbyl complexes by relativistic ab initio and DV-Xα calculations and gas-phase UV photoelectron spectroscopy, Organometallics, 13 (1994) 3810–3815.

[50] W. Chen, G. Lin, J. Xia, G. Wie, Y. Zhang and Z. Jin, Syntheses and crystal structures of $(\eta^5\text{-}C_5H_5)_3Ln(THF)$ (Ln = Ce, Er), J. Organomet. Chem., 467 (1994) 75–78.

[51] S. Wang, Y. Yu, Z. Ye and C. Qian, The formation and molecular structure of $(\eta^5\text{-}C_5H_5)_3Sm\cdot OC_4H_8$, J. Organomet. Chem., 464 (1994) 55–58.

[52] Z. Wu, Z. Xu, X. You, X. Zhou, X. Huang and J. Chen, Formation and crystal structures of $(C_5H_5)_3Sm(THF)$ and $(C_5H_5)_3Dy(THF)$, Polyhedron, 13 (1994) 379–384.

[53] S.Ya. Knjazhansky, I.Yu. Nomerotsky, B.M. Bulychev, V.K. Belsky and G.L. Soloveichik, Unprecedented coordination of the AlH_2^+ and Na^+ cations in the structure of the organometallic complex $[AlH_2(OC_4H_8)_4][(\eta^5\text{-}C_5H_5)_3Yb(\mu\text{-}Na)Yb(\eta^5\text{-}C_5H_5)_3]$, Organometallics, 13 (1994) 2075–2078.

[54] J. Ren, J. Guan and S. Jin, Synthesis and X-ray structure of an organolanthanum complex $[(^tBuCp)_3LaClLi(THF)_3]$, Polyhedron, 13 (1994) 2979–2982.

[55] Ch. Sun, G. Wei, Zh. Jin and W. Chen, Synthesis and crystal structure of $[Me_4C_2Cp_2SmCl\cdot THF]_2$, Polyhedron, 13 (1994) 1483–1487.

[56] G. Paolucci, R. D'Ippolito, Ch. Ye, J. Gräper and D.R. Fischer, New dinuclear bis(cyclopentadienyl)-lanthanoid chlorides containing $\eta^5\text{-}C_5H_4$ ligands linked by a metal-coordinated 2,6-dimethylenepyridyl unit, J. Organomet. Chem., 471 (1994) 97–104.

[57] J. Gräper, R.D. Fischer and G. Paolucci, Lanthanocene ($Ln = Pr^{III}$, Yb^{III}) chlorides involving tetramethyldisiloxane-interlinked cyclopentadienyl ligands, J. Organomet. Chem. 471 (1994) 85–87.

[58] Ch. Qian and D. Zhu, Studies on Organolanthanide complexes. Part 55. Synthesis of furan-bridged bis(cyclopentadienyl)lanthanide and yttrium chlorides, and ligand and metal tuning of reactivity of organolanthanide hydrides (in situ), J. Chem. Soc. Dalton. Trans., (1994) 1599–1603.

[59] W.E. Piers, G. Ferguson, and J.F. Gallagher, Sterically enforced linearity in a bridging telluride

ligand. X-ray structure of $\{(CH_3)_2Si[(t\text{-}C_4H_9)C_5H_3]_2Sc(PMe_3)\}_2(\mu\text{-}Te)\cdot C_6H_6$, Inorg. Chem., 33 (1994) 3784–3787.

[60] H. Schumann, M. Glanz and H. Hemling, Metallorganische Verbindungen der Lanthanoide, 90. — [(*tert*-Butylcyclopentadienyl)dimethyl(tetramethyl cyclopentadienyl)silan]-Komplexe von Lanthan, Neodym und Lutetium, Chem. Ber., 127 (1994) 2363–2367.

[61] Sh. Hajela and J.E. Bercaw. Competitive chain transfer by β-hydrogen and β-methyl elimination for the model Ziegler–Natta olefin polymerization system $[Me_2Si(\eta^5\text{-}C_5Me_4)_2]Sc\{CH_2CH(CH_3)_2\}(PMe_3)$, Organometallics, 13 (1994) 1147–1154.

[62] M.A. Giardello, V.P. Conticello, L. Brard, M. Sabat, A.L. Rheingold, Ch.L. Stern and T.J. Marks, Chiral organolanthanides designed for asymmetric catalysis. Synthesis, characterization, and configurational interconversions of chiral, C_1-symmetric organolanthanide halides, amides, and hydrocarbyls, J. Am. Chem. Soc., 116 (1994) 10212–10240.

[63] W.J. Evans, T.S. Gummersheimer, T.J. Boyle and J.W. Ziller, Synthesis and structure of new soluble organosamarium(II) reagents: $(indenyl)_2Sm(THF)$ and $(fluorenyl)_2Sm(THF)_2$, Organometallics, 13 (1994) 1281–1284.

[64] J. Jubb and S. Gambarotta, Dinitrogen reduction operated by a samarium macrocyclic complex. Encapsulation of dinitrogen into a Sm_2Li_4 metallic cage, J. Am. Chem. Soc., 116 (1994) 4477–4478.

[65] K. Mashima, Y. Nakayama and A. Nakamura, A new convenient preparation of monocyclooctatetraenyl–lanthanide complexes from metallic lanthanides and oxidants, J. Organomet. Chem., 473 (1994) 85–91.

[66] U. Kilimann, M. Schäfer, R. Herbst-Irmer and F.T. Edelmann, Cyclooctatetraenyl-Komplexe der frühen Übergangsmetalle und Lanthanoide. IV. Strukturechemie des anionisichen Sandwich-Komplexes $[Ce(COT)_2]^-$, J. Organomet. Chem., 469 (1994) C15–C18.

[67] U. Kilimann, M. Schäfer, R. Herbst-Irmer and F.T. Edelmann, Cyclooctatetraenyl-Komplexe der frühen Übergangsmetalle und Lanthanoide. III. Cyclooctatetraenyl-lanthanoidtriflate und -iodide: Neue Ausgangsmaterialen für die Organolanthanoid-Chemie, J. Organomet. Chem., 469 (1994) C10–C14.

[68] U. Kilimann and F.T. Edelmann, Cyclooctatetraenyl-Komplexe der frühen Übergangsmetalle und Lanthanoide. II. Neue Cyclooctatetraenyl-Halbsandwich-Komplexe des Yttriums, J. Organomet. Chem., 469 (1994) C5–C9.

[69] S. Zhang, G. Wie, and W. Chen, Synthesis and crystal structure of $\{(C_8H_8)Dy[\mu\text{-}OCH_2(CH_2)_2CH{=}CH_2](THF)\}_2$, Polyhedron, 13 (1994) 1927–1930.

[70] U. Kilimann, R. Herbst-Irmer, D. Stalke and F.T. Edelmann, An efficient access to organocerium(IV) complexes: synthesis and structure of bis[1,3,6-tris(trimethylsilyl)cyclooctatetraene]cerium(IV), Angew. Chem. Int. Ed. Engl., 33 (1994) 1618–1621.

[71] Y. Li, P.-F. Fu and T.J. Marks, Organolanthanide-catalyzed carbon-heteroatom bond formation. Observations on the facile, regiospecific cyclization of aminoalkynes, Organometallics, 13 (1994) 439–440.

[72] M.A. Giardello, V.P. Conticello, L. Brard, M.R. Gagne and T.J. Marks, Chiral organolanthanides designed for asymmetric catalysis. A kinetic and mechanistic study of enantioselective olefin hydroamination/cyclization and hydrogenation by C_1-symmetric $Me_2Si(Me_4C_5)(C_5H_3R^*)Ln$ complexes where R^* = chiral auxiliary, J. Am. Chem. Soc., 116 (1994) 10241–10254.

[73] X. Yang, A.M. Seyam, P.F. Fu and T.J. Marks, *exo*-Methylene-functionalized polyethylenes via ring-opening Ziegler polymerization. Product control in organolanthanide-catalyzed methylenecyclopropane polymerization-copolymerization, Macromolecules, 27 (1994) 4625–4626.

[74] W.J. Evans and H. Katsumata, Polymerization of ε-caprolactone by divalent samarium complexes, Macromolecules, 27 (1994) 2330–2332.

[75] W.J. Evans and H. Katsumata, Copolymerization of ethylene carbonate and ε-caprolactone using samarium complexes, Macromolecules, 27 (1994) 4011–4013.

[76] S. Onozawa, T. Sakakura and M. Tanaka, Lanthanoid-catalyzed aldehyde dimerization and its application to polyester synthesis, Chem. Lett., (1994) 531–534.

[77] S. Onozava, T. Sakakura and M. Tanaka, Hydrosilylation of dienes catalysed by $Cp^*_2NdCH(SiMe_3)_2$, Tetrahedron Lett., 35 (1994) 8177–8180.

[78] C. Qian, A. Qui, D. Zhu and X. Yang, Regioselective acylative cleavage of cyclic ether catalyzed by rare earth compounds, J. Mol. Catal., 87 (1994) 357–360.

[79] H. Yasuda, Preparation of lactone polymers at low temperature without depolymerization and thermal decomposition, Jpn. Kokai Tokkyo Koho JP 05 247 184[93 247 184] (Cl. C08G63/08), 24 September 1993, Appl. 92/81 697, 03 March 1992; 4pp., Chem. Abstr., 120 (1994) 120: 135475a.

[80] R.L. Geerts, Olefin polymerization with anionic organoyttrium complexes as catalysts, US Patent 5 244 991 (Cl. 526-141; C08F4/54), 14 September 1993, Appl. 775 389, 15 October 1991; 4 pp., Chem. Abstr. 120 (1994) 120: 218830p.

[81] K. Yokota, Polymerization catalysts for olefins, Jpn. Kokai Tokkyo Koho JP 06 41 232[94 41 232] (Cl. C08F10/00), 15 February 1994, Appl. 92/215 733, 22 July 1992; 7pp., Chem. Abstr. 121 (1994) 121: 134999h.

[82] T.K. Woo, L. Fan and T. Ziegler, A density functional study of chain growing and chain terminating steps in olefin polymerization by metallocene and constrained geometry catalysts, Organometallics, 13 (1994) 2252–2261.

[83] T.K. Woo, L. Fan and T. Ziegler, Density functional study of insertion step in olefin polymerization by metallocene and constrained geometry catalysts, Organometallics, 13 (1994) 432–433.

[84] E.P. Bierwagen, J.E. Bercaw and W.A. Goddard, III, Theoretical studies of Ziegler–Natta catalysis: structural variation and tacticity control, J. Am. Chem. Soc., 116 (1994) 1481–1489.

[85] A. Domingos, N. Marques, A. Pires de Matos, I. Santos and M. Silva, Hydrotris(pyrazolyl)borate chemistry of uranium(III) and uranium(IV). Synthesis of σ-hydrocarbyl derivatives of uranium(IV) and reactivity of $UCl_2R[HB(3,5\text{-}Me_2pz)_3]$ ($R = CH_2SiMe_3$, $CH(SiMe_3)_2$) and $UCl_2R[HB(3,5\text{-}Me_2pz)_3]$ toward ketones and aldehydes, Organometallics, 13 (1994) 654–662.

[86] P.G. Edwards, M.B. Hursthouse, K.M. Abdul Malik and J.S. Parry, Direct conversion of carbon monoxide to a coordinated secondary alcohol derivative by a thorium phosphido complex, J. Chem. Soc. Chem. Commun., (1994) 1249–1250.

[87] P. Gradoz, D. Baudry, M. Ephritikhine, M. Lance, M. Nierlich and J. Vigner, Tetramethylphospholyluranium complexes and their pentamethylcyclopentadienyl analogues, J. Organomet. Chem., 466 (1994) 107–118.

[88] A.F. England, C.J. Burns and S.L. Buchwald, New syntheses of $Cp^{\ddagger}_2Th(Ph)_2$ and $Cp^{\ddagger}_2Th(Me)(aryl)$ derivatives, Organometallics, 13 (1994) 3491–3495.

[89] L. Jia, X. Yang, C. Stern and T.J. Marks, Cationic d^0/f^0 metallocene catalysts. Properties of binuclear organoborane Lewis acid cocatalysts and weakly coordinating counteranions derived therefrom, Organometallics, 13 (1994) 3755–3757.

[90] F.G. Cloke, S.A. Hawkes, P.B. Hitchcock and P. Scott, Synthesis of tris(tetramethylcyclopentadienyl) derivatives of the actinide metals: molecular structure of $[UCl(\eta\text{-}C_5Me_4H)_3]$, Organometallics, 13 (1994) 2895–2897.

[91] R. Adam, C. Villiers and M. Ephritikhine, Reaction of saturated ketones with a trivalent uranium complex. Isolation and characterization of the alcoholate and enolate products. Tetrahedron Lett., 35 (1994) 573–574.

[92] X. Jemine, J. Goffart, P.C. Leverd and M. Ephritikhine, Organo-f-element thermochemistry. Absolute uranium–ligand bond disruption enthalpies of $[UL_3SX]$ complexes ($L = C_5H_4^tBu$, $C_5H_4SiMe_3$ or $C_9H_6SiMe_3$ and $X = Et$ or ^tBu), J. Organomet. Chem., 469 (1994) 55–57.

[93] D. Baudry, A. Dormond and I.A. Abdallaoui, Reactivity of U–H and U–C bonds in electron-poor cyclopentadienyluranium complexes: electronic effects, J. Organomet. Chem., 476 (1994) C15–C17.

[94] T. Arliguie, M. Lance, M. Nierlich, J. Vigner and M. Ephritikhine, Inverse cycloheptatrienyl sandwich complexes. Crystal structure of $[U(BH_4)_2(OC_4H_8)_5][(BH_4)_3U(\mu\text{-}\eta^7,\eta^7\text{-}C_7H_7)U(BH_4)_3]$, J. Chem. Soc. Chem. Commun., (1994) 847–848.

[95] P.C. Leverd, T. Arliguie, M. Lance, M. Nierlich, J. Vigner, M. Ephritikhine, Monocyclooctatetraene uranium thiolate complexes. Crystal structure of $[\{U(\eta\text{-}C_8H_8)(\mu\text{-}S^iPr)_2\}_2]$, J. Chem. Soc. Dalton Trans., (1994) 501–504.

[96] E.G. Samsel, Actinide metallocene catalysts for chain growth on aluminium alkyls. Eur. Pat. Appl. EP 574 854 (Cl. C07C2/88), 22 December 1993, US Appl. 900 387, 18 June 1992; 12 pp., Chem. Abstr., 121 (1994) 121: 86240e.